



# **NAVAL POSTGRADUATE SCHOOL**

**MONTEREY, CALIFORNIA**

## **THESIS**

**PERFORMANCE ANALYSIS OF THE LINK-16/JTIDS  
WAVEFORM WITH CONCATENATED CODING, SOFT  
DECISION REED-SOLOMON DECODING AND NOISE-  
NORMALIZATION**

by

Katsaros Charalampos

September 2010

Thesis Advisor:  
Second Reader:

R. Clark Robertson  
Terry Smith

**Approved for public release; distribution is unlimited**

THIS PAGE INTENTIONALLY LEFT BLANK

<b>REPORT DOCUMENTATION PAGE</b>			<i>Form Approved OMB No. 0704-0188</i>	
Public reporting burden for this collection of information is estimated to average 1 hour per response, including the time for reviewing instruction, searching existing data sources, gathering and maintaining the data needed, and completing and reviewing the collection of information. Send comments regarding this burden estimate or any other aspect of this collection of information, including suggestions for reducing this burden, to Washington headquarters Services, Directorate for Information Operations and Reports, 1215 Jefferson Davis Highway, Suite 1204, Arlington, VA 22202-4302, and to the Office of Management and Budget, Paperwork Reduction Project (0704-0188) Washington DC 20503.				
<b>1. AGENCY USE ONLY (Leave blank)</b>		<b>2. REPORT DATE</b> September 2010	<b>3. REPORT TYPE AND DATES COVERED</b> Master's Thesis	
<b>4. TITLE AND SUBTITLE</b> Performance Analysis of the Link-16/JTIDS Waveform with Concatenated Coding, Soft Decision Reed-Solomon Decoding, and Noise-Normalization			<b>5. FUNDING NUMBERS</b>	
<b>6. AUTHOR(S)</b> Charalampos Katsaros				
<b>7. PERFORMING ORGANIZATION NAME(S) AND ADDRESS(ES)</b> Naval Postgraduate School Monterey, CA 93943-5000			<b>8. PERFORMING ORGANIZATION REPORT NUMBER</b>	
<b>9. SPONSORING /MONITORING AGENCY NAME(S) AND ADDRESS(ES)</b> N/A			<b>10. SPONSORING/MONITORING AGENCY REPORT NUMBER</b>	
<b>11. SUPPLEMENTARY NOTES</b> The views expressed in this thesis are those of the author and do not reflect the official policy or position of the Department of Defense or the U.S. Government. IRB Protocol number _____.				
<b>12a. DISTRIBUTION / AVAILABILITY STATEMENT</b> Approved for public release; distribution is unlimited			<b>12b. DISTRIBUTION CODE</b>	
<b>13. ABSTRACT (maximum 200 words)</b>  <p>The Joint Tactical Information Distribution System (JTIDS) is a hybrid frequency-hopped, direct sequence spread spectrum system that employs a (31, 15) Reed-Solomon (RS) code for forward error correction coding. In this thesis, an alternative error correction coding scheme that uses concatenated coding with a (31, <math>k</math>) RS inner code and a rate 4/5 convolutional outer code is considered. In addition, a sequential diversity of two, consistent with the JTIDS double-pulse structure, is considered both for soft decision (SD) RS decoding and for soft diversity combining with noise-normalization. Both coherent and noncoherent detection are considered.</p> <p>Based on the analyses, the alternative JTIDS waveform outperforms the original in all cases considered. When only additive white Gaussian noise is present, the best performances, which result in a gain of about 1.4 dB relative to the existing JTIDS waveform, are achieved for (31, 23) RS and (31, 25) RS inner codes for coherent detection and for (31, 27) RS and (31, 29) RS inner codes for noncoherent detection. For these RS inner codes, a 23.0% and 33.0% improvement in system throughput is achieved, respectively, for coherent detection, and a 44.0% and 55.0% improvement in throughput is achieved, respectively, for noncoherent detection relative to the existing JTIDS waveform. Noise-normalization neutralizes the effects of pulse-noise interference, but no significant benefits are obtained from using SD RS decoding.</p>				
<b>14. SUBJECT TERMS</b> JTIDS, Link-16, soft decision (SD) Reed-Solomon (RS) codes, cyclic code-shift keying (CCSK), minimum-shift keying (MSK), convolutional codes, concatenated codes, noise-normalization, pulse-noise interference (PNI), diversity, additive white Gaussian noise (AWGN).			<b>15. NUMBER OF PAGES</b> 111	
			<b>16. PRICE CODE</b>	
<b>17. SECURITY CLASSIFICATION OF REPORT</b> Unclassified	<b>18. SECURITY CLASSIFICATION OF THIS PAGE</b> Unclassified	<b>19. SECURITY CLASSIFICATION OF ABSTRACT</b> Unclassified	<b>20. LIMITATION OF ABSTRACT</b> UU	

NSN 7540-01-280-5500

Standard Form 298 (Rev. 2-89)  
Prescribed by ANSI Std. Z39-18

THIS PAGE INTENTIONALLY LEFT BLANK

**Approved for public release; distribution is unlimited**

**PERFORMANCE ANALYSIS OF THE LINK-16/JTIDS WAVEFORM WITH  
CONCATENATED CODING, SOFT DECISION REED SOLOMON DECODING  
AND NOISE-NORMALIZATION**

Katsaros Charalampos  
Lieutenant Junior Grade, Hellenic Navy  
Bachelor of Naval Science, Hellenic Naval Academy, 2003

Submitted in partial fulfillment of the  
requirements for the degree of

**MASTER OF SCIENCE IN ELECTRONIC WARFARE SYSTEMS  
ENGINEERING**

from the

**NAVAL POSTGRADUATE SCHOOL  
September 2010**

Author: Katsaros Charalampos

Approved by: R. Clark Robertson  
Thesis Advisor

Terry Smith  
Second Reader

Dan C. Boger  
Chairman, Department of Information Sciences

THIS PAGE INTENTIONALLY LEFT BLANK

## ABSTRACT

The Joint Tactical Information Distribution System (JTIDS) is a hybrid frequency-hopped, direct sequence spread spectrum system that employs a (31, 15) Reed-Solomon (RS) code for forward error correction coding. In this thesis, an alternative error correction coding scheme that uses concatenated coding with a (31,  $k$ ) RS inner code and a rate 4/5 convolutional outer code is considered. In addition, a sequential diversity of two, consistent with the JTIDS double-pulse structure, is considered both for soft decision (SD) RS decoding and for soft diversity combining with noise-normalization. Both coherent and noncoherent detection are considered.

Based on the analyses, the alternative JTIDS waveform outperforms the original in all cases considered. When only additive white Gaussian noise is present, the best performances, which result in a gain of about 1.4 dB relative to the existing JTIDS waveform, are achieved for (31, 23) RS and (31, 25) RS inner codes for coherent detection and for (31, 27) RS and (31, 29) RS inner codes for noncoherent detection. For these RS inner codes, a 23.0% and 33.0% improvement in system throughput is achieved, respectively, for coherent detection, and a 44.0% and 55.0% improvement in throughput is achieved, respectively, for noncoherent detection relative to the existing JTIDS waveform. Noise-normalization neutralizes the effects of pulse-noise interference, but no significant benefits are obtained from using SD RS decoding.

THIS PAGE INTENTIONALLY LEFT BLANK



## TABLE OF CONTENTS

<b>I.</b>	<b>INTRODUCTION.....</b>	<b>1</b>
<b>A.</b>	<b>    THESIS OBJECTIVE.....</b>	<b>1</b>
<b>B.</b>	<b>    THESIS OUTLINE.....</b>	<b>2</b>
<b>II.</b>	<b>BACKGROUND .....</b>	<b>3</b>
<b>A.</b>	<b>    ALTERNATIVE LINK-16/JTIDS TYPE SYSTEM.....</b>	<b>3</b>
1.	Concatenated Codes.....	4
2.	Convolutional Codes.....	5
3.	Symbol-to-bit Conversion .....	8
4.	Reed-Solomon (RS) Codes .....	9
5.	Symbol Interleaver.....	10
6.	Cyclic Code-Shift Keying Baseband Symbol Modulation.....	10
7.	Pseudorandom Noise .....	12
8.	Minimum-Shift Keying Chip Modulation .....	12
<b>B.</b>	<b>    CHAPTER SUMMARY.....</b>	<b>13</b>
<b>III.</b>	<b>PERFORMANCE ANALYSIS OF COHERENT AND NONCOHERENT 32-ARY CCSK WITH CONCATENATED CODING, DIVERSITY AND SD RS DECODING IN AWGN .....</b>	<b>15</b>
<b>A.</b>	<b>    INTRODUCTION.....</b>	<b>15</b>
<b>B.</b>	<b>    COHERENT DEMODULATION OF 32-ARY CCSK WITH DIVERSITY IN AWGN.....</b>	<b>16</b>
<b>C.</b>	<b>    NONCOHERENT DEMODULATION OF 32-ARY CCSK WITH DIVERSITY IN AWGN.....</b>	<b>19</b>
<b>D.</b>	<b>    PERFORMANCE ANALYSIS OF COHERENT DEMODULATION OF 32-ARY CCSK WITH DIVERSITY IN AWGN.....</b>	<b>21</b>
<b>E.</b>	<b>    PERFORMANCE ANALYSIS OF NONCOHERENT DEMODULATION OF 32-ARY CCSK WITH DIVERSITY IN AWGN.....</b>	<b>22</b>
<b>F.</b>	<b>    COMPARISON OF THE PERFORMANCES OF THE ALTERNATIVE WAVEFORM OBTAINED WITH COHERENT AND NONCOHERENT DEMODULATION OF 32-ARY CCSK WITH DIVERSITY IN AWGN.....</b>	<b>24</b>
<b>G.</b>	<b>    COMPARISON OF THE PERFORMANCES OF THE ALTERNATIVE WAVEFORM OBTAINED WITH HARD DECISION AND SOFT DECISION RS DECODING OF 32-ARY CCSK WITH DIVERSITY IN AWGN.....</b>	<b>25</b>
<b>H.</b>	<b>    CHAPTER SUMMARY.....</b>	<b>26</b>
<b>IV.</b>	<b>PERFORMANCE ANALYSIS OF COHERENT 32-ARY CCSK WITH CONCATENATED CODING, DIVERSITY, SD RS DECODING AND NOISE-NORMALIZATION IN AWGN, AND PULSE-NOISE INTERFERENCE.....</b>	<b>29</b>

A.	COHERENT DEMODULATION OF 32-ARY CCSK WITH DIVERSITY AND NOISE-NORMALIZATION IN AWGN AND PNI ..	29
B.	PERFORMANCE ANALYSIS OF COHERENT DEMODULATION OF 32-ARY CCSK WITH DIVERSITY AND NOISE-NORMALIZATION IN AWGN AND PNI .....	35
C.	CHAPTER SUMMARY .....	47
V.	PERFORMANCE ANALYSIS OF NONCOHERENT 32-ARY CCSK WITH CONCATENATED CODING, DIVERSITY, SD RS DECODING AND NOISE-NORMALIZATION IN AWGN, AND PULSE-NOISE INTERFERENCE .....	49
A.	NONCOHERENT DEMODULATION OF 32-ARY CCSK WITH DIVERSITY AND NOISE-NORMALIZATION IN AWGN AND PNI ..	49
B.	PERFORMANCE ANALYSIS OF NONCOHERENT DEMODULATION OF 32-ARY CCSK WITH DIVERSITY AND NOISE-NORMALIZATION IN AWGN AND PNI .....	59
C.	COMPARISON OF THE PERFORMANCE OF THE ALTERNATIVE WAVEFORM WITH SLOPE DETECTION OR WITH QUADRATURE-CORRELATOR SQUARE-LAW DETECTION FOR NONCOHERENT DEMODULATION OF 32-ARY CCSK WITH DIVERSITY AND NOISE-NORMALIZATION IN AWGN AND PNI .....	72
D.	COMPARISON OF THE PERFORMANCE OF THE ALTERNATIVE WAVEFORM OBTAINED WITH HARD AND SOFT DECISION RS DECODING .....	77
E.	CHAPTER SUMMARY .....	81
VI.	CONCLUSIONS AND FUTURE WORK .....	83
	LIST OF REFERENCES .....	85
	INITIAL DISTRIBUTION LIST .....	87

## LIST OF FIGURES

Figure 1.	A JTIDS-type System Model Using the Alternative Error Control Coding Scheme (From [1]).	4
Figure 2.	Block Diagram of Concatenated Coding Communication System (From [3]).	5
Figure 3.	Rate $1/2$ Convolutional Code with Constraint Length $K = 3$ (From [4]).	6
Figure 4.	The 32-chip CCSK Sequences Chosen for JTIDS (From [9]).	11
Figure 5.	Receiver Structure of a JTIDS-type System Using the Alternative Error Correction Coding Scheme (From [1]).	15
Figure 6.	Continuous-phase BFSK or MSK Demodulator with Slope Detector. The Signal $m(t)$ is the Antipodal Information Signal (From [11]).	19
Figure 7.	Performance of 32-ary CCSK Using the Alternative Error Correction Coding Scheme in AWGN for Coherent Demodulation, a Diversity of Two, and Soft Decision RS Decoding.	22
Figure 8.	Performance of 32-ary CCSK Using the Alternative Error Correction Coding Scheme in AWGN for Noncoherent Demodulation, a Diversity of Two, and Soft Decision RS Decoding.	23
Figure 9.	Performance of 32-ary CCSK Using the Alternative Error Correction Coding Scheme in AWGN for RS (31, 23) and RS (31, 25) Inner Codes, Coherent and Noncoherent Demodulation, a Diversity of Two, and Soft Decision RS Decoding.	24
Figure 10.	Performance of 32-ary CCSK Using the Alternative Error Correction Coding Scheme in AWGN for RS (31, 23) and RS (31, 25) Inner Codes, a Diversity of Two, Hard and Soft Decision RS Decoding, and Coherent Demodulation.	25
Figure 11.	Performance of 32-ary CCSK Using the Alternative Error Correction Coding Scheme in AWGN for RS (31, 23) and RS (31, 25) Inner Codes, a Diversity of Two, Hard and Soft Decision RS Decoding, and Noncoherent Demodulation.	26
Figure 12.	FFH/BPSK Noise-normalized Receiver.	30
Figure 13.	Performance of 32-ary CCSK Using the Alternative Error Correction Coding Scheme for a RS (31, 25) Inner Code in Both AWGN and PNI for $\rho = 0.1$ , $\rho = 0.3$ , $\rho = 0.5$ , $\rho = 0.7$ and $\rho = 1.0$ , Coherent Demodulation, Soft Decision RS Decoding, a Diversity of Two, Noise-normalization, and $E_b/N_0 = 7.0$ dB.	36
Figure 14.	Performance of 32-ary CCSK Using the Alternative Error Correction Coding Scheme for a RS (31, 25) Inner Code in Both AWGN and PNI for $\rho = 0.5$ , Coherent Demodulation, Soft Decision RS Decoding, a Diversity of Two, and Noise-normalization when $E_b/N_0 = 6.0$ dB, $E_b/N_0 = 6.5$ dB, $E_b/N_0 = 10.0$ dB, $E_b/N_0 = 14.5$ dB, $E_b/N_0 = 15.0$ dB.	37

Figure 15.	Performance of 32-ary CCSK Using the Alternative Error Correction Coding Scheme in Both AWGN and PNI for $\rho = 0.1$ , Coherent Demodulation, Soft Decision RS Decoding, a Diversity of Two, Noise-normalization, and $E_b/N_0 = 6.0$ dB.....	40
Figure 16.	Performance of 32-ary CCSK Using the Alternative Error Correction Coding Scheme in Both AWGN and PNI for $\rho = 0.3$ , Coherent Demodulation, Soft Decision RS Decoding, a Diversity of Two, Noise-normalization, and $E_b/N_0 = 6.0$ dB.....	41
Figure 17.	Performance of 32-ary CCSK Using the Alternative Error Correction Coding Scheme in Both AWGN and PNI for $\rho = 0.5$ , Coherent Demodulation, Soft Decision RS Decoding, a Diversity of Two, Noise-normalization, and $E_b/N_0 = 6.0$ dB.....	41
Figure 18.	Performance of 32-ary CCSK Using the Alternative Error Correction Coding Scheme in Both AWGN and PNI for $\rho = 0.7$ , Coherent Demodulation, Soft Decision RS Decoding, a Diversity of Two, Noise-normalization, and $E_b/N_0 = 6.0$ dB.....	42
Figure 19.	Performance of 32-ary CCSK Using the Alternative Error Correction Coding Scheme in Both AWGN and PNI for $\rho = 1.0$ , Coherent Demodulation, Soft Decision RS Decoding, a Diversity of Two, Noise-normalization, and $E_b/N_0 = 6.0$ dB.....	42
Figure 20.	Performance of 32-ary CCSK Using the Alternative Error Correction Coding Scheme in Both AWGN and PNI for $\rho = 0.1$ , Coherent Demodulation, Soft Decision RS Decoding, a Diversity of Two, Noise-normalization, and $E_b/N_0 = 10.0$ dB.....	43
Figure 21.	Performance of 32-ary CCSK Using the Alternative Error Correction Coding Scheme in Both AWGN and PNI for $\rho = 0.3$ , Coherent Demodulation, Soft Decision RS Decoding, a Diversity of Two, Noise-normalization, and $E_b/N_0 = 10.0$ dB.....	43
Figure 22.	Performance of 32-ary CCSK Using the Alternative Error Correction Coding Scheme in Both AWGN and PNI for $\rho = 0.5$ , Coherent Demodulation, Soft Decision RS Decoding, a Diversity of Two, Noise-normalization, and $E_b/N_0 = 10.0$ dB.....	44
Figure 23.	Performance of 32-ary CCSK Using the Alternative Error Correction Coding Scheme in Both AWGN and PNI for $\rho = 0.7$ , Coherent Demodulation, Soft Decision RS Decoding, a Diversity of Two, Noise-normalization, and $E_b/N_0 = 10.0$ dB.....	44
Figure 24.	Performance of 32-ary CCSK Using the Alternative Error Correction Coding Scheme in Both AWGN and PNI for $\rho = 1.0$ , Coherent Demodulation, Soft Decision RS Decoding, a Diversity of Two, Noise-normalization, and $E_b/N_0 = 10.0$ dB.....	45

Figure 25.	Performance of 32-ary CCSK Using the Alternative Error Correction Coding Scheme in Both AWGN and PNI for $\rho = 0.3$ , Coherent Demodulation, Soft Decision RS Decoding, a Diversity of Two, Noise-normalization, and $E_b/N_0 = 15.0$ dB.....	45
Figure 26.	Performance of 32-ary CCSK Using the Alternative Error Correction Coding Scheme in Both AWGN and PNI for $\rho = 0.5$ , Coherent Demodulation, Soft Decision RS Decoding, a Diversity of Two, Noise-normalization, and $E_b/N_0 = 15.0$ dB.....	46
Figure 27.	Performance of 32-ary CCSK Using the Alternative Error Correction Coding Scheme in Both AWGN and PNI for $\rho = 0.7$ , Coherent Demodulation, Soft Decision RS Decoding, a Diversity of Two, Noise-normalization, and $E_b/N_0 = 15.0$ dB.....	46
Figure 28.	Performance of 32-ary CCSK Using the Alternative Error Correction Coding Scheme in Both AWGN and PNI for $\rho = 1.0$ , Coherent Demodulation, Soft Decision RS Decoding, a Diversity of Two, Noise-normalization, and $E_b/N_0 = 15.0$ dB.....	47
Figure 29.	The Quadrature-correlator Square-law Detector for an Input Signal $s(t)$ with Unknown Phase $\theta$ (After [11]). .....	49
Figure 30.	Noncoherent Noise-normalized FFH/BFSK Receiver (From [13]).....	51
Figure 31.	Performance of 32-ary CCSK Using the Alternative Error Correction Coding Scheme with Diversity and Noise-normalization in AWGN and PNI with $\rho = 0.1$ when $E_b/N_0 = 8.0$ dB.....	63
Figure 32.	Performance of 32-ary CCSK Using the Alternative Error Correction Coding Scheme with Diversity and Noise-normalization in AWGN and PNI with $\rho = 0.3$ when $E_b/N_0 = 8.0$ dB. ....	63
Figure 33.	Performance of 32-ary CCSK Using the Alternative Error Correction Coding Scheme with Diversity and Noise-normalization in AWGN and PNI with $\rho = 0.5$ when $E_b/N_0 = 8.0$ dB. ....	64
Figure 34.	Performance of 32-ary CCSK Using the Alternative Error Correction Coding Scheme with Diversity and Noise-normalization in AWGN and PNI with $\rho = 0.7$ when $E_b/N_0 = 8.0$ dB. ....	64
Figure 35.	Performance of 32-ary CCSK Using the Alternative Error Correction Coding Scheme with Diversity and Noise-normalization in AWGN and PNI with $\rho = 1.0$ when $E_b/N_0 = 8.0$ dB.....	65
Figure 36.	Performance of 32-ary CCSK Using the Alternative Error Correction Coding Scheme with Diversity and Noise-normalization in AWGN and PNI with $\rho = 0.1$ when $E_b/N_0 = 10.0$ dB.....	65
Figure 37.	Performance of 32-ary CCSK Using the Alternative Error Correction Coding Scheme with Diversity and Noise-normalization in AWGN and PNI with $\rho = 0.3$ when $E_b/N_0 = 10.0$ dB. ....	66

Figure 38.	Performance of 32-ary CCSK Using the Alternative Error Correction Coding Scheme with Diversity and Noise-normalization in AWGN and PNI with $\rho = 0.5$ when $E_b / N_o = 10.0$ dB. ....	66
Figure 39.	Performance of 32-ary CCSK Using the Alternative Error Correction Coding Scheme with Diversity and Noise-normalization in AWGN and PNI with $\rho = 0.7$ when $E_b / N_o = 10.0$ dB. ....	67
Figure 40.	Performance of 32-ary CCSK Using the Alternative Error Correction Coding Scheme with Diversity and Noise-normalization in AWGN and PNI with $\rho = 1.0$ when $E_b / N_o = 10.0$ dB. ....	67
Figure 41.	Performance of 32-ary CCSK Using the Alternative Error Correction Coding Scheme with Diversity and Noise-normalization in AWGN and PNI with $\rho = 0.3$ when $E_b / N_o = 13.0$ dB. ....	68
Figure 42.	Performance of 32-ary CCSK Using the Alternative Error Correction Coding Scheme with Diversity and Noise-normalization in AWGN and PNI with $\rho = 0.5$ when $E_b / N_o = 13.0$ dB. ....	68
Figure 43.	Performance of 32-ary CCSK Using the Alternative Error Correction Coding Scheme with Diversity and Noise-normalization in AWGN and PNI with $\rho = 0.7$ when $E_b / N_o = 13.0$ dB. ....	69
Figure 44.	Performance of 32-ary CCSK Using the Alternative Error Correction Coding Scheme with Diversity and Noise-normalization in AWGN and PNI with $\rho = 1.0$ when $E_b / N_o = 13.0$ dB. ....	69
Figure 45.	Performance of 32-ary CCSK Using the Alternative Error Correction Coding Scheme with Diversity and Noise-normalization in AWGN and PNI with $\rho = 0.3$ when $E_b / N_o = 15.0$ dB. ....	70
Figure 46.	Performance of 32-ary CCSK Using the Alternative Error Correction Coding Scheme with Diversity and Noise-normalization in AWGN and PNI with $\rho = 0.5$ when $E_b / N_o = 15.0$ dB. ....	70
Figure 47.	Performance of 32-ary CCSK Using the Alternative Error Correction Coding Scheme with Diversity and Noise-normalization in AWGN and PNI with $\rho = 0.7$ when $E_b / N_o = 15.0$ dB. ....	71
Figure 48.	Performance of 32-ary CCSK Using the Alternative Error Correction Coding Scheme with Diversity and Noise-normalization in AWGN and PNI with $\rho = 1.0$ when $E_b / N_o = 15.0$ dB. ....	71
Figure 49.	Performance of 32-ary CCSK Using the Alternative Error Correction Coding Scheme with Diversity and Noise-normalization in AWGN and PNI with $\rho = 0.3$ for Both Matched Filter and Slope Detection when $E_b / N_o = 12.0$ dB. ....	73
Figure 50.	Performance of 32-ary CCSK Using the Alternative Error Correction Coding Scheme with Diversity and Noise-normalization in AWGN and PNI with $\rho = 0.5$ for Both Matched Filter and Slope Detection when $E_b / N_o = 12.0$ dB. ....	74

Figure 51.	Performance of 32-ary CCSK Using the Alternative Error Correction Coding Scheme with Diversity and Noise-normalization in AWGN and PNI with $\rho = 0.7$ for Both Matched Filter and Slope Detection when $E_b / N_o = 12.0$ dB.....	74
Figure 52.	Performance of 32-ary CCSK Using the Alternative Error Correction Coding Scheme with Diversity and Noise-normalization in AWGN and PNI with $\rho = 1.0$ for Both Matched Filter and Slope Detection when $E_b / N_o = 12.0$ dB.....	75
Figure 53.	Performance of 32-ary CCSK Using the Alternative Error Correction Coding Scheme with Diversity and Noise-normalization in AWGN and PNI with $\rho = 0.3$ for Matched Filter Detection with $E_b / N_o = 15.0$ dB and Slope Detection with $E_b / N_o = 12.0$ dB.....	75
Figure 54.	Performance of 32-ary CCSK Using the Alternative Error Correction Coding Scheme with Diversity and Noise-normalization in AWGN and PNI with $\rho = 0.5$ for Matched Filter Detection with $E_b / N_o = 15.0$ dB and Slope Detection with $E_b / N_o = 12.0$ dB.....	76
Figure 55.	Performance of 32-ary CCSK Using the Alternative Error Correction Coding Scheme with Diversity and Noise-normalization in AWGN and PNI with $\rho = 0.7$ for Matched Filter Detection with $E_b / N_o = 15.0$ dB and Slope Detection with $E_b / N_o = 12.0$ dB.....	76
Figure 56.	Performance of 32-ary CCSK Using the Alternative Error Correction Coding Scheme with Diversity and Noise-normalization in AWGN and PNI with $\rho = 1.0$ for Matched Filter Detection with $E_b / N_o = 15.0$ dB and Slope Detection with $E_b / N_o = 12.0$ dB.....	77
Figure 57.	Performance of 32-ary CCSK Using the Alternative Error Correction Coding Scheme in AWGN and PNI with $\rho = 0.3$ , Diversity, Noise-normalization, Hard and Soft Decision RS Decoding, and Noncoherent Demodulation.....	79
Figure 58.	Performance of 32-ary CCSK Using the Alternative Error Correction Coding Scheme in AWGN and PNI with $\rho = 0.5$ , Diversity, Noise-normalization, Hard and Soft Decision RS Decoding, and Noncoherent Demodulation.....	79
Figure 59.	Performance of 32-ary CCSK Using the Alternative Error Correction Coding Scheme in AWGN and PNI with $\rho = 0.7$ , Diversity, Noise-normalization, Hard and Soft Decision RS Decoding, and Noncoherent Demodulation.....	80
Figure 60.	Performance of 32-ary CCSK Using the Alternative Error Correction Coding Scheme in AWGN and PNI with $\rho = 1.0$ , Diversity, Noise-normalization, Hard and Soft Decision RS Decoding, and Noncoherent Demodulation.....	80

THIS PAGE INTENTIONALLY LEFT BLANK



## LIST OF TABLES

Table 1.	Generator Polynomials and Information Weight Structure for Rate $4/5$ Convolutional Codes (From [5]).....	8
Table 2.	Conditional Probabilities of Symbol Error for the CCSK Sequence Chosen by JTIDS (From [10]). .....	12
Table 3.	Comparison of the Performance of the Original and the Alternative JTIDS Waveform for Different Values of $\rho$ for Coherent Demodulation when $E_b/N_0 = 6.0$ dB.....	38
Table 4.	Comparison of the Performance of the Original and the Alternative JTIDS Waveform for Different Values of $\rho$ for Coherent Demodulation when $E_b/N_0 = 10.0$ dB.....	39
Table 5.	Comparison of the Performance of the Original and the Alternative JTIDS Waveform for Different Values of $\rho$ for Coherent Demodulation when $E_b/N_0 = 15.0$ dB.....	40
Table 6.	Comparison of the Performance of the Original and the Alternative JTIDS Waveform for Different Values of $\rho$ for Noncoherent Demodulation when $E_b/N_0 = 8.0$ dB.....	60
Table 7.	Comparison of the Performance of the Original and the Alternative JTIDS Waveform for Different Values of $\rho$ for Noncoherent Demodulation when $E_b/N_0 = 10.0$ dB.....	60
Table 8.	Comparison of the Performance of the Original and the Alternative JTIDS Waveform for Different Values of $\rho$ for Noncoherent Demodulation when $E_b/N_0 = 13.0$ dB.....	61
Table 9.	Comparison of the Performance of the Original and the Alternative JTIDS Waveform for Different Values of $\rho$ for Noncoherent Demodulation when $E_b/N_0 = 15.0$ dB.....	62
Table 10.	Comparison of the Performance of the Alternative Waveform for Different Values of $\rho$ for Noncoherent Demodulation with Matched Filter Detection and Slope Detection with $E_b/N_0 = 12.0$ dB.....	72
Table 11.	Comparison of the Performance of the Alternative Waveform for Different Values of $\rho$ for Noncoherent Demodulation with Matched Filter Detection with $E_b/N_0 = 15.0$ dB and Slope Detection with $E_b/N_0 = 12.0$ dB.....	73
Table 12.	Comparison of the Performance of the Alternative Waveform for Different Values of $\rho$ for Noncoherent Hard and Soft Decision RS Decoding in AWGN and PNI with Noise Normalization when $E_b/N_0 = 8.0$ dB.....	78

THIS PAGE INTENTIONALLY LEFT BLANK

## EXECUTIVE SUMMARY

Link-16 is a highly integrated system designed to support the tactical data information exchange requirements of military applications. It is the basic communication tool for combined operations and provides secure and jam-resistant digital communication for both data and voice.

The Joint Tactical Information Distribution System (JTIDS) is the communication terminal of Link-16 and utilizes a  $(31, 15)$  Reed-Solomon (RS) code for channel coding, cyclic code-shift keying (CCSK) for 32-ary baseband symbol modulation, where each encoded symbol consists of five bits, and minimum-shift keying (MSK) for chip modulation. Transmission bandwidth and transmitter/receiver complexity are sacrificed for increased resistance to jamming and low probability of interception and detection, which are achieved by making use of frequency-hopping (FH) and direct sequence spread spectrum (DSSS) techniques. Finally, JTIDS uses the ultra high frequency (UHF) spectrum; hence, communications are limited to line-of-sight unless suitable relay platforms are available.

In this thesis, an alternative error correction coding scheme for the physical layer waveform of the JTIDS, which is consistent with the existing JTIDS error control coding scheme, is examined. The system considered uses concatenated coding with a  $(31, k)$  RS inner code and a rate  $4/5$  convolutional outer code. A sequential diversity of two, consistent with the JTIDS double-pulse structure, is assumed. In the receiver, soft decision RS decoding is employed to determine the transmitted symbols, and noise-normalization is utilized in the receiver when additive white Gaussian noise (AWGN) and pulse-noise interference (PNI) are both present to neutralize the interference effects. The benefits of using noise-normalization are examined in situations where PNI is used to represent a typical jammed operating environment.

The performance obtained with the alternative waveform for various  $(31, k)$  RS inner codes is compared with that obtained with the existing JTIDS waveform for the case where AWGN is the only noise present, as well as when both AWGN and PNI are present.

Based on the analyses, the author concludes that the alternative, compatible JTIDS waveform has better performance than the existing waveform for both coherent and noncoherent detection in AWGN, and when both AWGN and PNI are present. The best performance for coherent detection was found to be for  $(31,23)$  and  $(31,25)$  RS inner codes, which results in a gain of about 1.4 dB and a 23.0% and 33.0% improvement in system throughput, respectively, as compared to the existing JTIDS waveform. For noncoherent detection, best performance was found to be for  $(31,27)$  and  $(31,29)$  RS inner codes, which results in a gain of about 1.4 dB and 44.0% and 55.0% throughput improvement, respectively. Soft decision RS decoding improves the overall performance less than 1.0 dB relative to hard decision decoding, and therefore the benefits are negligible. Finally, when both AWGN and PNI are present, the use of a noise-normalized receiver was found to cancel the effects of PNI, forcing the jammer to adopt a continuous, full-band jamming strategy.

## LIST OF ACRONYMS AND ABBREVIATIONS

AWGN	Additive White Gaussian Noise
BCH	Bose Chaudhuri Hocquenghem
BFSK	Binary Frequency Shift Keying
BPSK	Binary Phase Shift Keying
CCSK	Cyclic Code-Shift Keying
DPSK	Differential Phase Shift Keying
DSSS	Direct Sequence Spread Spectrum
FEC	Forward Error Correction
FFH	Fast Frequency Hopping
GF	Golay Field
HD	Hard Decision
JTIDS	Joint Tactical Information Distribution System
MSK	Minimum Shift Keying
OQPSK	Offset Quadrature Phase Shift Keying
PN	Pseudorandom Noise
PNI	Pulse Noise Interference
PSD	Power Spectral Density
QPSK	Quadrature Phase Shift Keying
RS	Reed-Solomon
SNR	Signal to Noise Ratio
SD	Soft Decision
UHF	Ultra High Frequency

THIS PAGE INTENTIONALLY LEFT BLANK

## **ACKNOWLEDGMENTS**

I would like to devote this work to my lovely wife, Zacharenia Dimitrogiannaki, for her continuous support, her strength and courage, and the happiness that she brings to my life.

I would also like to express my gratitude and sincere appreciation to Professor Clark Robertson for his guidance, encouragement and support in order to complete this work. Finally, I would like to thank Lt. Col Terry Smith for his time spent serving as the second reader of this thesis.

THIS PAGE INTENTIONALLY LEFT BLANK



# **I. INTRODUCTION**

## **A. THESIS OBJECTIVE**

This thesis has two main objectives. The first is to investigate an alternative error correction coding scheme for the Joint Tactical Information Distribution System (JTIDS) physical layer waveform that is consistent with the existing JTIDS error control coding scheme. The alternative system to be considered uses concatenated coding. The outer code is a rate  $4/5$  convolutional code and the inner code is a  $(31, k)$  Reed-Solomon (RS) code. Alternating the value of  $k$  and, therefore, the overall code rate, the RS code that results in the best performance improvement is obtained. The initial analysis considers additive white Gaussian noise (AWGN) for both coherent and noncoherent detection. A sequential diversity of two, consistent with the double-pulse structure of JTIDS, is assumed. Hence, each symbol is transmitted twice on two different carrier frequencies. Finally, the effect on performance when soft decision RS decoding is assumed is examined.

The second main objective in this thesis is to examine the effects of using noise-normalization in the receiver. In military applications, there are other considerations that supersede conventional ones, such as the ability to reject hostile jamming. A noise-normalized receiver can minimize the effect of partial band interference/jamming, where jamming is spread over only a portion of the entire spread spectrum bandwidth. The system again uses the alternative error correction scheme with a diversity of two and soft decision RS decoding in both AWGN and pulse-noise interference (PNI) for both coherent and noncoherent detection.

Previous research has examined various enhancements and modifications to the JTIDS waveform. In particular, concatenated coding was examined in [1] and [2]. However, this is the first time that concatenated coding in combination with noise-normalization has been considered.

## **B. THESIS OUTLINE**

The thesis is organized into the introduction (Chapter I), background (Chapter II), and four additional chapters. An analysis of the performance of coherent and noncoherent 32-ary cyclic code-shift keying (CCSK) with concatenated coding, diversity of two, and soft decision RS decoding in AWGN is presented in Chapter III. In Chapter IV, the performance of coherent 32-ary CCSK with concatenated coding in AWGN and PNI with a diversity of two, soft decision decoding, and noise-normalization is analyzed. The performance of noncoherent 32-ary CCSK with concatenated coding in AWGN and PNI with a diversity of two, soft decision decoding, and noise-normalization is considered in Chapter V. Finally, in Chapter VI the conclusions based on the results obtained from the analyses in the previous chapters are presented.

## II. BACKGROUND

A brief description of the alternative JTIDS system and a series of basic concepts that are required in order for the reader to understand the analysis of the alternative waveform are provided in this chapter.

### A. ALTERNATIVE LINK-16/JTIDS TYPE SYSTEM

The existing JTIDS uses a 32-ary CCSK modulation scheme combined with a (31,15) RS code. In this thesis, the alternative scheme employs concatenated coding, which uses two levels of coding. In the transmitter, at first, a rate  $4/5$  convolutional encoder is used and, after the bit-to-symbol converter, a RS encoder follows. After encoding, the proposed JTIDS signal is the same as the existing JTIDS signal. Before the CCSK modulation, a symbol interleaver is applied and prior to transmission the CCSK sequence is converted to a direct sequence spread spectrum (DSSS) signal via binary phase-shift keying (BPSK) spreading using a 32-chip pseudorandom noise (PN) sequence. Finally, minimum-shift keying (MSK) is used for the waveform modulation. MSK is a continuous phase modulation scheme with differential encoding of the chips. In this thesis, at the receiver, soft decision RS decoding is considered to further improve the performance of the system.

The alternative JTIDS transceiver is shown in Figure 1. The top branch represents the transmitter and the bottom branch the receiver. At the receiver, the reception process is the reverse of the transmission process. After frequency de-hopping, MSK demodulation and de-scrambling, each 5-bit symbol is recovered by a CCSK demodulator. After symbol de-interleaving, the channel symbols are decoded by a RS decoder, and the inner code input symbols are recovered. Finally, a symbol-to-bit converter is applied before the convolutional decoder, which recovers the information bits.

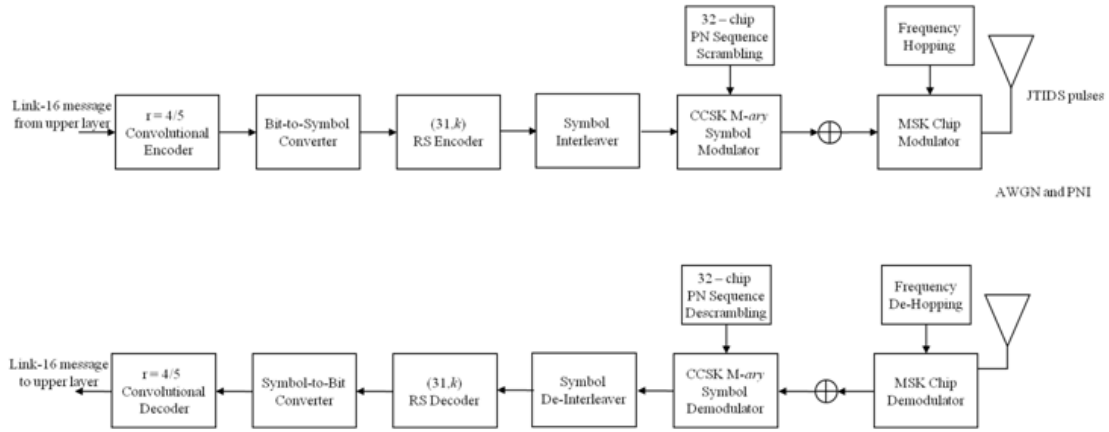


Figure 1. A JTIDS-type System Model Using the Alternative Error Control Coding Scheme (From [1]).

## 1. Concatenated Codes

A concatenated code consists of two separate codes that are combined to form a larger code. The first code, which takes the information bits directly, is referred to as the outer code and the second code is referred to as the inner code. In this thesis, the inner code is a RS code, and soft decision decoding is performed at the receiver in the inner decoder. The outer code is a convolutional code, and the outer decoder is a hard decision decoder.

Considering the concatenated coding scheme in Figure 2, the outer encoder takes  $k_o$  bits and generates an  $n_o$ -bit symbol. The inner encoder takes  $k_i$   $n_o$ -bit symbols and generates  $n_i$   $k_i$ -bit symbols. Thus, a concatenated block code having a block length  $n_i n_o$  and containing  $k_i k_o$  information bits is obtained.

The primary advantage of using concatenated coding is that a lower error rate is achieved than by using either of the constituent codes alone (RS or convolutional). The overall code rate of this concatenated code is [3]

$$r_{cc} = \frac{k_i k_o}{n_i n_o} \quad (2.1)$$

The error probability of concatenated codes can be evaluated by first calculating the bit error probability of the inner code and then applying the result to the error probability of the outer code.

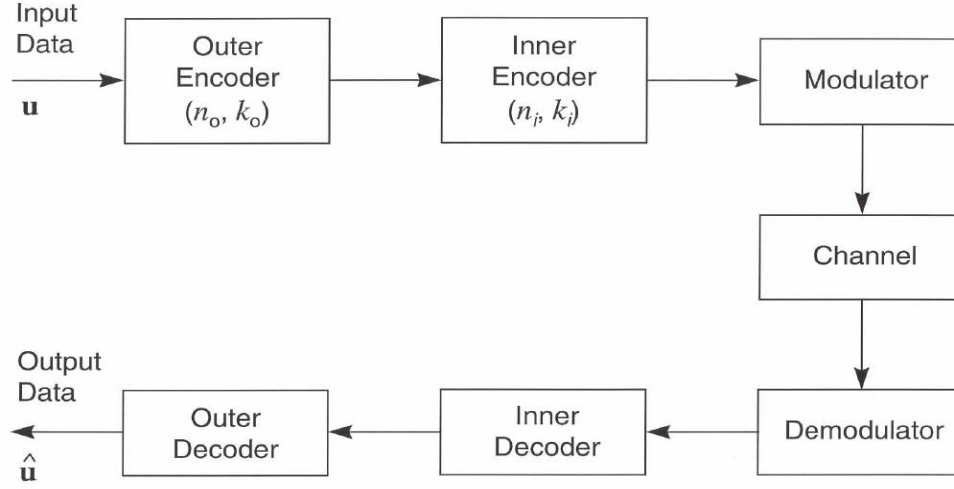


Figure 2. Block Diagram of Concatenated Coding Communication System (From [3]).

## 2. Convolutional Codes

A convolutional code is generated by passing the information bits to be transmitted through a finite state machine. Convolutional codes are linear and introduce redundant bits into the data stream through the use of linear shift registers. The code rate  $r$  for a convolutional code is defined as

$$r = \frac{k}{n} \quad (2.2)$$

where  $n$  is the number of output coded bits that are produced from  $k$  input information bits. Any particular state depends only on a finite number of past information bits. For a code with  $2^\nu$  states, the number of past information bits that determine a present state are between  $\nu$  and  $k\nu$  bits. The constraint length of the convolutional code is [4]

$$K = \nu + 1 \quad (2.3)$$

where  $\nu$  is the maximum number of shift registers. The shift registers store the state information of the convolutional encoder, and the constraint length relates to the number

of bits upon which the output depends. The output coded bits are obtained by the convolution (modulo-2) of the input information bits with the encoder generator sequences. In Figure 3, a rate  $1/2$  convolutional encoder is considered for illustration. The output sequences  $c_1(x)$  and  $c_2(x)$  are multiplexed (parallel-to-serial conversion) into a single sequence  $c$  for transmission that contains twice the number of information bits as the input stream. A convolutional code can become very complicated with various code rates and constraint lengths.

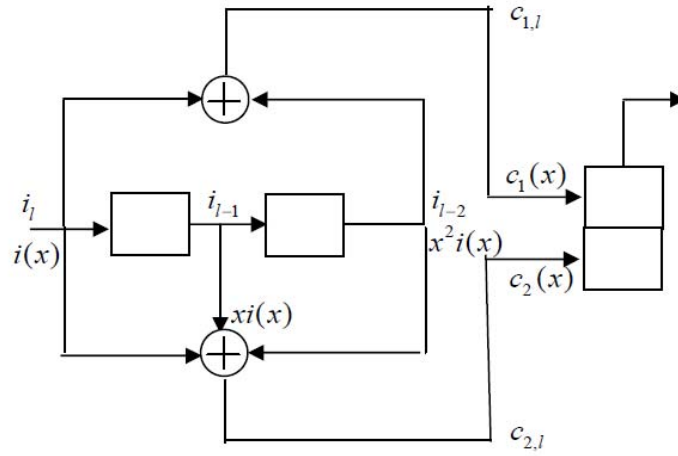


Figure 3. Rate  $1/2$  Convolutional Code with Constraint Length  $K = 3$  (From [4]).

Assume that  $P_2(d)$  is the probability of selecting a code sequence that is a Hamming distance  $d$  from the correct code sequence, and  $\beta_d$  is the sum of all possible information bit errors. The union bound on the coded bit error probability can be obtained by weighting  $P_2(d)$  with the information weight  $\beta_d$  of all paths of Hamming weight  $d$ . Since there are  $k$  information bits per branch for a rate  $r = k/n$  code, the union bound is given by [5]

$$P_b \leq \frac{1}{k} \sum_{d=d_{free}}^{\infty} \beta_d P_2(d) \quad (2.4)$$

where  $d_{free}$  is the free distance of the convolutional code . Free distance is defined as the minimum Hamming distance between any two code sequences. In order to evaluate the union bound for the bit error probability, one needs to calculate the pair-wise error probability  $P_2(d)$ , which is given by [5]

$$P_2(d) = \sum_{k=(d+1)/2}^d \binom{d}{k} p^k (1-p)^{n-k} \quad (2.5)$$

when  $d$  is even and

$$P_2(d) = \frac{1}{2} \binom{d}{d/2} p^{d/2} (1-p)^{d/2} + \sum_{k=d/2+1}^d \binom{d}{k} p^k (1-p)^{n-k} \quad (2.6)$$

when  $d$  is odd, where  $p$  is the channel probability of bit error.

In general, for a specific code rate and constraint length, it is best for the free distance to be as large as possible and  $\beta_d$  to be as small as possible. Most good convolutional codes have been found by computerized searches of large numbers of codes to find those that best meet these criteria.

In this thesis, a rate  $4/5$  convolutional encoder is considered. The weight structures of a  $r = 4/5$  code are displayed in Table 1, where in this case  $K$  denotes the total number of memory elements in the encoder (not the constraint length as before). For the proposed JTIDS alternate encoding scheme, the author considers the case where

$$B_{d_{free}} = 31 \text{ and } d_{free} = 5 \quad (2.7)$$

when  $K = 8$ .

$K$	Generators	$d_{free}$	$B_{d_{free}}$	$B_{d_{free}+1}$	$B_{d_{free}+2}$	$B_{d_{free}+3}$	$B_{d_{free}+4}$
2	5,7,7,5,5	1	1	-	-	-	-
3	15,17,17,15,15	3	14	-	-	-	-
4	23,35,35,23,35	3	11	-	-	-	-
5	53,75,75,75,75	4	40	-	-	-	-
6	133,171,133,133,133	4	12	-	-	-	-
7	247,371,371,247,371	5	168	-	-	-	-
8	561,753,561,753,561	5	31	-	-	-	-

Table 1. Generator Polynomials and Information Weight Structure for Rate  $4/5$  Convolutional Codes (From [5]).

### 3. Symbol-to-bit Conversion

For equiprobable orthogonal signals, all symbol errors are equiprobable and occur with probability [6]

$$\frac{1}{M-1} = \frac{1}{2^k-1}. \quad (2.8)$$

When a symbol error is made, not all the bits within the symbol are necessarily in error.

There are  $\binom{k}{n}$  ways in which  $n$  bits out of  $k$  may be in error. Hence, the average number of bit errors per  $k$ -bit symbol is [6]

$$\sum_{n=1}^k n \binom{k}{n} \frac{1}{2^k-1} = k \frac{2^{k-1}}{2^k-1}, \quad (2.9)$$

and the average bit error probability is the result in Equation (2.9) divided by  $k$ , the number of bits per symbol. Thus, [6]

$$P_b = \frac{2^{k-1}}{2^k-1} P_E \quad (2.10)$$

where  $P_E$  is the probability of symbol error for an  $M$ -ary orthogonal signal set.



#### 4. Reed-Solomon (RS) Codes

RS codes are nonbinary, Bose-Chaudhuri-Hocquenghem (BCH) codes. The encoding is performed on symbols in the appropriate Golay field (GF) instead of on bits. There are  $m$  bits per symbol. An  $(n, k)$  RS encoder takes  $k$  information symbols and generates  $n$  coded symbols. Thus, a code word has a total of  $mn$  coded bits. A  $t$ -error correcting RS code is characterized in symbols as follows [4]:

$$\text{code word length} \quad n = 2m - 1, \quad (2.11)$$

$$\text{parity-check block} \quad n - k = 2t, \quad (2.12)$$

$$\text{minimum Hamming distance} \quad d_{\min} = 2t + 1, \quad (2.13)$$

$$\text{and symbol error-correcting capability} \quad t. \quad (2.14)$$

Reed-Solomon codes achieve the largest possible code minimum distance for any linear code with the same encoder input and output block length. For RS codes, orthogonal signaling with  $M = 2^m$  and hard decision decoding, the probability of symbol and bit error is [7]

$$P_s \approx \frac{1}{n} \sum_{i=t+1}^n i \binom{n}{i} p_s^i (1 - p_s)^{n-i} \quad (2.15)$$

and

$$P_b \approx \frac{n+1}{n^2} \sum_{i=t+1}^n i \binom{n}{i} p_s^i (1 - p_s)^{n-i} \quad (2.16)$$

respectively, where  $p_s$  is the probability of coded, or channel, symbol error,  $t$  is the maximum number of corrected symbol errors per block,  $P_s$  is the probability of information symbol error and  $P_b$  is the probability of information bit error. Finally,  $(n+1)/n$  in Equation (2.16) is the average number of bit errors per symbol error.

## 5. Symbol Interleaver

Interleaving is frequently used in digital communications in order to improve the performance of forward error correction coding. Communication channels are not always memoryless; they can have memory. This means that the errors may be bursty and may not be independent.


An example of a channel with memory is a channel with multipath fading where signals arrive at the receiver over two or more paths of different lengths. In this case, signals generally arrive out of phase with each other, and the cumulative received signal is distorted over the burst period. Interleaving the coded message before transmission and de-interleaving after reception ameliorates this problem, because errors can be handled by the decoder as if they were random errors.

A symbol interleaver is a device that shuffles the symbols from several different code words so that the symbols from a specific code word are not transmitted sequentially. A symbol de-interleaver in the receiver reverses the process, putting the received symbols back into proper order before passing them on to the decoder.

## 6. Cyclic Code-Shift Keying Baseband Symbol Modulation

Cyclic code-shift keying is a modulation technique that utilizes a single  $M$ -chip baseband waveform to represent  $M$  symbols ( $M = 2^k$ ). The  $M$ -chip baseband waveform represents the all-zero symbol, whereas all remaining combinations of  $k$  bits are represented by  $M-1$  cyclical shifts of the initial  $M$ -chip baseband waveform [8].

In JTIDS, each 5-bit symbol is represented by a 32-chip sequence. The 32-CCSK unique chipping sequences are derived by cyclically shifting a starting sequence  $S_0$ , which is 01111100111010010000101011101100, one place to the left at a time in order to obtain all possible combinations of five bits. This procedure is illustrated in Figure 4. In the receiver, determining which 5-bit symbol was received is accomplished by computing the cross-correlation between the received 32-chip sequence and all possible 32-chip sequences. The decision is made by choosing the 5-bit symbol corresponding to the branch with the largest cross-correlation.

 **DIRECTION OF SHIFT**

5-Bit Symbol	32-Chip Sequence (CCSK Code Word)
00000	S0 = 01111100111010010000101011101100
00001	S1 = 11111001110100100001010111011000
00010	S2 = 11110011101001000010101110110001
00011	S3 = 11100111010010000101011101100011
00100	S4 = 11001110100100001010111011000111
•	
•	
•	
11111	S31 = 00111110011101001000010101110110

Figure 4. The 32-chip CCSK Sequences Chosen for JTIDS (From [9]).

An analytical upper bound on the probability of symbol error for the 32-chip CCSK sequence for JTIDS is given by [10]

$$P_s < \sum_{j=0}^{32} \zeta_{UB_j} \binom{32}{j} P_c^j (1 - P_c)^{32-j} \quad (2.17)$$

where  $P_s$  is the probability of demodulator symbol error,  $P_c$  is the probability of chip error at the output of the MSK chip demodulator, and  $\zeta_{UB_j}$  are the conditional probabilities of symbol error for CCSK. The conditional probabilities  $\zeta_{UB_j}$  of symbol error for the 32-CCSK sequence chosen for JTIDS are given in [10] and are reproduced in Table 2.

$N = j$	$\zeta_{UB_j}$
0	0
1	0
$\vdots$	$\vdots$
5	0
6	0
7	0.0015
8	0.0207
9	0.1166
10	0.4187
11	1.0
12	1.0
13	1.0
14	1.0
15	1.0
$\vdots$	$\vdots$
32	1.0

Table 2. Conditional Probabilities of Symbol Error for the CCSK Sequence Chosen by JTIDS (From [10]).

CCSK is a quasi-orthogonal modulation technique. Even though the probability of symbol error of the 32-chip CCSK is inferior to that of 32-orthogonal signaling, the advantage is that only one detector branch is required to recover the original symbol instead of thirty-two individual detector branches.

## 7. Pseudorandom Noise

In order to increase the transmission security of the JTIDS signal, the 32-chip CCSK sequence is scrambled (XOR) with a reference 32-chip PN sequence. The resulting sequence, after being modulated, is transmitted and appears to be a random signal because this signal appears to have the statistical properties of sampled white noise. Nevertheless, it is a deterministic periodic signal that is known only to the transmitter and the receiver and looks like noise to an unauthorized listener.

## 8. Minimum-Shift Keying Chip Modulation

Minimum-shift keying is a continuous binary frequency-shift keying (BFSK) modulation scheme with a minimum frequency spacing of  $1/2T_c$  ( $T_c$  is the chip duration).

This is the minimum separation for two FSK signals to be orthogonal; hence, this signaling technique is named “minimum-shift”. It is spectrally efficient with relatively low spectral sidelobes and can be detected either coherently or noncoherently.

## **B. CHAPTER SUMMARY**

The first part of this chapter was a brief description of the alternative JTIDS encoding scheme. Afterward, a brief analysis of each part of the alternative structure was addressed. In the next chapter, the performance of the alternative JTIDS waveform that uses concatenated coding and soft decision RS decoding with a diversity of two is examined for a channel with only AWGN present.

THIS PAGE INTENTIONALLY LEFT BLANK

### III. PERFORMANCE ANALYSIS OF COHERENT AND NONCOHERENT 32-ARY CCSK WITH CONCATENATED CODING, DIVERSITY AND SD RS DECODING IN AWGN

#### A. INTRODUCTION

In this chapter, the author examines the performance of the alternative JTIDS waveform for both coherent and noncoherent detection. The quality of the performance is measured by analyzing the bit error probability versus  $E_b/N_o$ , which is a version of signal-to-noise ratio (SNR) normalized by bandwidth and bit rate. The  $E_b/N_o$  required to achieve a designated level of performance is one of the most important figures of merit. It is dimensionless and allows a fair comparison of one system with another.

In Figure 5, the receiver of the alternative JTIDS is reproduced for convenience. The probability of bit error  $P_b$  at the output of the convolutional decoder of the alternative JTIDS-type receiver is calculated by evaluating four probabilities consecutively. These probabilities are as follows: probability of channel chip error  $p_c$  at the output of the MSK chip demodulator, the probability of channel symbol error  $p_s$  at the output of the CCSK symbol demodulator, the probability of symbol error  $P_s$  at the output of the RS decoder, and the probability of bit error  $p_b$  at the output of the symbol-to-bit converter.

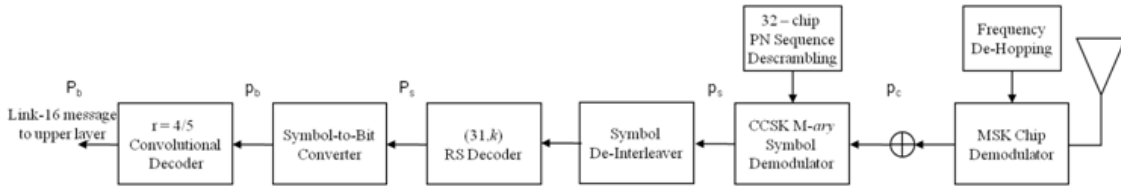


Figure 5. Receiver Structure of a JTIDS-type System Using the Alternative Error Correction Coding Scheme (From [1]).

In this thesis, during the analysis of the compatible JTIDS-type waveform it is assumed that frequency de-hopping is perfectly synchronized with the frequency-hopped waveform and that de-scrambling is perfectly synchronized.

First, coherent demodulation of the JTIDS waveform using the alternative error correction coding scheme in AWGN is considered, and subsequently, the performance for noncoherent demodulation in AWGN is examined.

## **B. COHERENT DEMODULATION OF 32-ARY CCSK WITH DIVERSITY IN AWGN**

When a coherent matched filter or correlator is used to recover the data chips, MSK has the same error performance as BPSK, quadrature phase-shift keying (QPSK), and offset quadrature phase-shift keying (OQPSK) [8]. In this case, the probability of chip error is given by [8]

$$P_c = Q\left(\sqrt{\frac{2E_c}{N_0}}\right) \quad (3.1)$$

where  $E_c$  is the average energy per chip,  $N_0$  is the one-sided power spectral density (PSD) of the AWGN, and  $Q(x)$  is the Gaussian integral with argument  $x$  given by

$$Q(x) = \frac{1}{\sqrt{2\pi}} \int_x^\infty e^{-\frac{y^2}{2}} dy. \quad (3.2)$$

In the transmitter, each 5-bit symbol is modulated with a 32-ary CCSK sequence, and each 5-bit symbol is represented by one of the cyclical shifts of a 32-chip starting sequence. For each symbol in the receiver,

$$E_s = 5E_b = 32E_c \quad (3.3)$$

where  $E_s$  is the average energy per symbol,  $E_b$  is the average energy per bit, and  $E_c$  is the average energy per cyclical shift. Moreover, the forward error correction (FEC) coding that allows the receiver to detect and correct errors implies

$$E_{b_c} = r_{cc} E_b \quad (3.4)$$



where  $r_{cc}$  is the code rate of the concatenated code and  $E_{b_c}$  is the energy per coded bit. Finally, the receiver receives the same symbol twice at different carrier frequencies (frequency diversity of  $L=2$ )

$$\begin{aligned} E_s &= 5E_b = LE_p = 5LE_{b''} \\ E_b &= LE_{b''} \end{aligned} \quad (3.5)$$

where  $E_p$  is the average energy per pulse and  $E_{b''}$  is the average energy per bit per pulse. Equations (3.1) through (3.5) lead to a probability of channel chip error of

$$p_c = Q\left(\sqrt{\frac{10r_{cc}LE_{b''}}{32N_0}}\right). \quad (3.6)$$

The demodulation of a CCSK symbol is independent of the FEC coding. The analytic expression for the probability of channel symbol error of a JTIDS-type waveform is obtained from Equation (2.17) by replacing  $P_s$  and  $P_c$  with  $p_s$  and  $p_c$ , respectively. That is,

$$p_s = \sum_{j=0}^{32} \zeta_{UB_j} \binom{32}{j} p_c^j (1-p_c)^{32-j} \quad (3.7)$$

where  $\zeta_{UB_j}$  are the conditional probabilities of channel symbol error given that  $j$  chip errors have occurred in the received, de-scrambled 32-chip sequence, and  $p_c$  is given by Equation (3.6).

In order to achieve a large error-correcting capability with a long block length, the alternative JTIDS uses a concatenated code. That is, two shorter codes in series are employed. From the brief description in the previous chapter, the first code is the outer code  $(n_o, k_o)$  with code rate  $r_o = n_o/k_o$  and is a rate  $4/5$  convolutional code, the second code is the inner code  $(n_i, k_i)$  with code rate  $r_i = n_i/k_i$  and is a RS code, and the overall

code rate of the waveform is  $r_{cc} = r_i r_o$ . The error probability of the concatenated codes is evaluated by first calculating the bit error probability of the inner code and then the error probability of the outer code.

As discussed in Chapter II, the encoding/decoding for RS codes is performed on symbols instead of bits. If a memoryless channel is assumed, the probability of symbol error is given by Equation (2.15)

$$P_s \approx \frac{1}{n} \sum_{i=t_{HD}+1}^n i \binom{n}{i} p_s^i (1-p_s)^{n-i} \quad (3.8)$$

where  $p_s$  is the probability of channel symbol error in Equation (3.7). Since soft decision (SD) RS decoding is assumed, the error correcting capability  $t$  is assumed to be

$$t_{SD} = t_{HD} + 1 \equiv t \quad (3.9)$$

where  $t_{SD}$  is the error correcting capability for SD RS decoding and  $t_{HD}$  is the error correcting capability for hard decision (HD) RS decoding. The probability of information bit error  $P_b$  of a JTIDS-type waveform is given by Equation (2.16), repeated below for convenience,

$$P_b \approx \frac{n+1}{n^2} \sum_{i=t+1}^n i \binom{n}{i} p_s^i (1-p_s)^{n-i} \quad (3.10)$$

and provides the probability of bit error at the output of the symbol-to-bit converter. The probability of bit error of convolutional codes was presented in the previous chapter and is reproduced here for convenience. The pairwise error probability when  $d$  is even according to Equation (2.5) is

$$P_2(d) = \sum_{k=(d+1)/2}^d \binom{d}{k} P_b^k (1-P_b)^{n-k} \quad (3.11)$$

where  $P_b$  the probability of bit error at the output of the symbol-to-bit converter in Equation (3.10) and  $d$  is the free distance of the convolutional code. Finally, the bit error probability at the output of the rate  $4/5$  convolutional decoder is obtained from Equation

(2.4) by taking into consideration the values of  $B_{d_{free}}$  and  $d_{free}$  in Equation (2.7) and the pairwise error probability  $P_2(d)$  in Equation (3.11). The bounded bit error probability in Equation (2.4) is reproduced below for convenience,

$$P_b \leq \frac{1}{k} \sum_{d=d_{free}}^{\infty} \beta_d P_2(d) \quad (3.12)$$

where the first term in the sum dominates for reasonable values of  $P_2(d)$ . Equation (3.12) identifies the probability of error bounds used for coherent demodulation of the alternate JTIDS waveform in subsequent analysis.

### C. NONCOHERENT DEMODULATION OF 32-ARY CCSK WITH DIVERSITY IN AWGN

Noncoherent MSK can be demodulated using either a matched filter envelope detector or a quadrature correlator-square detector. When either of these equivalent detectors is applied, their performance is identical to noncoherent BFSK [11]. The bit error probability of noncoherent BFSK is given by [8]

$$P_b = \frac{1}{2} e^{-E_b/2N_o} \quad (3.13)$$

An alternative way of noncoherently detecting an MSK signal is by using a slope detector instead of matched filters or correlators. This method takes advantage of the fact that BFSK and MSK are digital FM signals, which means that the modulating information signals are digital. Therefore, both BFSK and MSK can be demodulated by a slope detector used for FM demodulation [11].

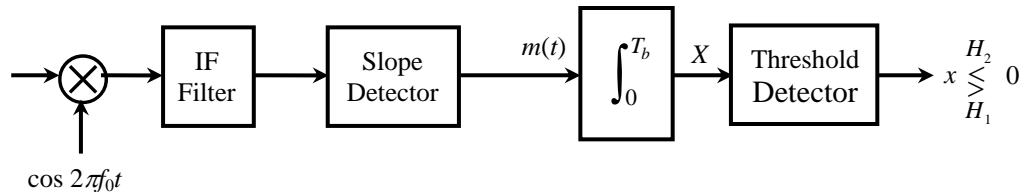


Figure 6. Continuous-phase BFSK or MSK Demodulator with Slope Detector. The Signal  $m(t)$  is the Antipodal Information Signal (From [11]).

A demodulator that uses a slope detector is illustrated in Figure 6. The IF filter is used in order to reject the out-of-band noise and restrict the frequency band of the signal. Its bandwidth is sufficiently broad so that the distortion of the modulated signal can be ignored. The demodulation is done by the slope detector, and the output is proportional to the angle of the input signal, assuming that the slope detector has an ideal characteristic. The integrator, with integration time  $T_b$ , approximates a post-detection low pass filter. The polarity of the samples at the output of the threshold detector determines the transmitted bits. The bit error probability is given by [11]

$$P_b = e^{-E_b/N_0}. \quad (3.14)$$

Demodulation with a slope detector is superior to noncoherent demodulation with either a matched filter envelope detector or a quadrature correlator-square detector. Furthermore, its performance is approximately that of an optimum noncoherent differential phase-shift keying (DPSK) demodulator.

When a diversity of two is employed, where each symbol is transmitted twice on two different carrier frequencies, the probability of error for binary DPSK is obtained from [6]

$$P = \frac{1}{2^{2L-1}} e^{-\frac{LE_c}{N_o}} \sum_{n=0}^{L-1} c_n \left( \frac{LE_c}{N_o} \right)^n \quad (3.15)$$

where

$$c_n = \frac{1}{n!} \sum_{k=0}^{L-1-n} \binom{2L-1}{k}. \quad (3.16)$$

The probability of channel chip error for noncoherent demodulation is obtained from Equations (3.15) and (3.16) by taking into consideration Equations (3.1) through (3.5) to get

$$P_c = \frac{1}{2^{2L-1}} e^{-\left( L \frac{5Lr_{cc}}{32} \frac{E_b''}{N_o} \right)} \sum_{n=0}^{L-1} c_n \left( L \frac{5Lr_{cc}}{32} \frac{E_b''}{N_o} \right)^n. \quad (3.17)$$

The probability of channel symbol error  $p_s$  at the output of the CCSK symbol demodulator, the probability of symbol error  $P_s$  at the output of the RS decoder, the probability of bit error  $p_b$  at the output of the symbol-to-bit converter, and the probability of bit error  $P_b$  at the output of convolutional decoder are evaluated in the same way as for coherent demodulation using Equations (3.7) through (3.12).

#### **D. PERFORMANCE ANALYSIS OF COHERENT DEMODULATION OF 32-ARY CCSK WITH DIVERSITY IN AWGN**

Evaluating the overall probability of error of the system at the output of the convolutional decoder by applying Equations (3.1) through (3.12), the author tries to optimize the performance of the alternative waveform by changing the value of  $k$  and, therefore, the code rate of the waveform. Specifically, substituting the code rates of the rate  $4/5$  outer convolutional encoder and the inner RS  $(31, k)$  encoder into Equation (2.1), the code rate of the waveform is given by

$$r_{cc} = \frac{4}{5} \frac{k}{31}. \quad (3.18)$$

The performance of the alternative waveform for various  $k$  values and the performance of the existing JTIDS waveform are shown in Figure 7. The quality of the performance is measured by analyzing the bit error probability versus  $E_b/N_o$ , where a satisfactory probability of error for reliable communications is considered to be  $P_b = 10^{-5}$ . The ratio  $E_b/N_o$  is the average energy per bit per pulse-to-noise power spectral density. It is obvious that in all cases the alternative compatible JTIDS-type waveform outperforms the existing waveform. Moreover, the best performances are achieved for RS  $(31, 23)$  and RS  $(31, 25)$  inner codes, where  $E_b/N_o = 2.6$  dB is required. For the same probability of error, the existing JTIDS waveform requires  $E_b/N_o = 4.0$  dB. Thus, there is a gain of about 1.4 dB and an increase in system throughput of approximately 23.0% and 33.0%, respectively.

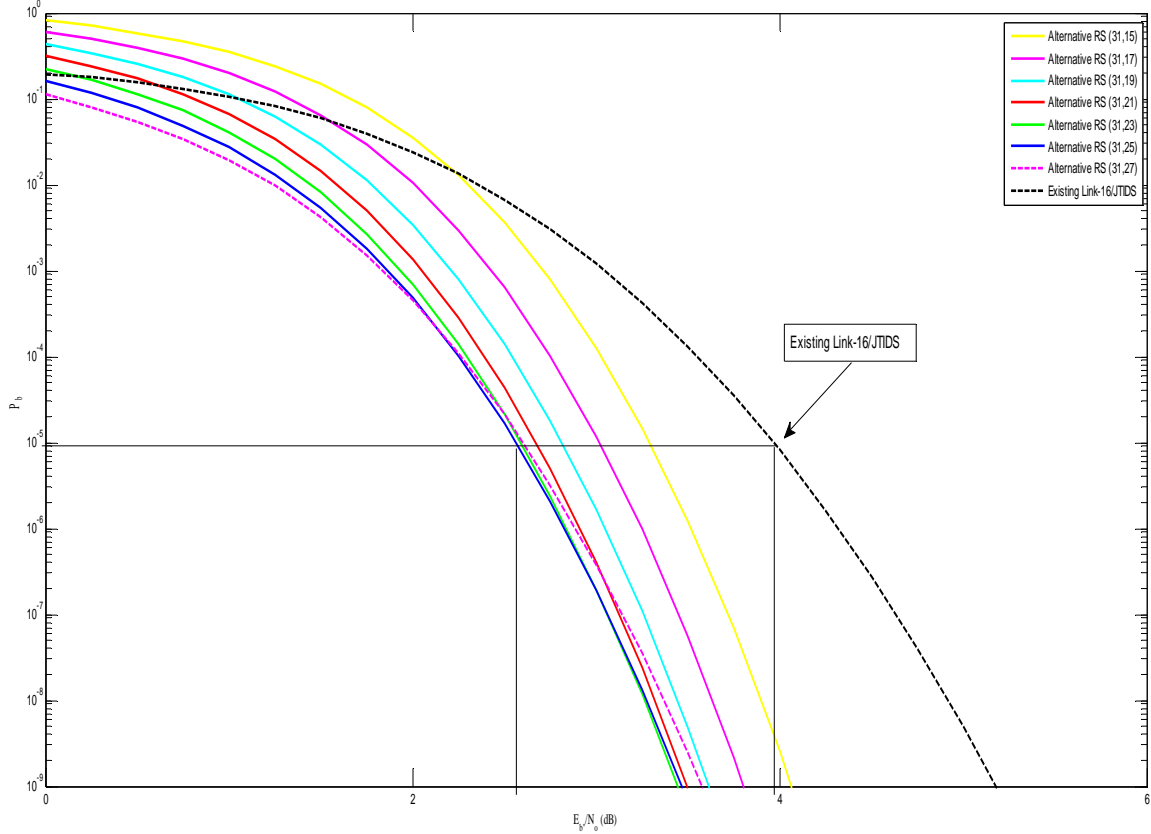


Figure 7. Performance of 32-ary CCSK Using the Alternative Error Correction Coding Scheme in AWGN for Coherent Demodulation, a Diversity of Two, and Soft Decision RS Decoding.

#### E. PERFORMANCE ANALYSIS OF NONCOHERENT DEMODULATION OF 32-ARY CCSK WITH DIVERSITY IN AWGN

The overall probability of error at the output of the convolutional decoder for noncoherent demodulation is obtained in the same way as for the coherent case but using Equation (3.17) instead of Equation (3.6) for the evaluation of the probability of chip error. Once again, the author tries to optimize the performance of the alternative waveform by changing the value of  $k$  and, therefore, the code rate of the waveform.

The performance of the alternative waveform for various  $k$  values and the performance of the existing JTIDS are shown in Figure 8. The quality of the performance is evaluated by analyzing the bit error probability versus  $E_b/N_o$ . It can be seen that in all cases the alternative compatible JTIDS-type waveform outperforms the original

waveform. Moreover, the best performances are achieved for the higher code rate waveforms and, specifically, for RS (31, 27) and RS (31, 29), which require  $E_b/N_o = 4.6$  dB. For the same probability of error, the existing JTIDS requires  $E_b/N_o = 6.0$  dB. Thus, there is again a gain of about 1.4 dB and an increase in system throughput of approximately 44.0% and 55.0%, respectively.

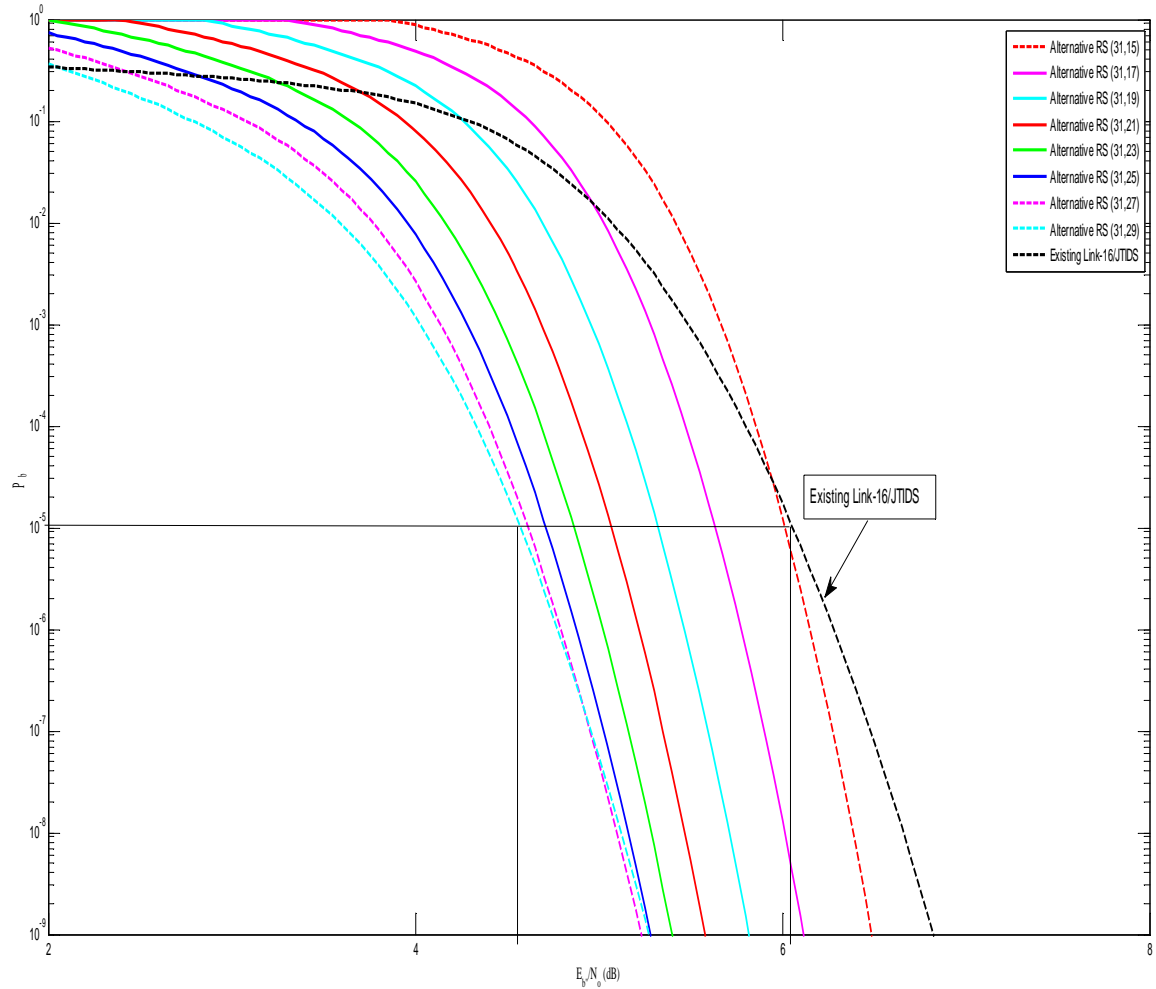


Figure 8. Performance of 32-ary CCSK Using the Alternative Error Correction Coding Scheme in AWGN for Noncoherent Demodulation, a Diversity of Two, and Soft Decision RS Decoding.

## F. COMPARISON OF THE PERFORMANCES OF THE ALTERNATIVE WAVEFORM OBTAINED WITH COHERENT AND NONCOHERENT DEMODULATION OF 32-ARY CCSK WITH DIVERSITY IN AWGN

For purposes of comparison, the performances obtained for both the coherent and noncoherent demodulation of the alternative waveform with RS (31, 23) and RS (31, 25) are plotted in Figure 9. In the case of coherent demodulation for  $P_b = 10^{-5}$ , the alternative waveform for RS (31, 23) and RS (31, 25) requires  $E_b/N_o = 2.6$  dB, but for noncoherent demodulation,  $E_b/N_o = 4.9$  dB and  $E_b/N_o = 4.7$  dB are required, respectively. Hence, there is a gain of 2.3 dB or 2.1 dB, respectively, with coherent as opposed to noncoherent demodulation.

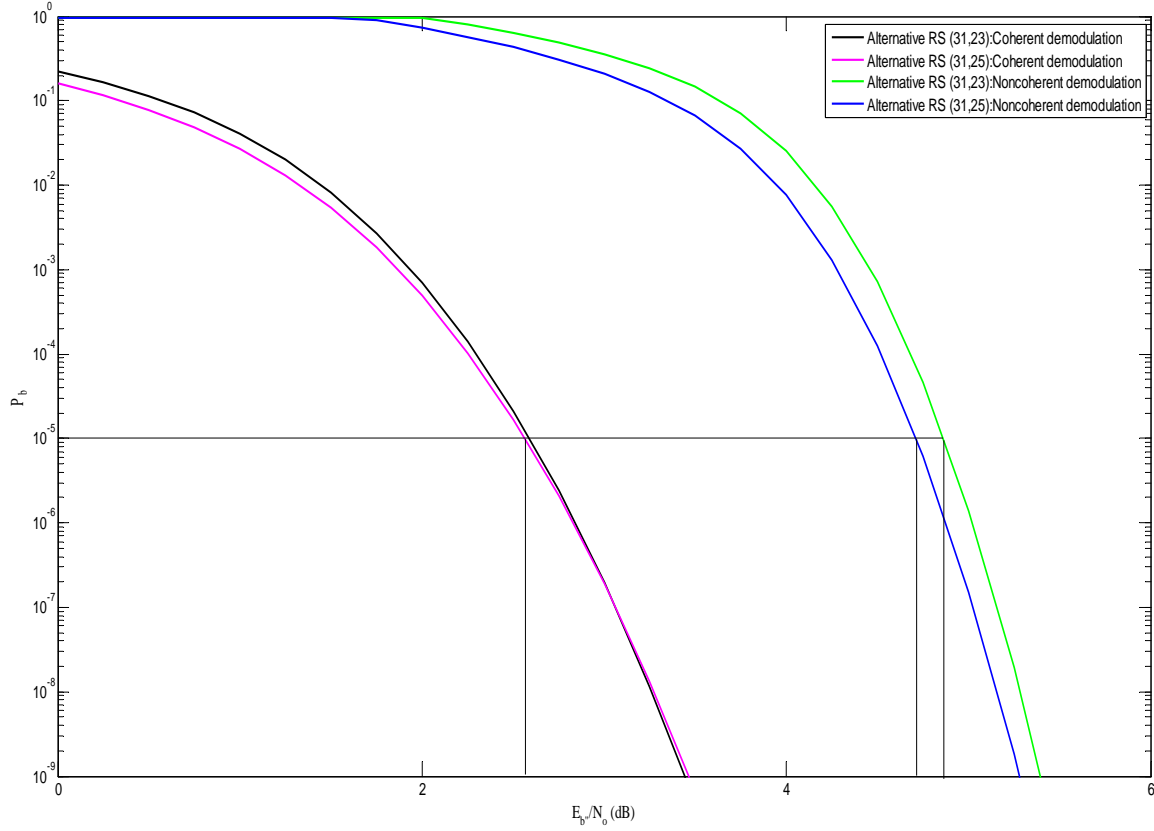


Figure 9. Performance of 32-ary CCSK Using the Alternative Error Correction Coding Scheme in AWGN for RS (31, 23) and RS (31, 25) Inner Codes, Coherent and Noncoherent Demodulation, a Diversity of Two, and Soft Decision RS Decoding.



### G. COMPARISON OF THE PERFORMANCES OF THE ALTERNATIVE WAVEFORM OBTAINED WITH HARD DECISION AND SOFT DECISION RS DECODING OF 32-ARY CCSK WITH DIVERSITY IN AWGN

This section examines the benefits of using soft decision RS decoding instead of hard decision RS decoding for both coherent and noncoherent case. In Figures 10 and 11, the results for RS (31, 23) and RS (31, 25) inner codes for coherent and noncoherent detection, respectively, are plotted. It is obvious that the advantages are negligible since the gain is less than 1.0 dB (approximately 0.5 dB) in both cases. Therefore, the price of having a simpler receiver with hard decision decoding is not high and is preferred.

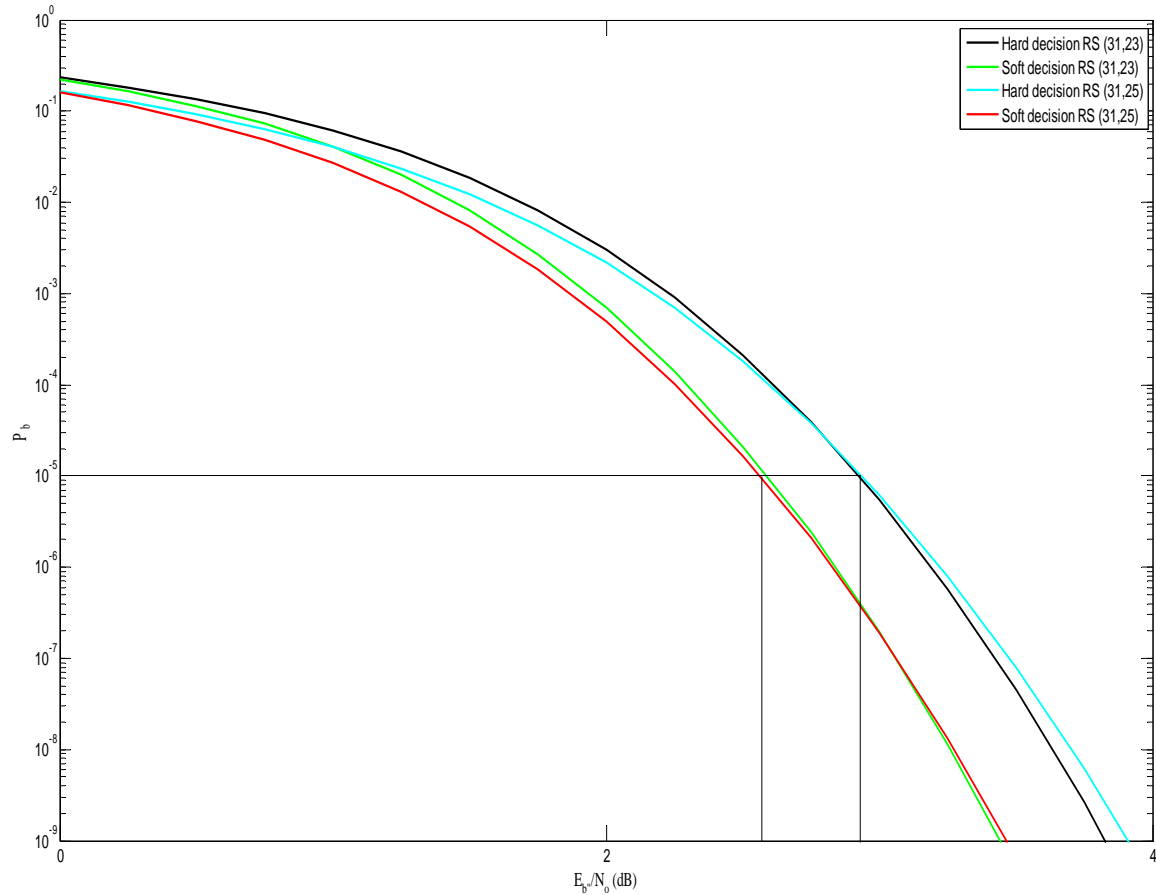


Figure 10. Performance of 32-ary CCSK Using the Alternative Error Correction Coding Scheme in AWGN for RS (31, 23) and RS (31, 25) Inner Codes, a Diversity of Two, Hard and Soft Decision RS Decoding, and Coherent Demodulation.

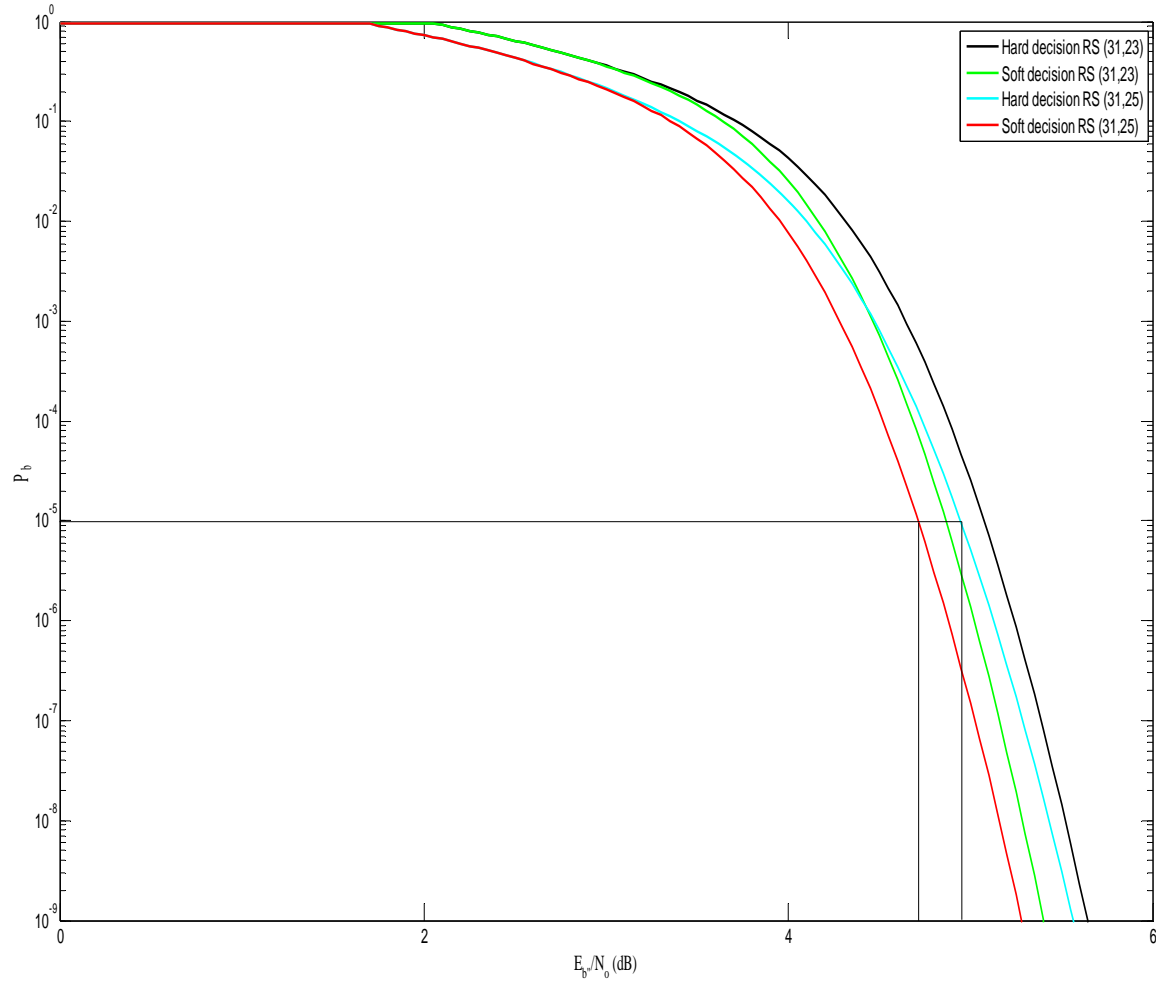


Figure 11. Performance of 32-ary CCSK Using the Alternative Error Correction Coding Scheme in AWGN for RS (31, 23) and RS (31, 25) Inner Codes, a Diversity of Two, Hard and Soft Decision RS Decoding, and Noncoherent Demodulation.

## H. CHAPTER SUMMARY

In this chapter, the effects of AWGN on the performance of the alternative waveform were examined. The author concluded that the performance of the existing waveform was inferior compared to the alternative waveform for both coherent and noncoherent demodulation. The benefits of using soft decision RS decoding in the receiver were trivial.

In Chapter IV, a different environment is considered where both AWGN and PNI are present. In such hostile conditions, noise-normalization is introduced in order to neutralize the effects of pulse interference. In Chapter IV, the alternative error correction coding scheme and the existing JTIDS waveform are examined for coherent demodulation only. Noncoherent detection performance for the alternative error correction coding scheme relative to the existing JTIDS is considered in Chapter V.

THIS PAGE INTENTIONALLY LEFT BLANK

## **IV. PERFORMANCE ANALYSIS OF COHERENT 32-ARY CCSK WITH CONCATENATED CODING, DIVERSITY, SD RS DECODING AND NOISE-NORMALIZATION IN AWGN, AND PULSE-NOISE INTERFERENCE**

### **A. COHERENT DEMODULATION OF 32-ARY CCSK WITH DIVERSITY AND NOISE-NORMALIZATION IN AWGN AND PNI**

As discussed in the previous chapter, MSK can be viewed as a special case of OQPSK with sinusoidal pulse shaping. When a matched filter or correlator is used to recover the data chip, MSK has the same error performance as BPSK, QPSK, and OQPSK [8].

Suppose the receiver is attacked by a band-limited, noise-like signal that is turned on and off systematically. Let  $\rho$  be the fraction of time the jammer is turned on, and assume that the jammer does not turn on or off during a bit interval. Noise-normalization is used at the receiver in order to neutralize the effects of partial-band or pulse-noise interference and de-emphasize jammed hops with respect to unjammed hops.

Next, consider the fast frequency-hopping (FFH)/BPSK noise-normalized receiver with diversity  $L=2$  in Figure 12. After the voltage multiplier, which is commonly referred to as a mixer, and assuming perfect de-hopping, an integrator circuit integrates the signal over the duration of one hop (i.e.,  $T_h$ ). The integrator acts as a low pass filter and provides optimum detection in AWGN. The integrator output is normalized by the measured noise power  $\sigma_k$  of hop  $\kappa$ . The decision variable  $z$  of the receiver is formed by the analog summation of the noise-normalized integrator output  $z_\kappa$ . The signal output is routed to a comparator where the final decision for the bit takes place. The influence of jammed hops on the overall decision statistics is minimized due to noise-normalization.

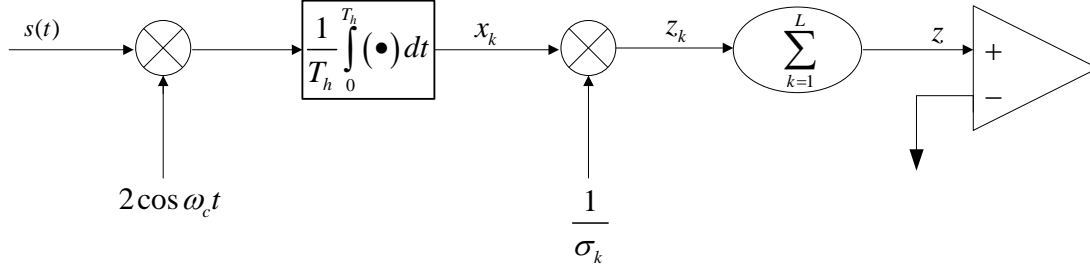


Figure 12. FFH/BPSK Noise-normalized Receiver.

If  $\rho$  is the fraction of the spread spectrum bandwidth that is jammed, then  $\rho$  is the probability that a hop is jammed, and  $1-\rho$  is the probability that narrowband interference is not present. The PSD of the partial-band noise interference is  $N_I/2\rho$ . In addition to the narrowband interference, the signal also suffers from AWGN with PSD  $N_o/2$ . Thus, the total noise PSD is given by

$$N_T = N_o + \frac{N_I}{\rho}. \quad (4.1)$$

If the equivalent noise bandwidth of the receiver is  $B$  Hz, then for each jammed (subscript  $j$ ) and unjammed (subscript  $o$ ) hop, respectively, the noise power is given by

$$\sigma_\kappa^2 = \sigma_{\kappa_j}^2 = \left( N_o + \frac{N_I}{\rho} \right) B = \frac{N_o + \frac{N_I}{\rho}}{T_h} \quad (4.2)$$

and

$$\sigma_\kappa^2 = \sigma_{\kappa_o}^2 = N_o B = \frac{N_o}{T_h}. \quad (4.3)$$

For a FFH/BPSK receiver with a fixed bit rate and diversity  $L$ , the hop rate is given by

$$R_h = LR_b \Rightarrow T_h = \frac{T_b}{L} \quad (4.4)$$

and the average energy per bit  $E_b$  is related to the average energy per hop  $E_h$  by

$$E_b = LE_h \Rightarrow E_h = \frac{E_b}{L}. \quad (4.5)$$

The random variable  $x_k$  at the integrator output is a Gaussian random variable with probability density function

$$f_{x_k}(x_k) = \frac{1}{\sqrt{2\pi}\sigma_k} \exp\left(-\frac{(x_k - \bar{x}_k)^2}{2\sigma_k^2}\right) \quad (4.6)$$

with  $\bar{x}_k = \sqrt{2}A_c$  ( $A_c$  is the digital signaling waveshape amplitude). The noise-normalized integrator output  $z_k$  is given by

$$z_k = \frac{x_k}{\sigma_k}. \quad (4.7)$$

The probability density function of the noise-normalized variable  $z_k$  prior to diversity combining is

$$\begin{aligned} f_{z_k}(z_k) &= \left| \frac{dx_k}{dz_k} \right| f_{x_k}(\sigma_k z_k) \\ &= \sigma_k \frac{1}{\sqrt{2\pi}\sigma_k} \exp\left(-\frac{(\sigma_k z_k - \sqrt{2}A_c)^2}{2\sigma_k^2}\right) \\ &= \frac{1}{\sqrt{2\pi}} \exp\left(-\frac{\sigma_k^2 \left(z_k - \frac{\sqrt{2}A_c}{\sigma_k}\right)^2}{2\sigma_k^2}\right) \\ f_{z_k}(z_k) &= \frac{1}{\sqrt{2\pi}} \exp\left(-\frac{\left(z_k - \frac{\sqrt{2}A_c}{\sigma_k}\right)^2}{2}\right). \end{aligned} \quad (4.8)$$

From Equation (4.8), it can be inferred that  $\sigma_{z_k}^2 = 1$  and  $\bar{z}_k = \frac{\sqrt{2}A_c}{\sigma_k}$ .

The random variable  $z$  results from the summation of the Gaussian random variables  $z_k$ . Therefore, it is also a Gaussian random variable with its mean and variance given by the following equations:

$$\bar{z} = \sum_{k=1}^{L=2} \bar{z}_k \quad (4.9)$$

and

$$\sigma_z^2 = \sum_{k=1}^{L=2} \sigma_{z_k}^2 = 1 + 1 = 2. \quad (4.10)$$

Consequently, when none of the hops is jammed, the mean of the random variable  $z$  is obtained from Equation (4.9) and Equation (4.4) with  $L = 2$  to get

$$\bar{z} = \frac{2\sqrt{2}A_c}{\sigma_{k_o}} = \frac{2\sqrt{2}A_c}{\sqrt{\frac{N_o}{T_h}}} = \frac{2\sqrt{2}A_c}{\sqrt{\frac{N_o}{T_b/2}}} = \frac{2A_c\sqrt{T_b}}{\sqrt{N_o}}. \quad (4.11)$$

Similarly, if one of the hops is jammed, the mean of the random variable  $z$  is

$$\begin{aligned} \bar{z} &= \frac{\sqrt{2A_c}}{\sigma_{k_j}} + \frac{\sqrt{2A_c}}{\sigma_{k_o}} = \sqrt{2A_c} \left[ \frac{(T_h)^{\frac{1}{2}}}{\sqrt{N_o + \frac{N_I}{p}}} + \frac{(T_h)^{\frac{1}{2}}}{\sqrt{N_o}} \right] \\ &= \sqrt{2A_c} \left[ \frac{\left(\frac{T_b}{2}\right)^{\frac{1}{2}}}{\sqrt{N_o + \frac{N_I}{p}}} + \frac{\left(\frac{T_b}{2}\right)^{\frac{1}{2}}}{\sqrt{N_o}} \right] \\ \bar{z} &= A_c \left[ \frac{\sqrt{T_b}}{\sqrt{N_o + \frac{N_I}{p}}} + \frac{\sqrt{T_b}}{\sqrt{N_o}} \right]. \end{aligned} \quad (4.12)$$

Finally, if both hops are jammed, the mean of the random variable  $z$  is

$$\begin{aligned} \bar{z} &= \frac{2\sqrt{2}A_c}{\sigma_{k_j}} = \frac{2\sqrt{2}A_c}{\sqrt{\frac{N_o + \frac{N_I}{\rho}}{T_h}}} = \frac{2\sqrt{2}A_c}{\sqrt{\frac{N_o + \frac{N_I}{\rho}}{T_b/2}}} \\ \bar{z} &= \frac{2A_c\sqrt{T_b}}{\sqrt{N_o + \frac{N_I}{\rho}}}. \end{aligned} \quad (4.13)$$



The figure of merit for a digital receiver is the probability of bit error. For the receiver in Figure 12, this probability is given by [12]

$$p_b = Q\left(\frac{\bar{z}}{\sigma_k}\right) = Q\left(\sqrt{\frac{\bar{z}^2}{\sigma_k^2}}\right) = Q\left(\sqrt{\frac{\bar{z}^2}{2}}\right). \quad (4.14)$$

Therefore, the probability of error when none of the hops are jammed ( $p_{b0}$ ), when one out of two hops is jammed ( $p_{b1}$ ), and when both hops are jammed ( $p_{b2}$ ) are obtained by using Equations (4.11) through (4.13) in Equation (4.14) to get

$$\begin{aligned} p_{b0} &= Q\left(\sqrt{\frac{\bar{z}^2}{2}}\right) = Q\left(\sqrt{\frac{2A_c^2 T_b}{N_o}}\right), \\ p_{b0} &= Q\left(\sqrt{\frac{2E_b}{N_o}}\right), \end{aligned} \quad (4.15)$$

$$\begin{aligned} p_{b1} &= Q\left(\sqrt{\frac{\bar{z}^2}{2}}\right) = Q\left(\sqrt{\frac{A_c^2 T_b \left[\frac{1}{\sqrt{N_o + N_I/\rho}} + \frac{1}{\sqrt{N_o}}\right]^2}{2}}\right), \\ p_{b1} &= Q\left(\sqrt{\frac{1}{2} \frac{1}{\sqrt{(E_b/N_o)^{-1} + (E_b/N_I)^{-1}/\rho}} + \sqrt{E_b/N_o}}\right), \end{aligned} \quad (4.16)$$

and

$$\begin{aligned} p_{b2} &= Q\left(\sqrt{\frac{\bar{z}^2}{2}}\right) = Q\left(\sqrt{\frac{2A_c^2 T_b}{N_o + N_I/\rho}}\right), \\ p_{b2} &= Q\left(\sqrt{\frac{2}{(E_b/N_o)^{-1} + (E_b/N_I)^{-1}/\rho}}\right). \end{aligned} \quad (4.17)$$

In JTIDS, at the receiver, an MSK coherent chip demodulator is used to recover the original scrambled 32-sequence on a chip-by-chip basis. Therefore,  $T_b$  must be replaced by  $T_c$  and  $E_b$  by  $E_c$  in Equations (4.15), (4.16) and (4.17) to get

$$p_{c0} = Q\left(\sqrt{\frac{2E_c}{N_o}}\right), \quad (4.18)$$

$$p_{c1} = Q\left(\frac{1}{\sqrt{2}} \frac{1}{\sqrt{(E_c/N_o)^{-1} + (E_c/N_I)^{-1} \frac{1}{\rho}}} + \sqrt{\frac{E_c}{N_o}}\right), \quad (4.19)$$

and

$$p_{c2} = Q\left(\sqrt{\frac{2}{(E_c/N_o)^{-1} + (E_c/N_I)^{-1} \frac{1}{\rho}}}\right). \quad (4.20)$$

The relationship of average energy per chip  $E_c$  to the average energy per bit  $E_b$  is obtained from Equations (3.3) through (3.5) and is given by

$$E_c = \frac{5r_{cc}E_b}{32}. \quad (4.21)$$

Finally, Equations (4.18), (4.19) and (4.20) become

$$p_{c0} = Q\left(\sqrt{\frac{10r_{cc}}{32} \frac{E_b}{N_o}}\right), \quad (4.22)$$

$$p_{c1} = Q\left(\sqrt{\frac{5r_{cc}}{64}} \frac{1}{\sqrt{(E_b/N_o)^{-1} + (E_b/N_I)^{-1} \frac{1}{\rho}}} + \sqrt{\frac{E_b}{N_o}}\right), \quad (4.23)$$

and

$$p_{c2} = Q\left(\sqrt{\frac{10r_{cc}}{32} \frac{1}{(E_b/N_o)^{-1} + (E_b/N_I)^{-1} \frac{1}{\rho}}}\right). \quad (4.24)$$

After the 32-chip sequence is de-scrambled, the CCSK symbol demodulator detects the 5-bit symbol. The probability of symbol error given that  $i$  hops are jammed was given in Equation (3.7) and is reproduced below for convenience:

$$p_{s(i)} = \sum_{j=0}^{32} \zeta_{UB_j} \binom{32}{j} p_{c(i)}^j (1 - p_{c(i)})^{32-j}. \quad (4.25)$$

The total probability of symbol error of a FFH system with a diversity of  $L = 2$  is

$$\begin{aligned} p_s &= \sum_{i=0}^L \binom{L}{i} \rho^i (1 - \rho)^{L-i} \quad p_{s(i)} = \sum_{i=0}^{L=2} \binom{L}{i} \rho^i (1 - \rho)^{L-i} \quad p_{s(i)} \\ &= (1 - \rho)^2 p_{s0} + 2\rho(1 - \rho) p_{s1} + \rho^2 p_{s2}. \end{aligned} \quad (4.26)$$

The probability of symbol error  $P_s$  at the output of the RS decoder, the probability of bit error  $p_b$  at the output of the symbol-to-bit converter, and the probability of bit error  $P_b$  at the output of the convolutional decoder are evaluated in the same way as in Chapter III by applying Equations (3.8) through (3.12).

## B. PERFORMANCE ANALYSIS OF COHERENT DEMODULATION OF 32-ARY CCSK WITH DIVERSITY AND NOISE-NORMALIZATION IN AWGN AND PNI

In this paragraph, the performance of the alternative waveform as well as that of the existing JTIDS waveform for different values of  $\rho$  is examined. The code rate  $r_{cc}$  of the alternative waveform is changed to optimize performance. In Figure 13, it is observed that the PNI, instead of degrading the performance of the alternative waveform relative to barrage noise interference, results in superior performance. This is the result of the noise-normalized receiver, which de-emphasizes the jammed hops with respect to unjammed hops and thus minimizes the influence of jammed hops on the overall decision statistics. Furthermore, in Figure 13 it is observed that the alternative waveform converges to a specific value of error probability, at which point changes in  $\rho$  do not affect the performance of the system. This value of course is different for different levels of  $E_b/N_0$ .

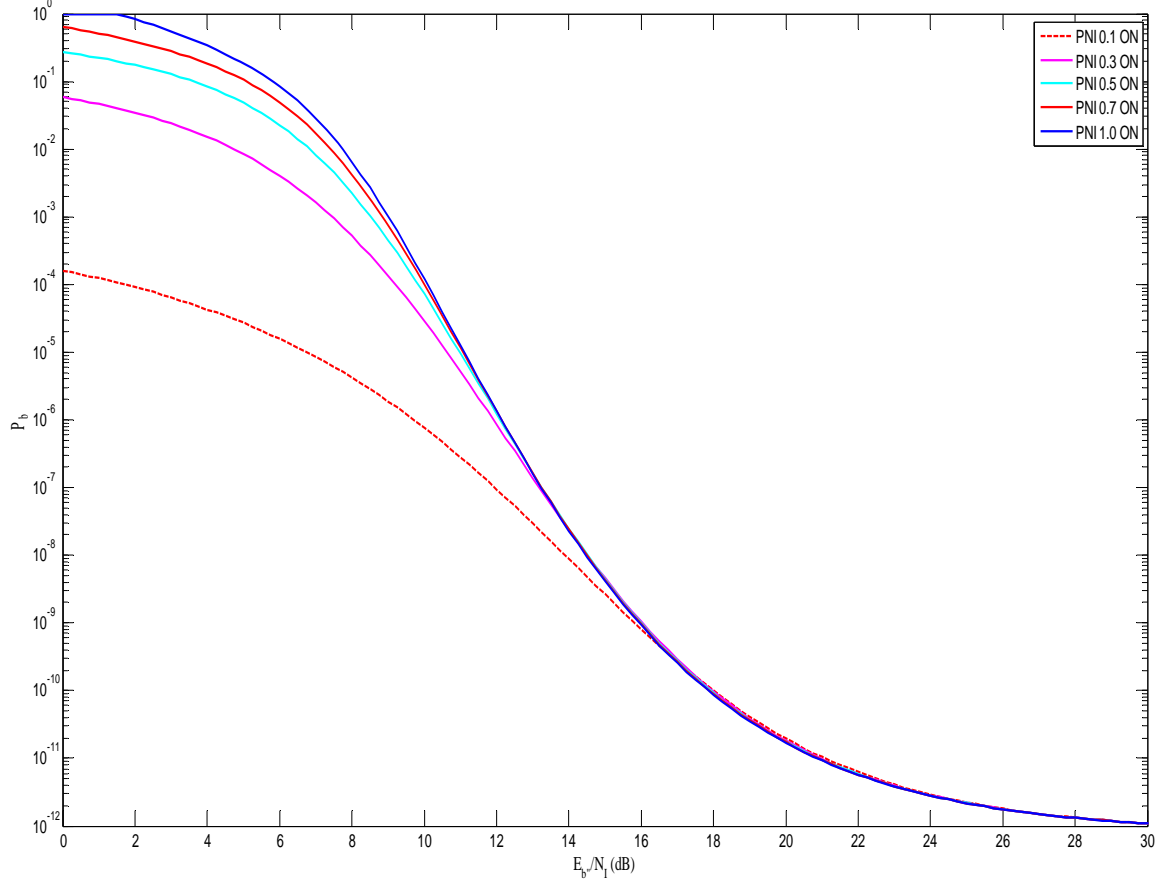


Figure 13. Performance of 32-ary CCSK Using the Alternative Error Correction Coding Scheme for a RS (31, 25) Inner Code in Both AWGN and PNI for  $\rho = 0.1$ ,  $\rho = 0.3$ ,  $\rho = 0.5$ ,  $\rho = 0.7$  and  $\rho = 1.0$ , Coherent Demodulation, Soft Decision RS Decoding, a Diversity of Two, Noise-normalization, and  $E_b/N_0 = 7.0$  dB.

In Figure 14, the alternative waveform with inner RS (31, 25) code is plotted. The fraction of time when the PNI is on remains constant and equal to  $\rho = 0.5$ . In this plot, the bit energy-to-noise power spectral density ( $E_b/N_0$ ) is the variable that changes. When  $E_b/N_0$  is near 6.0 dB, very small changes cause a huge difference in the system's performance; for example, when  $E_b/N_0$  increases from 6.0 dB to 6.5 dB, the system's performance is improved about 1.1 dB. On the other hand, when such an increase occurs and  $E_b/N_0$  is near 15.0 dB the system's performance is not affected at all. Therefore, the system's sensitivity depends significantly on the changes of  $E_b/N_0$  when the signal power relative to noise is low.

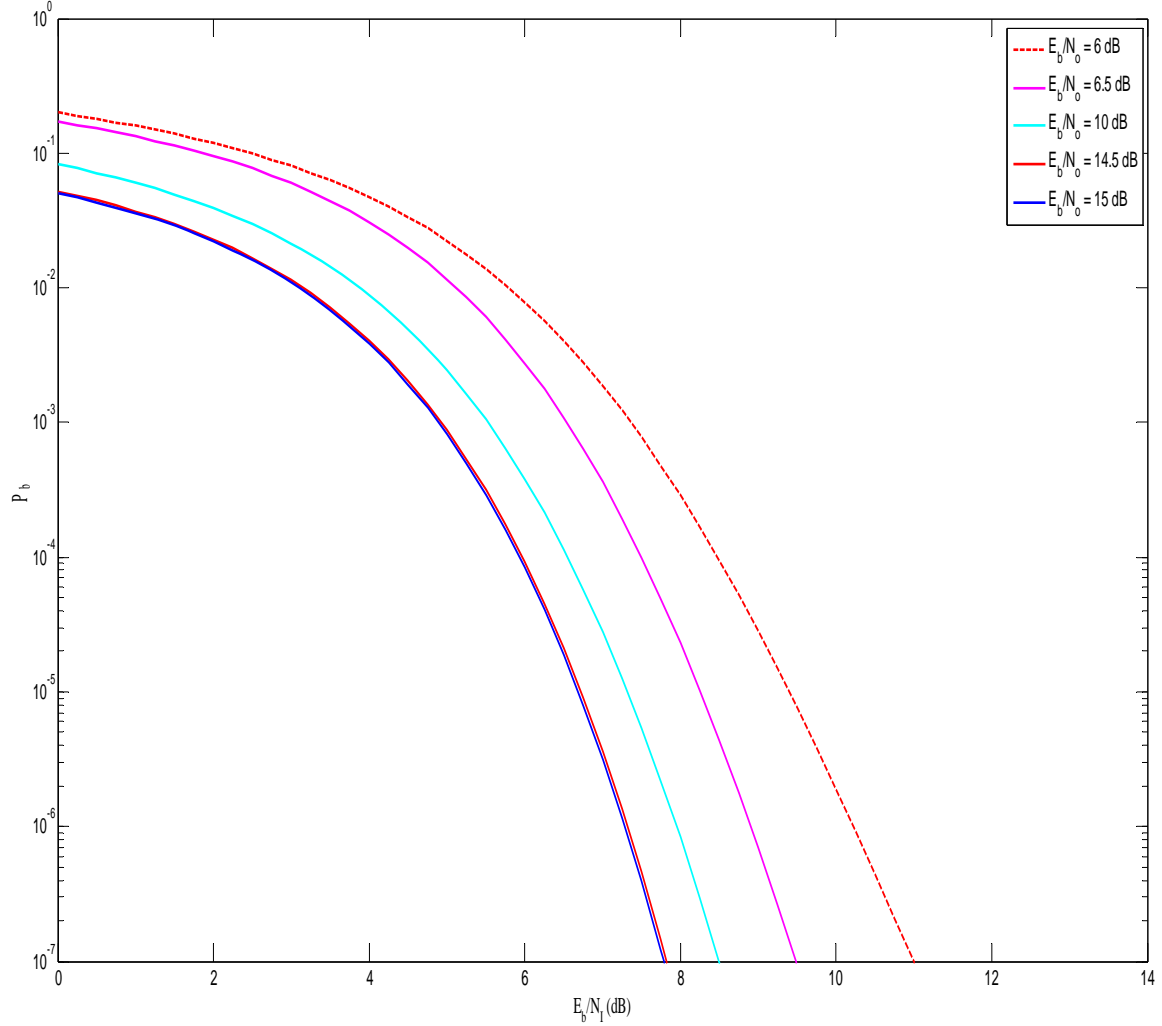


Figure 14. Performance of 32-ary CCSK Using the Alternative Error Correction Coding Scheme for a RS (31, 25) Inner Code in Both AWGN and PNI for  $\rho = 0.5$ , Coherent Demodulation, Soft Decision RS Decoding, a Diversity of Two, and Noise-normalization when  $E_b/N_0 = 6.0$  dB,  $E_b/N_0 = 6.5$  dB,  $E_b/N_0 = 10.0$  dB,  $E_b/N_0 = 14.5$  dB,  $E_b/N_0 = 15.0$  dB.

The performance results of the noise-normalized alternative waveform for various  $k$  of the inner RS (31,  $k$ ) code and of the noise-normalized actual JTIDS waveform are summarized in Tables 3, 4 and 5. The quality of the performance is measured by analyzing the bit error probability versus  $E_b/N_0$ , where the probability of error is taken to be  $P_b = 10^{-5}$ .

From Table 3, which is based on Figures 15 through 19, it can be seen that the original JTIDS waveform and the alternative waveform for lower rate codes have very poor performance when  $E_b/N_0 = 6.0\text{dB}$ . Only the higher rate codes ( $17 < k < 29$ ) yield satisfactory performances and, specifically, the most favorable are given by the RS (31, 23) and RS (31, 25) codes. The use of the noise-normalized receiver neutralizes the effects of partial-band interference since the performance of the system for  $\rho < 1$  relative to barrage noise interference ( $\rho = 1$ ) is approximately the same or slightly better.

$P_b$	$\rho$	$\kappa=15$ $E_b / N_I$ (dB)	$\kappa=17$ $E_b / N_I$ (dB)	$\kappa=19$ $E_b / N_I$ (dB)	$\kappa=21$ $E_b / N_I$ (dB)	$\kappa=23$ $E_b / N_I$ (dB)	$\kappa=25$ $E_b / N_I$ (dB)	$\kappa=27$ $E_b / N_I$ (dB)	Existing $E_b / N_I$ (dB)
$10^{-5}$	0.1	inferior	inferior	19.4	16.4	15.2	15.2	16.0	inferior
$10^{-5}$	0.3	inferior	inferior	19.75	17.1	16.1	15.93	16.4	inferior
$10^{-5}$	0.5	inferior	inferior	19.83	17.2	16.1	15.93	16.4	inferior
$10^{-5}$	0.7	inferior	inferior	19.92	17.2	16.2	15.9	16.4	inferior
$10^{-5}$	1.0	inferior	inferior	19.9	16.11	16.23	15.9	16.4	inferior

Table 3. Comparison of the Performance of the Original and the Alternative JTIDS Waveform for Different Values of  $\rho$  for Coherent Demodulation when  $E_b/N_0 = 6.0\text{dB}$ .

The summarized performance results for the alternative waveform and the existing JTIDS waveform in a more favorable environment where  $E_b/N_0 = 10.0\text{dB}$  are shown in Table 4, which is based on Figures 20 through 24. In this case, the best performances are obtained for  $\rho = 0.1$ . It is clear that the performance of the system degrades as the fraction of time where the PNI is on ( $\rho$ ) increases. Moreover, in this case the worst performance is with barrage noise interference ( $\rho = 1$ ). This phenomenon is due to the noise-normalized receiver and, thus, the jammer gains no advantage by using pulse-noise interference. Consequently, the jammer is obliged to spread its power over the entire spread spectrum bandwidth, thus reducing the maximum jamming power spectral density.

Furthermore, the lower rate code alternative waveform has better performance than the higher rate code when  $\rho < 0.5$ . For example, when  $\rho = 0.3$  the alternative

waveform with inner code RS (31, 15) compared to that with RS (31, 27) requires a signal-to-noise interference ratio ( $E_b / N_I$ ) that is 3.8 dB less. Nevertheless, when  $\rho$  increases the alternative waveform has approximately the same performance for the various code rates  $r_{cc}$  (less than 1.0 dB difference).

Finally, the actual JTIDS waveform with noise-normalization has poorer performance than the alternative waveform in all cases, but the benefits of noise-normalization still exist for the original JTIDS waveform.

$P_b$	$\rho$	$\kappa=15$ $E_b / N_I$ (dB)	$\kappa=17$ $E_b / N_I$ (dB)	$\kappa=19$ $E_b / N_I$ (dB)	$\kappa=21$ $E_b / N_I$ (dB)	$\kappa=23$ $E_b / N_I$ (dB)	$\kappa=25$ $E_b / N_I$ (dB)	$\kappa=27$ $E_b / N_I$ (dB)	Existing $E_b / N_I$ (dB)
$10^{-5}$	0.1	superior	superior	superior	superior	superior	superior	superior	superior
$10^{-5}$	0.3	2.7	2.7	2.7	3.5	4.4	5.5	6.5	9.0
$10^{-5}$	0.5	7.2	6.9	6.9	6.9	7.0	7.3	7.7	9.8
$10^{-5}$	0.7	8.2	7.8	7.6	7.5	7.5	7.6	7.8	10.0
$10^{-5}$	1.0	8.3	8.2	7.9	7.7	7.6	7.6	7.6	10.0

Table 4. Comparison of the Performance of the Original and the Alternative JTIDS Waveform for Different Values of  $\rho$  for Coherent Demodulation when  $E_b / N_0 = 10.0$  dB.

In Table 5, which is based on Figures 25 through 28, the summarized performance results for the alternative waveform and the existing JTIDS in an extremely favorable environment where  $E_b / N_0 = 15.0$  dB are shown. Essentially, the same conclusions are reached as when  $E_b / N_0 = 6.0$  dB. Specifically, the performance of the system degrades as the fraction of time when the PNI is on ( $\rho$ ) is increased, and the performance of the original JTIDS waveform with noise-normalization is poorer than the alternative waveform. The lower code rate alternative waveforms have better performance than the higher code rate waveforms when  $\rho < 0.7$  instead of  $\rho < 0.5$  ( $E_b / N_0 = 6.0$  dB case). Finally, noise-normalization is still effective for both the compatible JTIDS-type waveform and the existing waveform and, thus, the jammer is again forced to adopt full-band (barrage) interference.

$P_b$	$\rho$	$\kappa=15$ $E_b / N_I$ (dB)	$\kappa=17$ $E_b / N_I$ (dB)	$\kappa=19$ $E_b / N_I$ (dB)	$\kappa=21$ $E_b / N_I$ (dB)	$\kappa=23$ $E_b / N_I$ (dB)	$\kappa=25$ $E_b / N_I$ (dB)	$\kappa=27$ $E_b / N_I$ (dB)	Existing $E_b / N_I$ (dB)
$10^{-5}$	0.1	superior	superior	superior	superior	superior	superior	superior	superior
$10^{-5}$	0.3	superior	superior	superior	superior	superior	2.5	5.1	5.3
$10^{-5}$	0.5	4.0	4.6	5.1	5.5	5.9	6.3	6.7	8.0
$10^{-5}$	0.7	6.4	6.3	6.3	6.3	6.3	6.4	6.6	8.0
$10^{-5}$	1.0	7.0	6.6	6.4	6.2	6.1	6.1	6.1	7.7

Table 5. Comparison of the Performance of the Original and the Alternative JTIDS Waveform for Different Values of  $\rho$  for Coherent Demodulation when  $E_b/N_0 = 15.0$  dB.

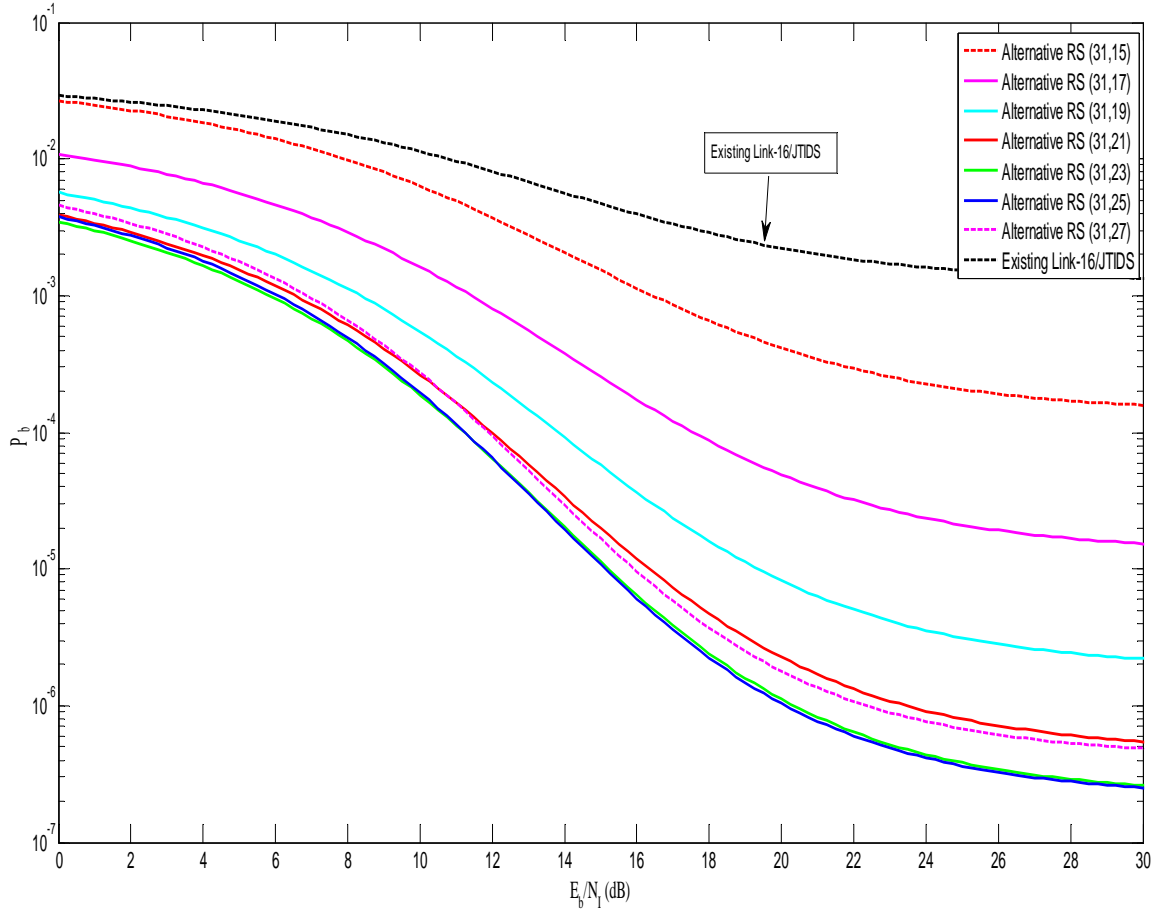


Figure 15. Performance of 32-ary CCSK Using the Alternative Error Correction Coding Scheme in Both AWGN and PNI for  $\rho = 0.1$ , Coherent Demodulation, Soft Decision RS Decoding, a Diversity of Two, Noise-normalization, and  $E_b/N_0 = 6.0$  dB.



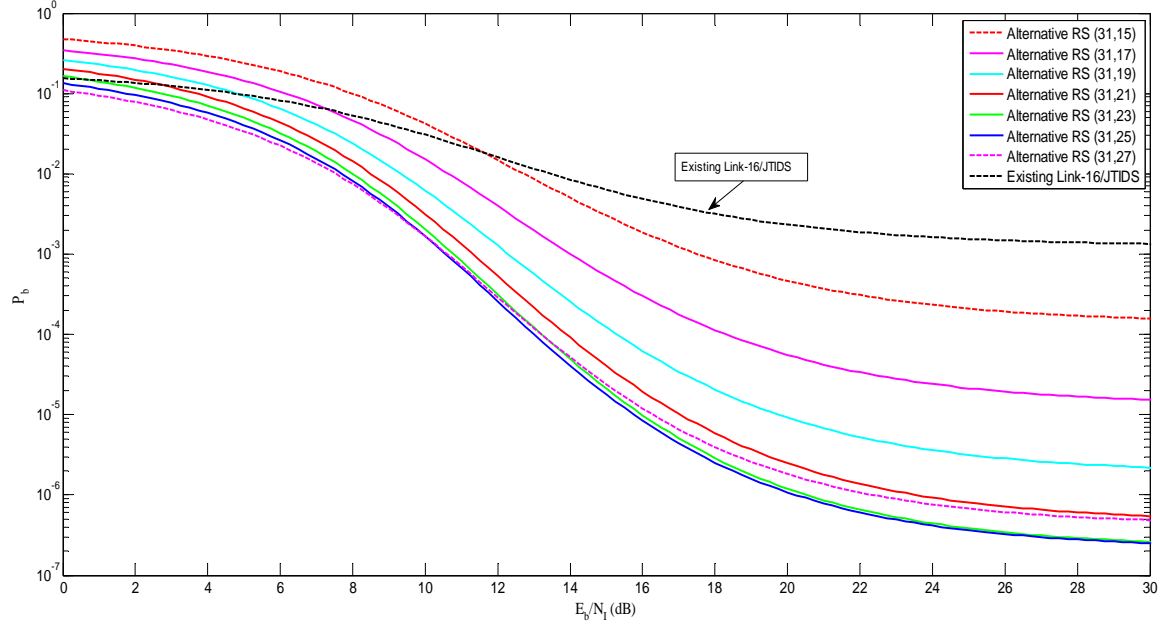


Figure 16. Performance of 32-ary CCSK Using the Alternative Error Correction Coding Scheme in Both AWGN and PNI for  $\rho = 0.3$ , Coherent Demodulation, Soft Decision RS Decoding, a Diversity of Two, Noise-normalization, and  $E_b/N_0 = 6.0$  dB.

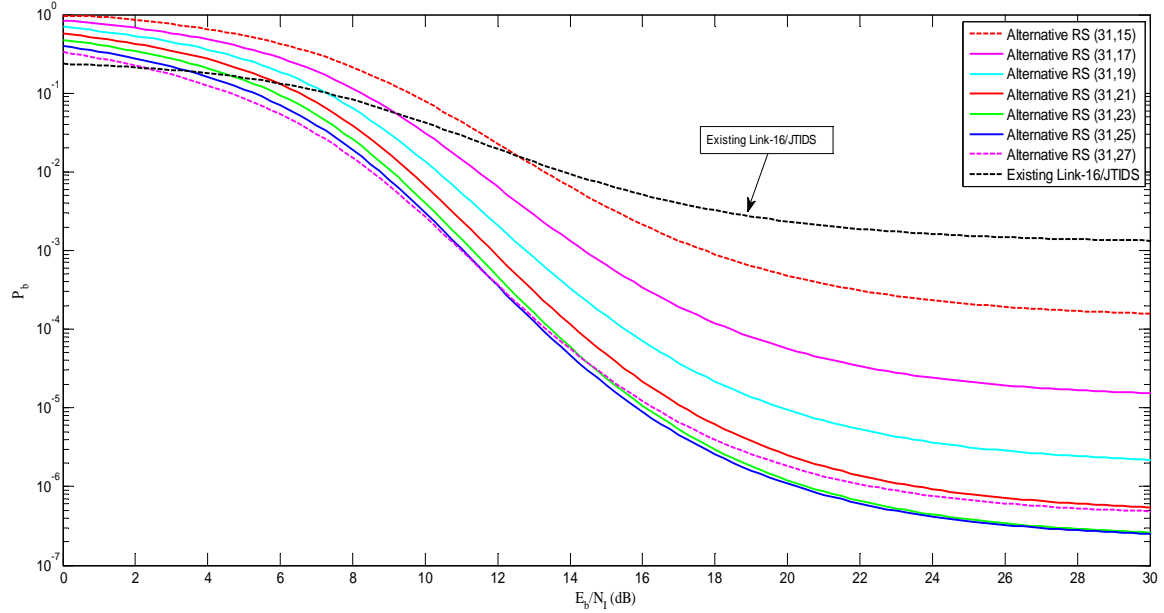


Figure 17. Performance of 32-ary CCSK Using the Alternative Error Correction Coding Scheme in Both AWGN and PNI for  $\rho = 0.5$ , Coherent Demodulation, Soft Decision RS Decoding, a Diversity of Two, Noise-normalization, and  $E_b/N_0 = 6.0$  dB.

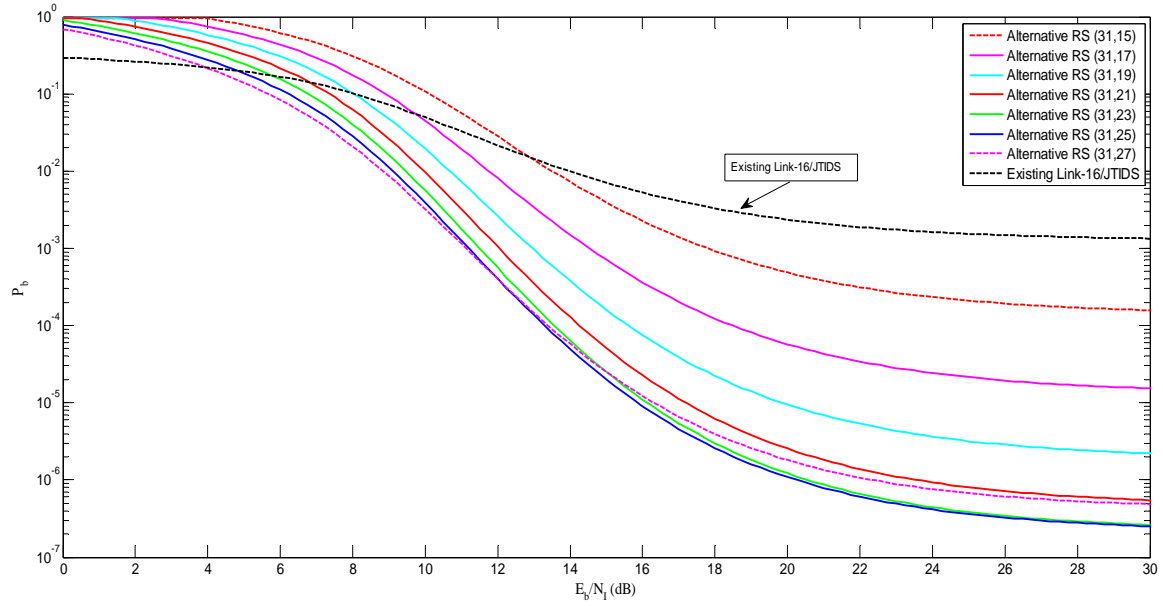


Figure 18. Performance of 32-ary CCSK Using the Alternative Error Correction Coding Scheme in Both AWGN and PNI for  $\rho = 0.7$ , Coherent Demodulation, Soft Decision RS Decoding, a Diversity of Two, Noise-normalization, and  $E_b/N_0 = 6.0$  dB.

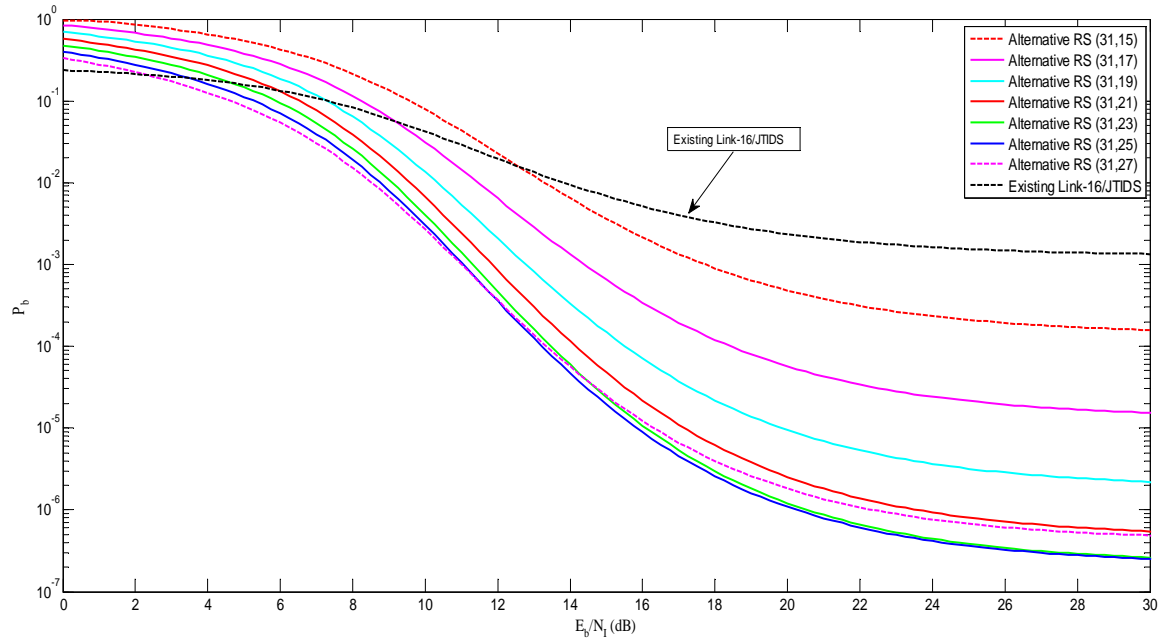


Figure 19. Performance of 32-ary CCSK Using the Alternative Error Correction Coding Scheme in Both AWGN and PNI for  $\rho = 1.0$ , Coherent Demodulation, Soft Decision RS Decoding, a Diversity of Two, Noise-normalization, and  $E_b/N_0 = 6.0$  dB.

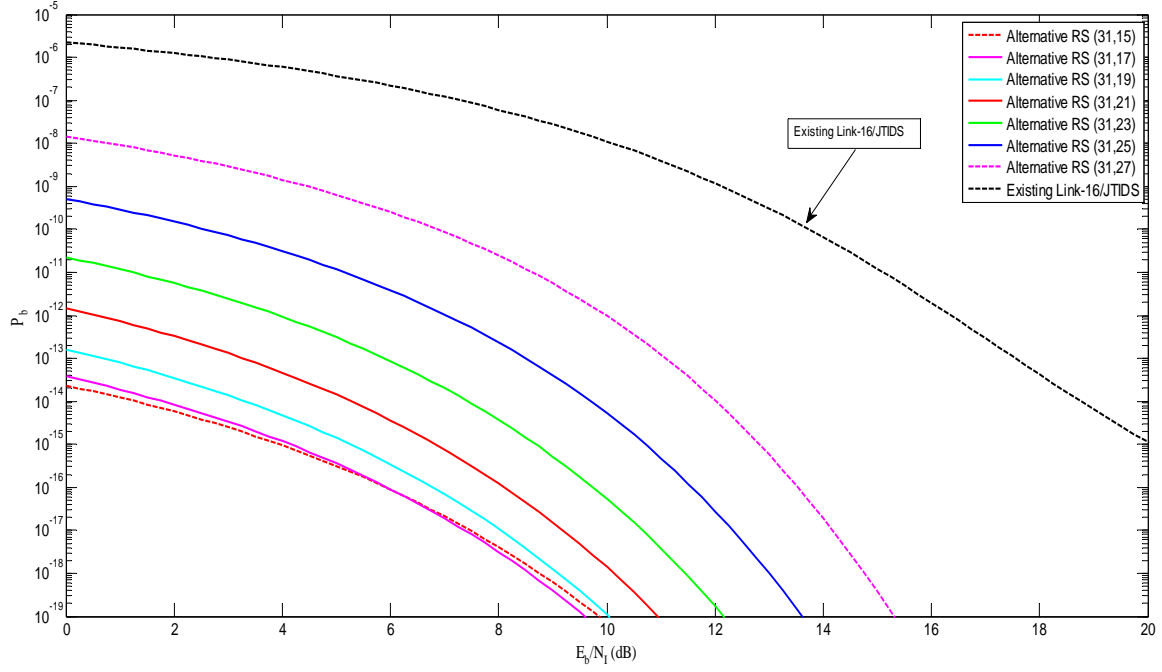


Figure 20. Performance of 32-ary CCSK Using the Alternative Error Correction Coding Scheme in Both AWGN and PNI for  $\rho = 0.1$ , Coherent Demodulation, Soft Decision RS Decoding, a Diversity of Two, Noise-normalization, and  $E_b/N_0 = 10.0$  dB.

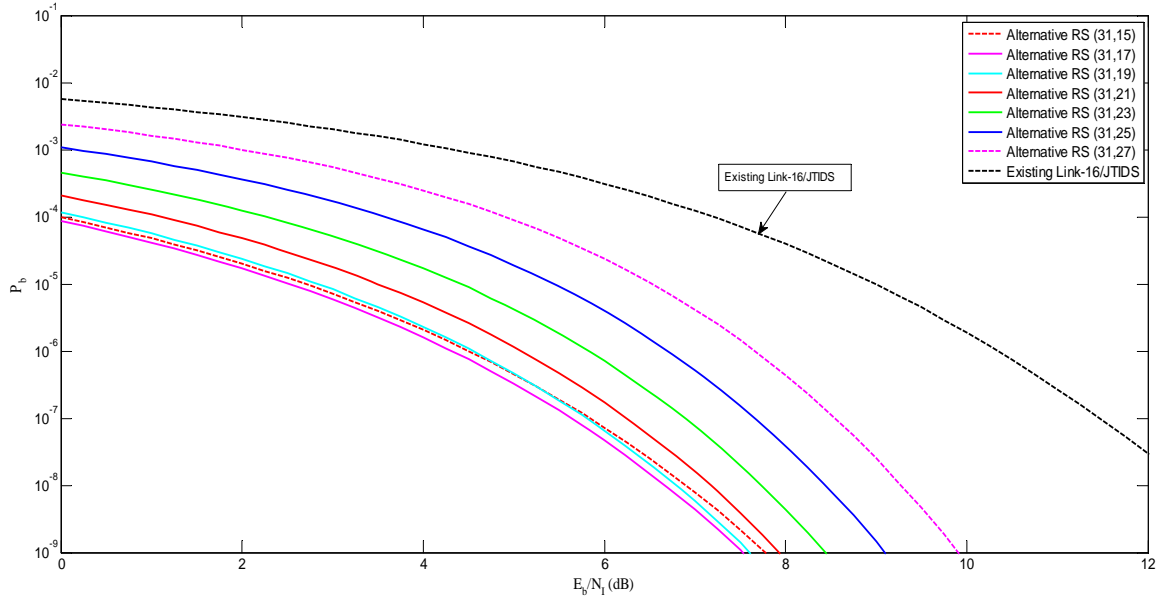


Figure 21. Performance of 32-ary CCSK Using the Alternative Error Correction Coding Scheme in Both AWGN and PNI for  $\rho = 0.3$ , Coherent Demodulation, Soft Decision RS Decoding, a Diversity of Two, Noise-normalization, and  $E_b/N_0 = 10.0$  dB.

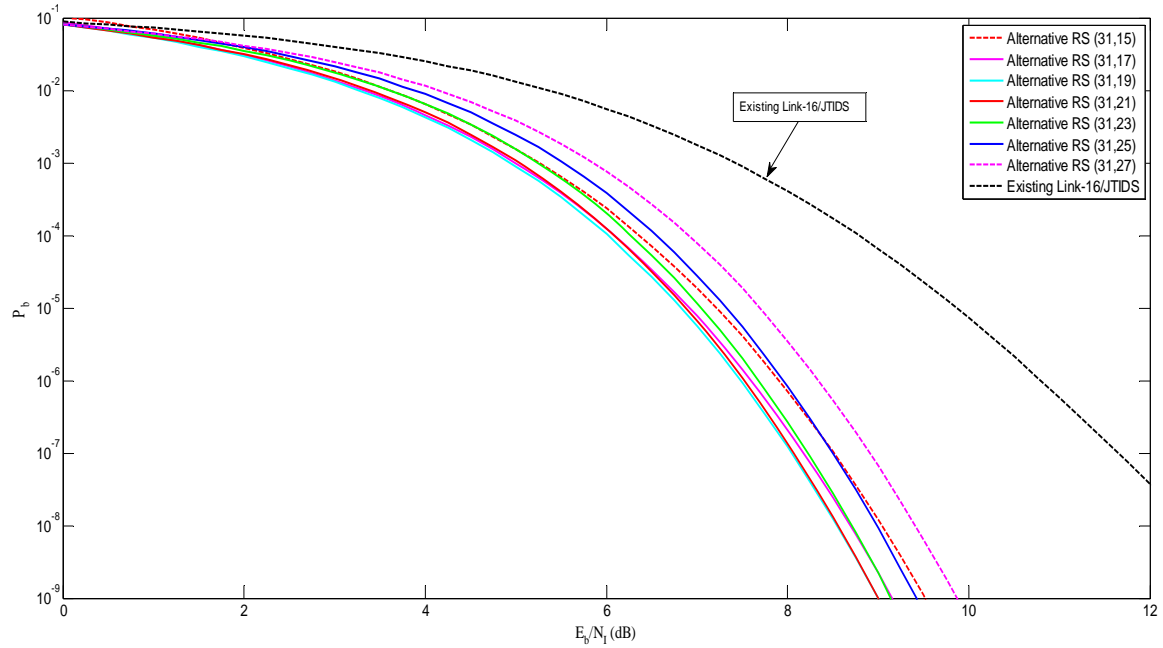


Figure 22. Performance of 32-ary CCSK Using the Alternative Error Correction Coding Scheme in Both AWGN and PNI for  $\rho = 0.5$ , Coherent Demodulation, Soft Decision RS Decoding, a Diversity of Two, Noise-normalization, and  $E_b/N_0 = 10.0$  dB.

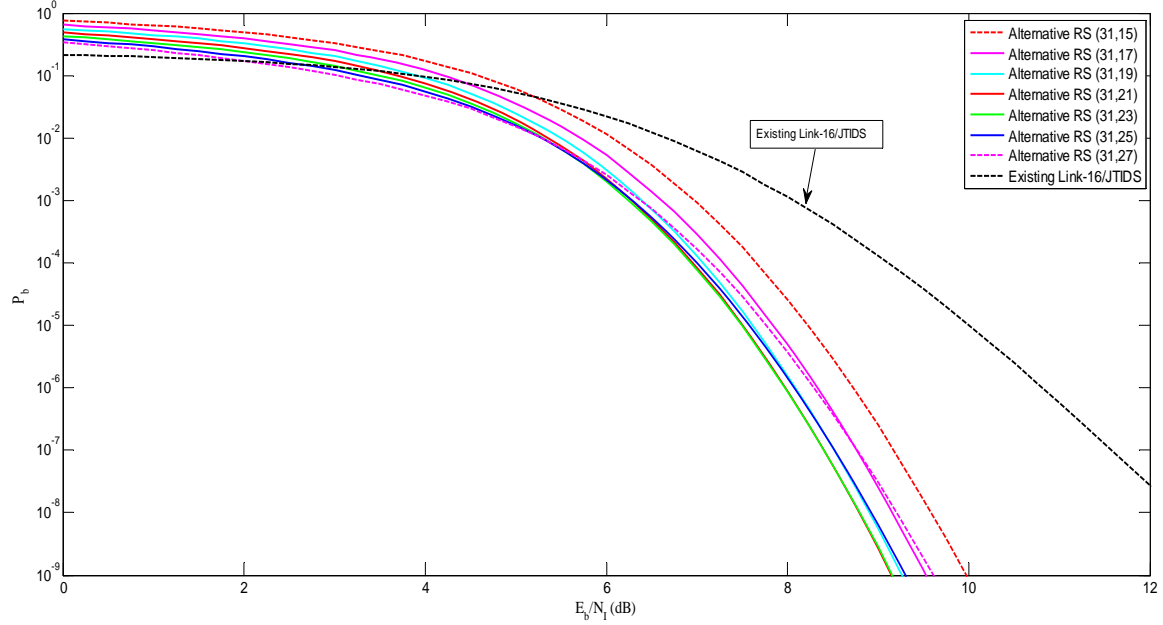


Figure 23. Performance of 32-ary CCSK Using the Alternative Error Correction Coding Scheme in Both AWGN and PNI for  $\rho = 0.7$ , Coherent Demodulation, Soft Decision RS Decoding, a Diversity of Two, Noise-normalization, and  $E_b/N_0 = 10.0$  dB.

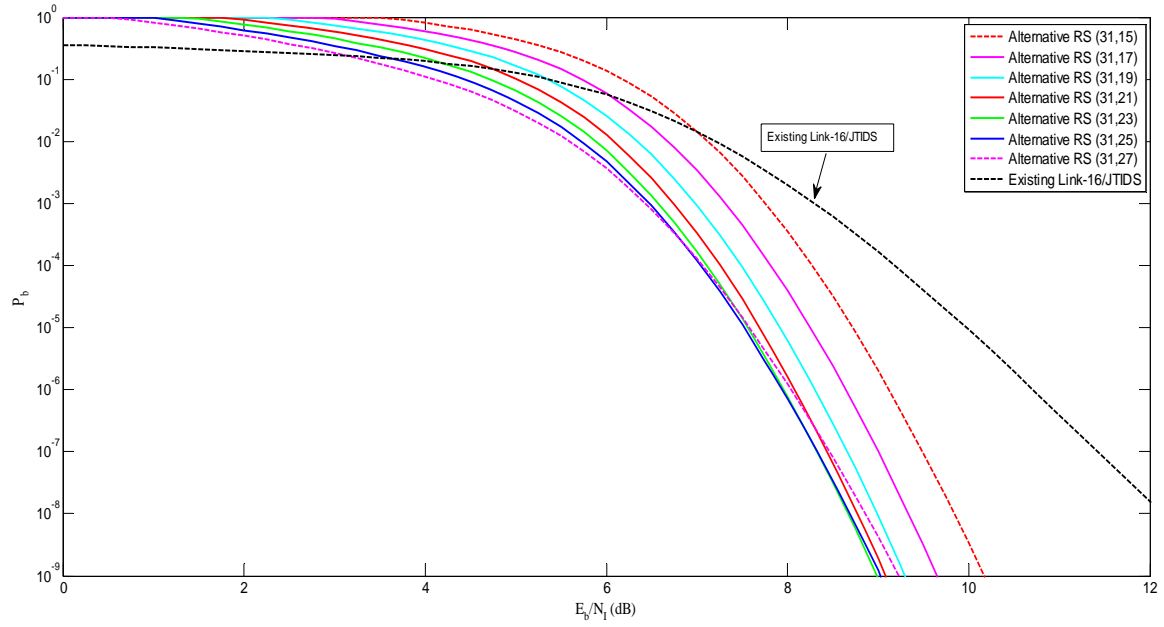


Figure 24. Performance of 32-ary CCSK Using the Alternative Error Correction Coding Scheme in Both AWGN and PNI for  $\rho = 1.0$ , Coherent Demodulation, Soft Decision RS Decoding, a Diversity of Two, Noise-normalization, and  $E_b/N_0 = 10.0$  dB.

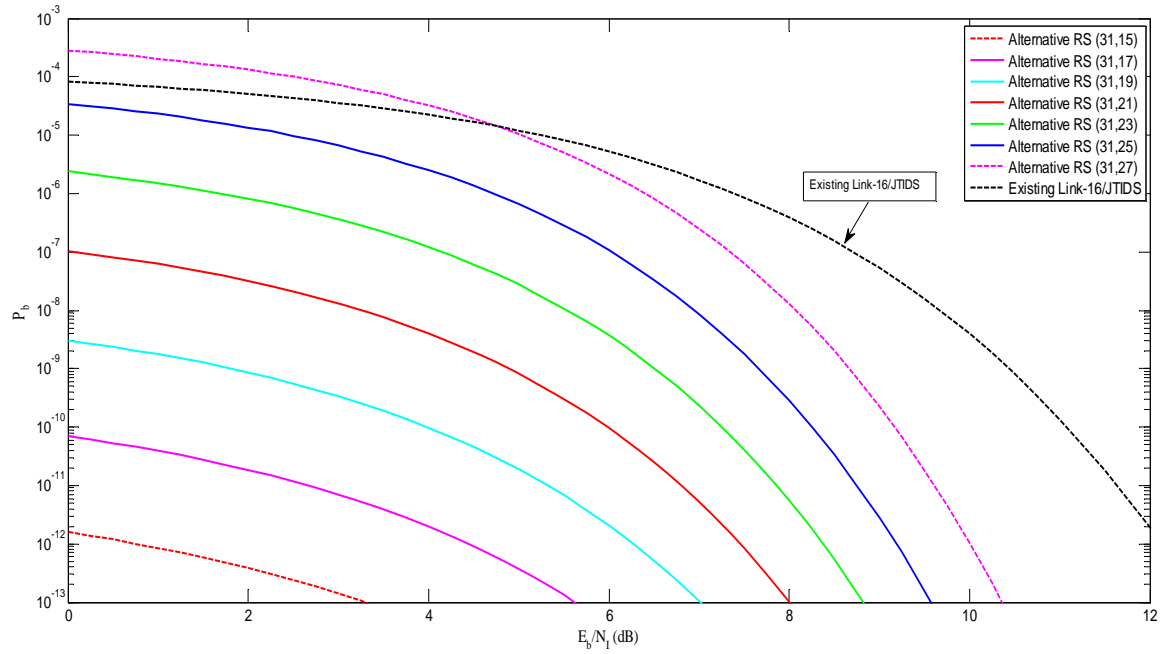


Figure 25. Performance of 32-ary CCSK Using the Alternative Error Correction Coding Scheme in Both AWGN and PNI for  $\rho = 0.3$ , Coherent Demodulation, Soft Decision RS Decoding, a Diversity of Two, Noise-normalization, and  $E_b/N_0 = 15.0$  dB.

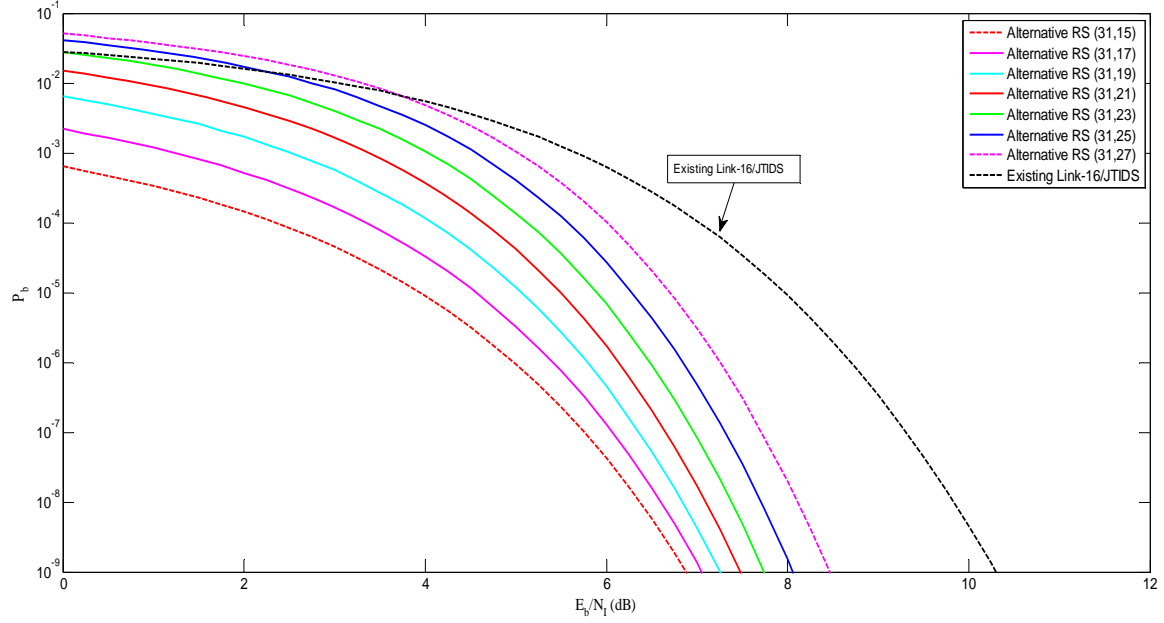


Figure 26. Performance of 32-ary CCSK Using the Alternative Error Correction Coding Scheme in Both AWGN and PNI for  $\rho = 0.5$ , Coherent Demodulation, Soft Decision RS Decoding, a Diversity of Two, Noise-normalization, and  $E_b/N_0 = 15.0$  dB.

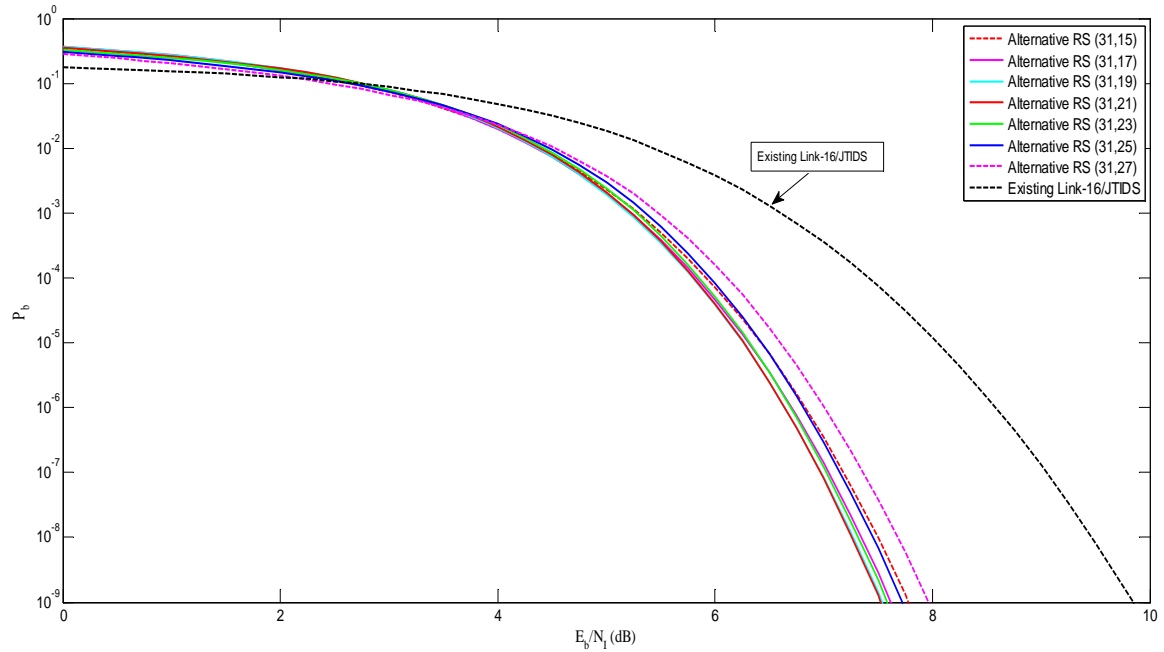


Figure 27. Performance of 32-ary CCSK Using the Alternative Error Correction Coding Scheme in Both AWGN and PNI for  $\rho = 0.7$ , Coherent Demodulation, Soft Decision RS Decoding, a Diversity of Two, Noise-normalization, and  $E_b/N_0 = 15.0$  dB.

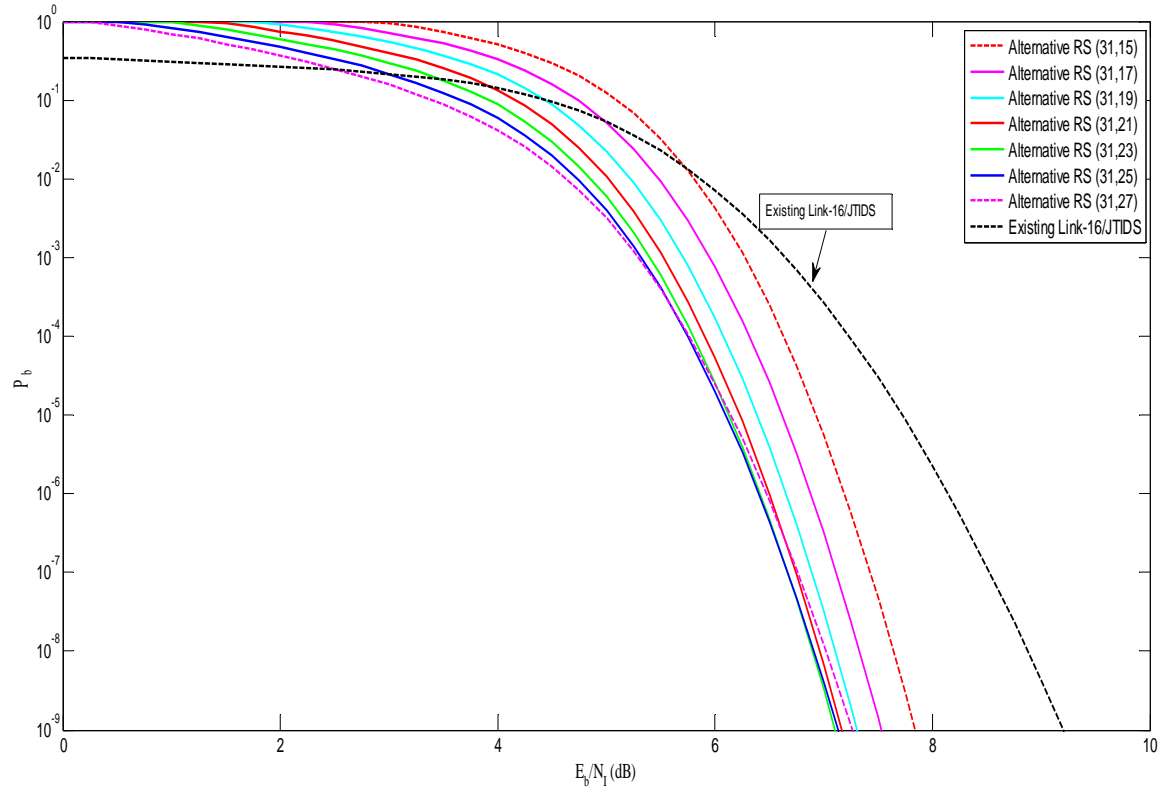


Figure 28. Performance of 32-ary CCSK Using the Alternative Error Correction Coding Scheme in Both AWGN and PNI for  $\rho = 1.0$ , Coherent Demodulation, Soft Decision RS Decoding, a Diversity of Two, Noise-normalization, and  $E_b/N_0 = 15.0$  dB.

### C. CHAPTER SUMMARY

In this chapter, the performance of the alternative waveform with a diversity of two, soft decision RS decoding, and noise-normalization in AWGN and PNI was investigated for coherent demodulation. The impact of the noise-normalized receiver on the degradation of the effects of pulse-noise interference was shown to be an effective way to protect communication signals from hostile interference. The author concluded that the performance of the existing waveform was inferior as compared to the alternative waveform in all cases. In Chapter V, the performance of the alternative waveform is examined in the same conditions for noncoherent demodulation.

THIS PAGE INTENTIONALLY LEFT BLANK



## V. PERFORMANCE ANALYSIS OF NONCOHERENT 32-ARY CCSK WITH CONCATENATED CODING, DIVERSITY, SD RS DECODING AND NOISE-NORMALIZATION IN AWGN, AND PULSE-NOISE INTERFERENCE

### A. NONCOHERENT DEMODULATION OF 32-ARY CCSK WITH DIVERSITY AND NOISE-NORMALIZATION IN AWGN AND PNI

Based on the analysis of noncoherent demodulation in Chapter III, the most effective way of detecting an MSK signal is by taking advantage of the fact that it is a digital FM signal and using a slope detector. The performance of a slope detector is approximated with that of an optimum noncoherent DPSK demodulator. DPSK is a special case of noncoherent orthogonal modulation with  $T_s = 2T_b$  and  $E_s = 2E_b$  [6]. For purposes of illustration, consider the quadrature-correlator square detector shown in Figure 29.

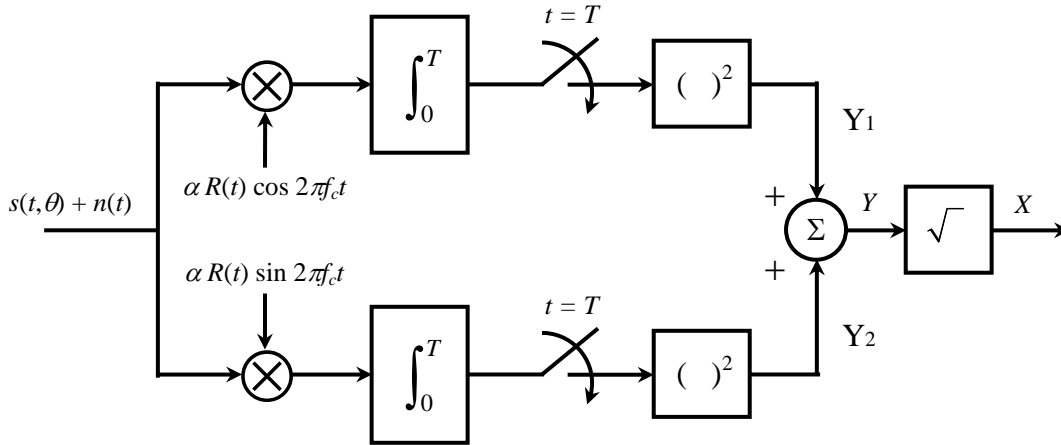


Figure 29. The Quadrature-correlator Square-law Detector for an Input Signal  $s(t)$  with Unknown Phase  $\theta$  (After [11]).

The decision statistic in Figure 29 is a function of two independent random variables  $Y_1$  and  $Y_2$  that can be either Ricean or Rayleigh. In practice, the square root operation in Figure 29 is often omitted because the decision variable  $Y$  produces the same decision as  $X$ . When the decision variable  $Y$  is the sum of two squared-Gaussian

random variables with a non-zero mean, then  $Y$  is a Ricean random variable with probability density function [11]

$$f_y(y) = \frac{1}{2\sigma^2} e^{-(y+a^2)/2\sigma^2} I_0\left(\frac{\sqrt{ya}}{\sigma^2}\right), \quad y \geq 0 \quad (5.1)$$

where

$$a^2 = s_{0,I}^2(T) + s_{0,Q}^2(T) \approx \alpha^2 E^2$$

and

$$\sigma^2 = \frac{\alpha^2 EN_0}{2}.$$

When the signal  $s(t)$  is not present, then  $Y$  is simply the square root of the sum of two squared, zero-mean Gaussian random variables with variance  $\sigma^2$ . Thus,  $Y$  is a Rayleigh random variable with a probability density function

$$f_y(y) = \frac{x}{2\sigma^2} e^{-y/2\sigma^2}, \quad y \geq 0 \quad (5.2)$$

where

$$\sigma^2 = \frac{\alpha^2 EN_0}{2}.$$

Suppose the receiver is attacked by a band-limited, noise-like signal that is turned on and off systematically. As before, let  $\rho$  be the fraction of time the jammer is turned on and assume that the jammer does not turn on or off during a channel bit interval. The jammer's PSD is  $N_I/2\rho$ . With DPSK the assumption is that two consecutive bits either are jammed or unjammed, i.e., the case where one bit is jammed and the other bit is unjammed is neglected. This is valid if the jammed bit sequence is long. For a noncoherent detector, the probability of error for DPSK is equivalent to that of orthogonal BFSK with twice the SNR [6].

In this thesis, the effects of partial-band interference are minimized by using a noncoherent noise-normalized receiver. In Figure 30, a BFSK noise-normalized

receiver is illustrated where a frequency synthesizer is utilized to de-hop the receiving signal.

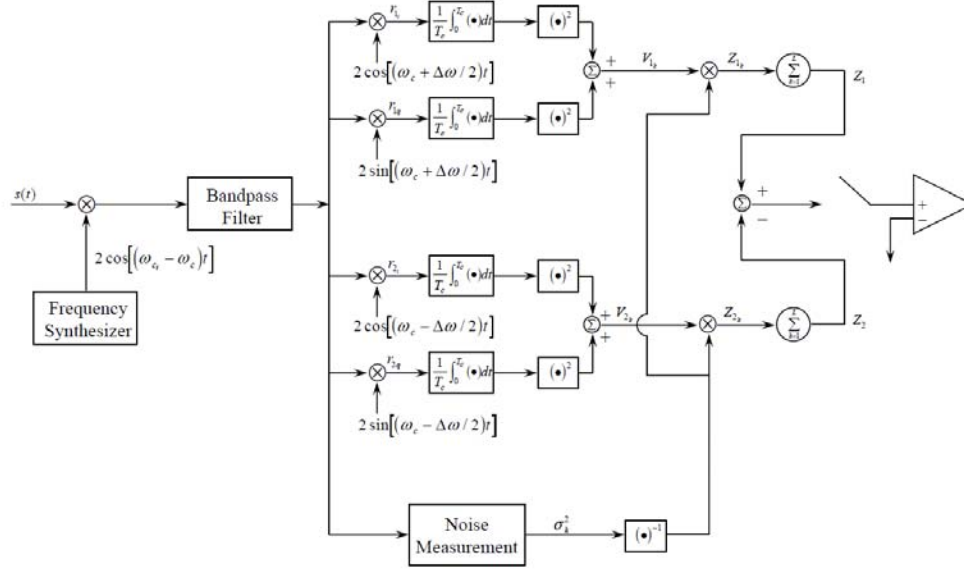


Figure 30. Noncoherent Noise-normalized FFH/BFSK Receiver (From [13]).

From Equations (5.1) and (5.2), the probability density functions (pdf) of the random variables  $V_{1\kappa}$  and  $V_{2\kappa}$  are given by

$$f_{V_{1\kappa}}(v_{1\kappa}) = \frac{1}{2\sigma_{\kappa}^2} \exp\left[-\frac{(V_{1\kappa} + 2A_c^2)}{2\sigma_{\kappa}^2}\right] I_0\left(\frac{A_c\sqrt{2V_{1\kappa}}}{\sigma_{\kappa}^2}\right) \quad (5.3)$$

and

$$f_{V_{2\kappa}}(v_{2\kappa}) = \frac{1}{2\sigma^2} \exp\left[-\frac{V_{2\kappa}}{2\sigma_{\kappa}^2}\right] \quad (5.4)$$

where the signal is assumed to be present on branch 1. If  $z_{1\kappa}$  and  $z_{2\kappa}$  are the noise-normalized random variables prior to diversity combining, then

$$z_{1\kappa} = \frac{V_{1\kappa}}{\sigma_k^2} \quad (5.5)$$

and

$$z_{2\kappa} = \frac{V_{2\kappa}}{\sigma_k^2}. \quad (5.6)$$

The probability density function of the noise-normalized random variable  $z_{1\kappa}$  prior to diversity combining is obtained by using Equations (5.3) and (5.5) in

$$\begin{aligned} f_{z_{1\kappa}}(z_{1\kappa}|1) &= \left| \frac{d_{v_{1\kappa}}}{d_{z_{1\kappa}}} \right| f_{v_{1\kappa}}(\sigma_k^2 z_{1\kappa}|1) = \sigma_k^2 f_{v_{1\kappa}}(\sigma_k^2 z_{1\kappa}|1) \\ &= \frac{1}{2} \exp \left[ -\frac{(z_{1\kappa} + 2A_c^2/\sigma_k^2)}{2} \right] I_o \left( \frac{A_c \sqrt{2z_{1\kappa}}}{\sigma_k} \right). \end{aligned} \quad (5.7)$$

Likewise, from Equations (5.4) and (5.6), the probability density function of the noise-normalized random variable  $z_{2\kappa}$  is

$$\begin{aligned} f_{z_{2\kappa}}(z_{2\kappa}|1) &= \left| \frac{dv_{2\kappa}}{dz_{2\kappa}} \right| f_{v_{2\kappa}}(\sigma_k^2 z_{2\kappa}|1) = \sigma_k^2 f_{v_{2\kappa}}(\sigma_k^2 z_{2\kappa}|1) \\ &= \frac{1}{2} \exp \left[ -\frac{z_{2\kappa}}{2} \right]. \end{aligned} \quad (5.8)$$

Since each hop is assumed to be independent and  $i$  out of  $L$  hops are jammed, then

$$f_{z_1}(z_1|1, i) = f_{z_{1\kappa_j}}^{\otimes i}(z_{1\kappa_j}|1) \otimes f_{z_{1\kappa}}^{\otimes (L-i)}(z_{1\kappa}|1) \quad (5.9)$$

and

$$f_{z_2}(z_2|1) = f_{z_{2\kappa}}^{\otimes L}(z_{2\kappa}|1). \quad (5.10)$$

Taking the Laplace transform of Equations (5.9) and (5.10), the results are

$$F_{z_1}(s|1, i) = F_{z_{1\kappa_j}}^i(s|1) F_{z_{1\kappa}}^{(L-i)}(s|1) \quad (5.11)$$

and

$$F_{z_2}(s_2|1) = F_{z_{2\kappa}}^L(s_2|1), \quad (5.12)$$

where the  $j$  subscript indicates a jammed hop. In order to compute the Laplace transforms of Equations (5.11) and (5.12), the following identities are used:

$$\text{a. Shifting property: } \mathfrak{F}\{e^{at} f(t)\} = F(s-a); \quad (5.13)$$

$$\text{b. } \mathfrak{I} \left\{ a^{-\frac{\nu}{2}} z^{\frac{\nu}{2}} I_{\nu}(2\sqrt{az}) \right\} = \frac{1}{s^{\nu+1}} \exp(a/s), \nu > -1; \quad (5.14)$$

and

$$\text{c. } \mathfrak{I}(\exp(-at)) = \frac{1}{s+a}. \quad (5.15)$$

By applying the above properties to Equations (5.7) and (5.8), one gets the following:

$$\begin{aligned} F_{z_{1\kappa}}(s|1) &= \int_0^{\infty} f_{z_{1\kappa}}(z_{1\kappa}|1) \exp(-sz_{1\kappa}) dz_{1\kappa} \\ &= \mathfrak{I} \left\{ \frac{1}{2} \exp \left[ -\frac{(z_{1\kappa} + 2A_c^2/\sigma_{\kappa}^2)}{2} \right] I_o \left( \frac{A_c \sqrt{2z_{1\kappa}}}{\sigma_{\kappa}} \right) \right\} \\ &= \mathfrak{I} \left\{ \frac{1}{2} \exp \left[ -\frac{(z_{1\kappa} + 2A_c^2/\sigma_{\kappa}^2)}{2} \right] I_o \left( 2\sqrt{\frac{A_c^2 z_{1\kappa}}{2\sigma_{\kappa}^2}} \right) \right\} \\ &= \frac{1}{2} \exp \left( -\frac{A_c^2}{\sigma_{\kappa}^2} \right) \mathfrak{I} \left\{ \exp \left[ -\frac{z_{1\kappa}}{2} \right] I_o \left( 2\sqrt{\frac{A_c^2 z_{1\kappa}}{2\sigma_{\kappa}^2}} \right) \right\} \\ &= \frac{1}{2} \exp \left( -\frac{A_c^2}{\sigma_{\kappa}^2} \right) \mathfrak{I} \left\{ I_o \left( 2\sqrt{\frac{A_c^2 z_{1\kappa}}{2\sigma_{\kappa}^2}} \right) \right\} \Big|_{s=s+\frac{1}{2}} \\ &= \frac{1}{2} \frac{1}{s+\frac{1}{2}} \exp \left( -\frac{A_c^2}{\sigma_{\kappa}^2} \right) \exp \left( \frac{A_c^2}{2\sigma_{\kappa}^2} \frac{1}{s+\frac{1}{2}} \right) \\ &= \frac{1}{2} \frac{1}{s+\frac{1}{2}} \exp \left( -\frac{A_c^2}{\sigma_{\kappa}^2} \left( \frac{s}{s+\frac{1}{2}} \right) \right) \end{aligned} \quad (5.16)$$

and

$$\begin{aligned} F_{z_{2\kappa}}(s|1) &= \int_0^{\infty} f_{z_{2\kappa}}(z_{2\kappa}|1) \exp(-sz_{2\kappa}) dz_{2\kappa} \\ &= \mathfrak{I} \left( \frac{1}{2} \exp \left[ -\frac{z_{2\kappa}}{2} \right] \right) = \frac{1}{2} \frac{1}{s+\frac{1}{2}}. \end{aligned} \quad (5.17)$$

Finally, combining Equation (5.11) with Equation (5.16) and Equation (5.12) with Equation (5.17) leads to

$$F_{z_1}(s|1, i) = \frac{1}{2^L} \left( \frac{1}{s + \frac{1}{2}} \right)^L \exp \left( -A_c^2 \left( \frac{i}{\sigma_{\kappa_j}^2} + \frac{L-i}{\sigma_{\kappa}^2} \right) \left( \frac{s}{s + \frac{1}{2}} \right) \right) \quad (5.18)$$

and

$$F_{z_2}(s_2|1) = \frac{1}{2^L} \left( \frac{1}{s + \frac{1}{2}} \right)^L \quad (5.19)$$

where  $\sigma_{\kappa_j}^2$  and  $\sigma_{\kappa}^2$  are the noise power of jammed hop and unjammed hop, respectively.

In order to calculate Equations (5.18) and (5.19) in the time domain, the inverse Laplace transform is obtained by taking advantage of the following properties:

$$\text{a. } \mathfrak{I}^{-1} \left\{ \frac{1}{s^{v+1}} \exp(a/s) \right\} = a^{-\frac{v}{2}} z^{\frac{v}{2}} I_v(2\sqrt{az}), v > -1; \quad (5.20)$$

$$\text{b. } \mathfrak{I}^{-1} \left( \frac{n!}{(s-a)^{n+1}} \right) = z^n \exp(az), s > a; \quad (5.21)$$

and

$$\text{c. shifting property: } \mathfrak{I}^{-1}(F(s-a)) = f(z) \exp(az), s > |a|. \quad (5.22)$$

From Equation (5.18) and setting  $n(i) = \left( \frac{i}{\sigma_{\kappa_j}^2} + \frac{L-i}{\sigma_{\kappa}^2} \right)$ , the following is obtained:

$$\begin{aligned} F_{z_1}(s|1, i) &= \frac{1}{2^L} \left( \frac{1}{s} \right)^L \exp \left( -A_c^2 n(i) \frac{s - \frac{1}{2}}{s} \right) \Bigg|_{s=s+\frac{1}{2}} \\ &= \frac{1}{2^L} \exp(-A_c^2 n(i)) \left[ \frac{1}{s^{(L-1)+1}} \exp \left( \frac{A_c^2 n(i)}{2} \left( \frac{1}{s} \right) \right) \right] \Bigg|_{s=s+\frac{1}{2}} \end{aligned}$$

$$\begin{aligned}
&\Rightarrow \mathfrak{I}^{-1}\left(F_{z_1}(s|1,i)\right) = f_{z_1}(s|1,i) \\
&= \frac{1}{2^L} z_1^{\frac{L-1}{2}} \frac{1}{\left(\frac{A_c^2 n(i)}{2}\right)^{\frac{L-1}{2}}} I_{L-1}\left(A_c \sqrt{2n(i)z_1}\right) \exp\left(-A_c^2 n(i)\right) \exp\left(-\frac{z_1}{2}\right) \\
&= \frac{z_1^{\frac{L-1}{2}}}{2\left[2A_c^2 n(i)\right]^{\frac{L-1}{2}}} \exp\left(-\frac{z_1 + 2A_c^2 n(i)}{2}\right) I_{L-1}\left(A_c \sqrt{2n(i)z_1}\right). \quad (5.23)
\end{aligned}$$

Likewise for branch 2, where the signal is not present,

$$\begin{aligned}
\mathfrak{I}^{-1}\left(F_{z_2}(s|1)\right) &= f_{z_2}(z_2|1) = \mathfrak{I}^{-1}\left(\frac{1}{2^L} \left(\frac{1}{s + \frac{1}{2}}\right)^L\right) \\
&= \frac{1}{2^L} \frac{z_2^{L-1}}{(L-1)!} \exp\left(-\frac{1}{2} z_2\right). \quad (5.24)
\end{aligned}$$

Finally, the random variables  $z_1$  and  $z_2$  are independent because their noise components are independent due to the orthogonality of the two signals. The error probability is equal to the average symbol error. Thus, when  $i$  bits are jammed

$$\begin{aligned}
P_s(i) &= \Pr(z_1 < z_2 | 1, i) = \int_0^\infty \int_{z_1}^\infty f_{z_1 z_2}(z_1, z_2 | 1, i) dz_2 dz_1 \\
&= \int_0^\infty f_{z_1}(z_1 | 1, i) \left[ \int_{z_1}^\infty f_{z_2}(z_2 | 1) dz_2 \right] dz_1 \\
P_s(i) &= \int_0^\infty f_{z_1}(z_1 | 1, i) \left[ \int_{z_1}^\infty \frac{1}{2^L} \frac{z_2^{L-1}}{(L-1)!} \exp\left(-\frac{1}{2} z_2\right) dz_2 \right] dz_1. \quad (5.25)
\end{aligned}$$

Using the identities

$$1. \int_0^u x^m \exp(-ax) dx = \frac{m!}{a^{m+1}} - \exp(-au) \sum_{k=0}^m \frac{m! u^k}{k! a^{m-k+1}}, u, \mu > 0, \quad (5.26)$$

$$2. \int_0^\infty x^{m'-1} \exp(-a'x) dx = \frac{\Gamma(m')}{a^{m'}}, \quad (5.27)$$

and

$$3. \Gamma(m') = (m' - 1)! \quad (5.28)$$

and setting  $m = L - 1$ ,  $a = \frac{1}{2}$ ,  $m' = L$  and  $a' = \frac{1}{2}$  in Equation (5.25), one gets the following:

$$\begin{aligned} P_s(i) &= \int_0^\infty f_{z_1}(z_1|1, i) \left[ \frac{1}{(L-1)!2^L} \left[ \int_0^\infty z_2^{L-1} \exp\left(-\frac{1}{2} z_2\right) dz_2 - \int_0^{z_1} z_2^{L-1} \exp\left(-\frac{1}{2} z_2\right) dz_2 \right] \right] dz_1 \\ &= \int_0^\infty f_{z_1}(z_1|1, i) \left[ \exp\left(\frac{-z_1}{2}\right) \sum_{n=0}^{L-1} \frac{z_1^n}{2^n n!} \right] dz_1 = \sum_{n=0}^{L-1} \int_0^\infty f_{z_1}(z_1|1, i) \exp\left(\frac{-z_1}{2}\right) \frac{z_1^n}{2^n n!} dz_1 \\ P_s(i) &= \sum_{n=0}^{L-1} \int_0^\infty \frac{z_1^{\frac{L-1}{2}}}{2 \left[ 2A_c^2 n(i) \right]^{\frac{L-1}{2}}} \exp\left(-\frac{z_1 + 2A_c^2 n(i)}{2}\right) I_{L-1}\left(A_c \sqrt{2n(i)z_1}\right) \\ &\times \exp\left(\frac{-z_1}{2}\right) \frac{z_1^n}{2^n n!} dz_1. \end{aligned} \quad (5.29)$$

In order to evaluate the integral in Equation (5.29), the following identities are used:

$$a. \int_0^\infty x^{\frac{m+n}{2}} \exp(-ax) J_n(2\beta\sqrt{x}) dx = \frac{m! \beta^n \exp\left(-\frac{\beta^2}{\alpha}\right)}{a^{m+n+1}} L_m^n\left(\frac{\beta^2}{\alpha}\right), \quad (5.30)$$

$$b. \text{Laguerre polynomial: } L_m^n\left(\frac{\beta^2}{\alpha}\right) = \sum_{p=0}^m \frac{(-1)^p}{p!} \binom{m+n}{m-p} \left(\frac{\beta^2}{\alpha}\right)^p, \quad (5.31)$$

and

$$c. I_n(z) = (-j)^n J_n(jz). \quad (5.32)$$

Setting  $n = L - 1$ ,  $m = n$ ,  $a = 1$  and  $\beta = \frac{jA_c \sqrt{2n(i)}}{2}$  in Equation (5.29), the following is obtained:



$$\begin{aligned}
P_s(i) &= \sum_{n=0}^{L-1} \int_0^\infty z_1^{n+\frac{L-1}{2}} \exp(-z_1) I_{L-1}(A_c \sqrt{2n(i)} \sqrt{z_1}) \exp(-A_c^2 n(i)) \frac{1}{2[2A_c^2 n(i)]^{\frac{L-1}{2}}} \frac{1}{2^n n!} dz_1 \\
&= \sum_{n=0}^{L-1} \int_0^\infty z_1^{n+\frac{L-1}{2}} \exp(-z_1) (-j)^{L-1} J_{L-1}(j A_c \sqrt{2n(i)} \sqrt{z_1}) \exp(-A_c^2 n(i)) \frac{1}{2[2A_c^2 n(i)]^{\frac{L-1}{2}}} \frac{1}{2^n n!} dz_1 \\
&= \sum_{n=0}^{L-1} n! \left( \frac{j A_c \sqrt{2n(i)}}{2} \right)^{L-1} \exp\left(\frac{A_c^2 n(i)}{2}\right) (-j)^{L-1} \exp(-A_c^2 n(i)) \frac{1}{2[2A_c^2 n(i)]^{\frac{L-1}{2}}} \frac{1}{2^n n!} \times \\
&\quad \times L_n^{L-1}\left(-\frac{A_c^2 n(i)}{2}\right) \\
&= \sum_{n=0}^{L-1} \frac{1}{2^{n+1}} \exp\left(-\frac{A_c^2 n(i)}{2}\right) (-j)^{L-1} (j)^{L-1} \frac{1}{2^{L-1}} (2A_c^2 n(i))^{\frac{L-1}{2}} \frac{1}{[2A_c^2 n(i)]^{\frac{L-1}{2}}} L_n^{L-1}\left(-\frac{A_c^2 n(i)}{2}\right) \\
&= \sum_{n=0}^{L-1} \exp\left(-\frac{A_c^2 n(i)}{2}\right) \frac{1}{2^{n+L}} L_n^{L-1}\left(-\frac{A_c^2 n(i)}{2}\right) = \exp\left(-\frac{A_c^2 n(i)}{2}\right) \sum_{n=0}^{L-1} \frac{1}{2^{n+L}} \sum_{\rho=0}^n \frac{(-1)^\rho}{\rho!} \binom{L+n-1}{n-\rho} \times \\
&\quad \times \left(-\frac{A_c^2 n(i)}{2}\right)^\rho \\
P_s(i) &= \exp\left(-\frac{A_c^2 n(i)}{2}\right) \sum_{n=0}^{L-1} \frac{1}{2^{n+L}} \sum_{\rho=0}^n \frac{1}{\rho!} \binom{L+n-1}{n-\rho} \left(\frac{A_c^2 n(i)}{2}\right)^\rho. \tag{5.33}
\end{aligned}$$

Recalling that DPSK is a special case of noncoherent orthogonal modulation with  $T_s = 2T_b$  and  $E_s = 2E_b$ , then

$$\frac{A_c^2 n(i)}{2} = \frac{A_c^2}{2} \left( \frac{i}{\sigma_{\kappa_j}^2} + \frac{L-i}{\sigma_{\kappa}^2} \right) = \frac{A_c^2}{2} \left( \frac{i}{\frac{N_o + N_I/\rho}{2T_b}} + \frac{L-i}{\frac{N_o}{2T_b}} \right) = E_b \left( \frac{i}{N_o + N_I/\rho} + \frac{L-i}{N_o} \right) \tag{5.34}$$

Substituting Equation (5.34) into Equation (5.33), the result is

$$P_b(i) = \exp(-\gamma_b) \sum_{n=0}^{L-1} \frac{1}{2^{n+L}} \sum_{\rho=0}^n \frac{1}{\rho!} \binom{L+n-1}{n-\rho} (\gamma_b)^\rho \tag{5.35}$$

where

$$\gamma_b = E_b \left( \frac{i}{N_o + \frac{N_I}{\rho}} + \frac{L-i}{N_o} \right). \quad (5.36)$$

In JTIDS, an MSK chip demodulator is used at the receiver to recover the original scrambled 32-sequence on chip-by-chip basis. Hence,  $T_b$  must be replaced by  $T_c$  and  $E_b$  by  $E_c$  in Equations (5.35) and (5.36). Therefore,

$$P_c(i) = \exp(-\gamma_c) \sum_{n=0}^{L-1} \frac{1}{2^{n+L}} \sum_{\rho=0}^n \frac{1}{\rho!} \binom{L+n-1}{n-\rho} (\gamma_c)^\rho \quad (5.37)$$

and

$$\gamma_c = E_c \left( \frac{i}{N_o + \frac{N_I}{\rho}} + \frac{L-i}{N_o} \right). \quad (5.38)$$

The relationship of average energy per chip  $E_c$  with the average energy per bit  $E_b$  is given by Equations (3.1) through (3.4) and results in

$$E_c = \frac{5r_{cc} E_b}{32}. \quad (5.39)$$

Finally, combining Equations (5.37), (5.38) and (5.39), one gets the chip error probability

$$P_c(i) = \exp(-\gamma_c) \sum_{n=0}^{L-1} \frac{1}{2^{n+L}} \sum_{\rho=0}^n \frac{1}{\rho!} \binom{L+n-1}{n-\rho} (\gamma_c)^\rho \quad (5.40)$$

where

$$\gamma_c = \frac{5r_{cc} E_b}{32} \left( \frac{i}{N_o + \frac{N_I}{\rho}} + \frac{L-i}{N_o} \right). \quad (5.41)$$

After the 32-chip sequence is de-scrambled, the CCSK symbol demodulator detects the 5-bit symbol. The probability of symbol error given that  $i$  hops are jammed is given by Equation (3.7) and reproduced below for convenience:

$$p_{s(i)} = \sum_{j=0}^{32} \zeta_{UB_j} \binom{32}{j} p_{c(i)}^j (1 - p_{c(i)})^{32-j}. \quad (5.42)$$

The total probability of symbol error of a FFH system with diversity of  $L = 2$  is

$$p_s = \sum_{i=0}^{L-2} \binom{L}{i} \rho^i (1 - \rho)^{L-i} p_{s(i)},$$

$$p_s = (1 - \rho)^2 p_{s0} + 2\rho(1 - \rho) p_{s1} + \rho^2 p_{s2}. \quad (5.43)$$

The probability of symbol error  $P_s$  at the output of the RS decoder, the probability of bit error  $p_b$  at the output of the symbol-to-bit converter, and the probability of bit error  $P_b$  at the output of the convolutional decoder are evaluated in the same way as for coherent demodulation in Chapter III using Equations (3.8) through (3.12).

#### **B. PERFORMANCE ANALYSIS OF NONCOHERENT DEMODULATION OF 32-ARY CCSK WITH DIVERSITY AND NOISE-NORMALIZATION IN AWGN AND PNI**

Noncoherent demodulation always has worse performance than coherent demodulation. Based on the analysis, both the alternative waveform and the original JTIDS waveform cannot achieve reliable communications when noncoherent detection is employed and  $E_b / N_o < 7.0$  dB. If  $E_b / N_o = 8.0$  dB, then only the higher code rate alternative waveforms can achieve satisfactory performance. However, in this case the signal power must be much higher than the noise interference power ( $E_b / N_i \gg 1$ ). The use of the noise-normalized receiver again neutralizes the effects of partial-band interference since the performance of the system for  $\rho < 1$  relative to barrage noise interference ( $\rho = 1$ ) is approximately the same or better. These performance results are summarized in Table 6, which is based on the results shown in Figures 31 through 35.

$P_b$	$\rho$	$\kappa=15$ $E_b / N_I$ (dB)	$\kappa=17$ $E_b / N_I$ (dB)	$\kappa=19$ $E_b / N_I$ (dB)	$\kappa=21$ $E_b / N_I$ (dB)	$\kappa=23$ $E_b / N_I$ (dB)	$\kappa=25$ $E_b / N_I$ (dB)	$\kappa=27$ $E_b / N_I$ (dB)	Existing JTIDS $E_b / N_I$ (dB)
$10^{-5}$	0.1	inferior	inferior	inferior	inferior	23.0	19.7	18.4	inferior
$10^{-5}$	0.3	inferior	inferior	inferior	inferior	23.4	19.9	18.6	inferior
$10^{-5}$	0.5	inferior	inferior	inferior	inferior	23.3	19.9	18.6	inferior
$10^{-5}$	0.7	inferior	inferior	inferior	inferior	23.5	20.0	18.5	inferior
$10^{-5}$	1	inferior	inferior	inferior	inferior	23.5	20.0	18.6	inferior

Table 6. Comparison of the Performance of the Original and the Alternative JTIDS Waveform for Different Values of  $\rho$  for Noncoherent Demodulation when  $E_b/N_0 = 8.0$  dB.

As the signal-to-noise ratio  $E_b/N_o$  increases, the benefits of using noise-normalization become more obvious. In Table 7, the performance results of the alternative waveform with noise-normalization and those for the existing JTIDS waveform with noise-normalization when  $E_b/N_o = 10.0$  dB are summarized. The results presented in Table 7 are based on the results shown in Figures 36 through 40.

$P_b$	$\rho$	$\kappa=15$ $E_b / N_I$ (dB)	$\kappa=17$ $E_b / N_I$ (dB)	$\kappa=19$ $E_b / N_I$ (dB)	$\kappa=21$ $E_b / N_I$ (dB)	$\kappa=23$ $E_b / N_I$ (dB)	$\kappa=25$ $E_b / N_I$ (dB)	$\kappa=27$ $E_b / N_I$ (dB)	Existing JTIDS $E_b / N_I$ (dB)
$10^{-5}$	0.1	superior	superior	superior	superior	superior	superior	superior	13.5
$10^{-5}$	0.3	14.9	13.0	11.8	11.2	11.1	11.2	11.6	16.3
$10^{-5}$	0.5	15.7	14.0	13.1	12.5	12.1	11.9	11.9	16.4
$10^{-5}$	0.7	15.9	14.3	13.2	12.6	12.2	11.8	11.7	16.4
$10^{-5}$	1	16.0	14.4	13.3	12.5	12.0	11.6	11.4	16.3

Table 7. Comparison of the Performance of the Original and the Alternative JTIDS Waveform for Different Values of  $\rho$  for Noncoherent Demodulation when  $E_b/N_0 = 10.0$  dB.

It can be inferred from Table 7 that the existing JTIDS waveform performs worse than the alternative one in all cases. For  $\rho = 0.1$  (i.e., 10% jam interval) the performance with the alternative waveform is outstanding and always provides reliable communications. The higher rate code alternative waveforms have superior performance

as compared to the lower rate codes. The performance of the alternative waveform is not affected in a significant manner by increasing  $\rho$  when  $\rho > 0.5$ . The noise-normalized receiver mitigates the effects of partial-band interference, and the interferer is forced to abandon the partial-band interference strategy and adopt full-band interference. Finally, the degradation of the performance of noncoherent demodulation relative to coherent demodulation is extremely large for both the alternative and the original JTIDS waveform.

In Chapter III, it was observed that for the optimum alternative waveforms with either RS (31, 23) or RS (31, 25) inner codes in AWGN, where noise-normalization did not need to be employed, there was a gain of 2.3 dB and 2.2 dB, respectively, with coherent as opposed to noncoherent demodulation. Increasing the ratio  $E_b / N_o$  by 3.0 dB, the author investigates the difference in the performance of coherent and noncoherent demodulation in the new environment with both AWGN and PNI, and noise-normalization is utilized to degrade the effects of pulse-noise interference on the overall performance of the system. In Table 8, the performance results for the alternative waveform with noise-normalization and those for the existing JTIDS waveform with noise-normalization when  $E_b / N_o = 13.0$  dB are shown. The results in Table 8 are based on the results shown in Figures 41 through 44.

$P_b$	$\rho$	$\kappa=15$ $E_b / N_I$ (dB)	$\kappa=17$ $E_b / N_I$ (dB)	$\kappa=19$ $E_b / N_I$ (dB)	$\kappa=21$ $E_b / N_I$ (dB)	$\kappa=23$ $E_b / N_I$ (dB)	$\kappa=25$ $E_b / N_I$ (dB)	$\kappa=27$ $E_b / N_I$ (dB)	Existing JTIDS $E_b / N_I$ (dB)
$10^{-5}$	0.1	superior	superior	superior	superior	superior	superior	superior	superior
$10^{-5}$	0.3	superior	superior	superior	superior	3.1	8.5	9.9	11
$10^{-5}$	0.5	10.1	10.0	10.0	10.0	10.1	10.2	10.3	12.1
$10^{-5}$	0.7	11.2	10.7	10.4	10.1	10.0	9.8	9.8	11.8
$10^{-5}$	1	11.3	10.6	10.1	9.8	9.5	9.2	9.1	11.3

Table 8. Comparison of the Performance of the Original and the Alternative JTIDS Waveform for Different Values of  $\rho$  for Noncoherent Demodulation when  $E_b / N_o = 13.0$  dB.

By comparing Tables 4 and 8, one can conclude that despite the difference of 3.0 dB in  $E_b/N_0$  between coherent and noncoherent demodulation (10.0 dB and 13.0 dB, respectively) the performance of the alternative waveform with either RS (31, 23) or RS (31, 25) inner codes and coherent demodulation is still better by 2.0 dB to 3.0 dB for the various values of  $\rho$  examined. Therefore, in a hostile environment where pulse-noise interference and AWGN are present, the use of coherent demodulation at the receiver is more important, and the capability to employ coherent demodulation is a significant advantage in an electronic warfare environment.

For comparison purposes, the performance results for the alternative waveform in extremely favorable transmitting conditions, where  $E_b/N_0 = 15.0$  dB, are summarized in Table 9, which is based on the results shown in Figures 45 through 48.

The alternative waveform again outperforms relative to the existing JTIDS waveform, especially, for the inner RS (31,  $\kappa$ ) codes where  $\kappa < 23$  and  $\rho < 0.5$ . Finally, the degradation of the performance due to noncoherent demodulation instead of coherent demodulation is not as large as when  $E_b/N_0 = 10.0$  dB. For  $\rho < 0.5$  the performance of the alternative waveform with RS (31,  $\kappa$ ) when  $\kappa < 23$  is outstanding. For larger values of  $\rho$  the difference does not exceed 5.0 dB, and as  $\rho$  increases the degradation due to noncoherent detection becomes smaller.

$P_b$	$\rho$	$\kappa=15$ $E_b/N_i$ (dB)	$\kappa=17$ $E_b/N_i$ (dB)	$\kappa=19$ $E_b/N_i$ (dB)	$\kappa=21$ $E_b/N_i$ (dB)	$\kappa=23$ $E_b/N_i$ (dB)	$\kappa=25$ $E_b/N_i$ (dB)	$\kappa=27$ $E_b/N_i$ (dB)	Existing $E_b/N_i$ (dB)
$10^{-5}$	0.1	superior	superior	superior	superior	superior	superior	superior	superior
$10^{-5}$	0.3	superior	superior	superior	superior	superior	8.3	9.7	10.6
$10^{-5}$	0.5	9.3	9.4	9.5	9.6	9.7	9.8	9.9	11.5
$10^{-5}$	0.7	10.4	10.1	9.8	9.6	9.5	9.4	9.4	11.0
$10^{-5}$	1	10.3	9.8	9.4	9.1	8.8	8.6	8.5	10.3

Table 9. Comparison of the Performance of the Original and the Alternative JTIDS Waveform for Different Values of  $\rho$  for Noncoherent Demodulation when  $E_b/N_0 = 15.0$  dB.

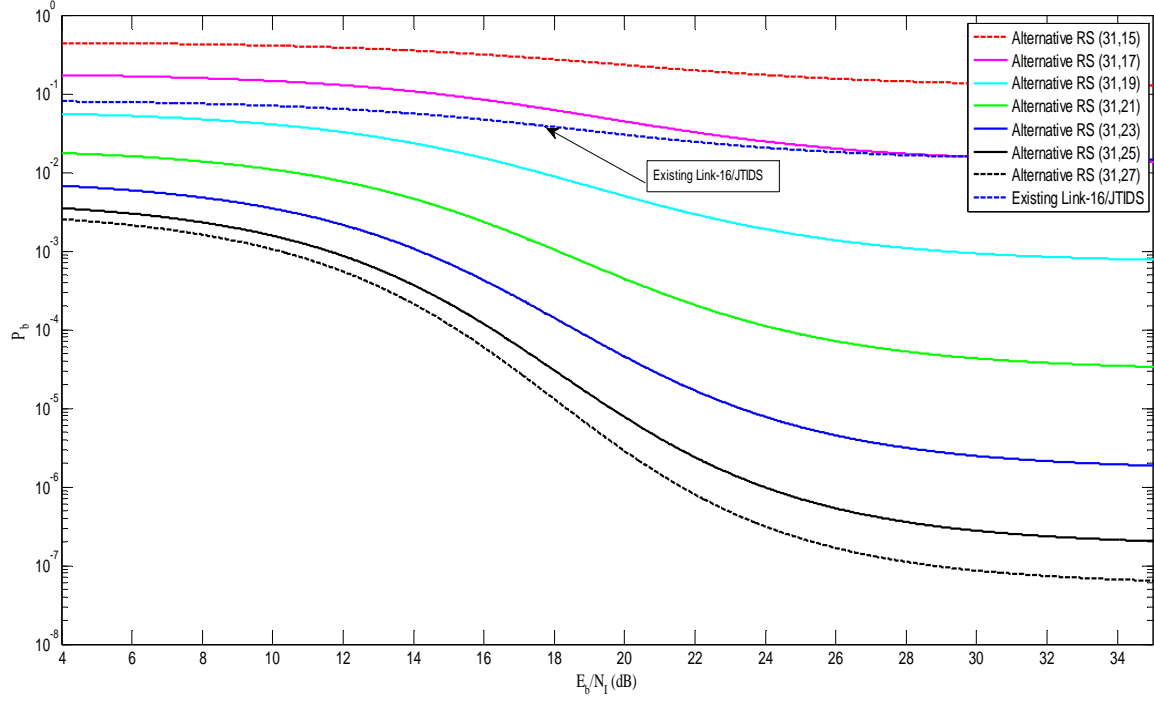


Figure 31. Performance of 32-ary CCSK Using the Alternative Error Correction Coding Scheme with Diversity and Noise-normalization in AWGN and PNI with  $\rho = 0.1$  when  $E_b / N_o = 8.0\text{dB}$ .

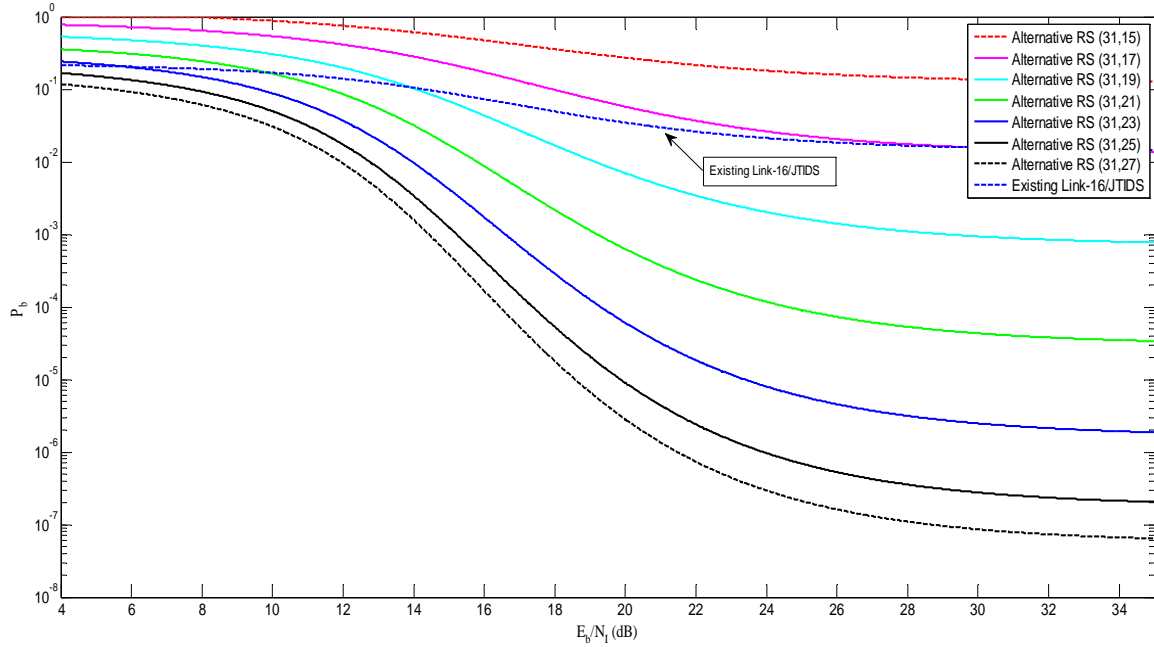


Figure 32. Performance of 32-ary CCSK Using the Alternative Error Correction Coding Scheme with Diversity and Noise-normalization in AWGN and PNI with  $\rho = 0.3$  when  $E_b / N_o = 8.0\text{dB}$ .

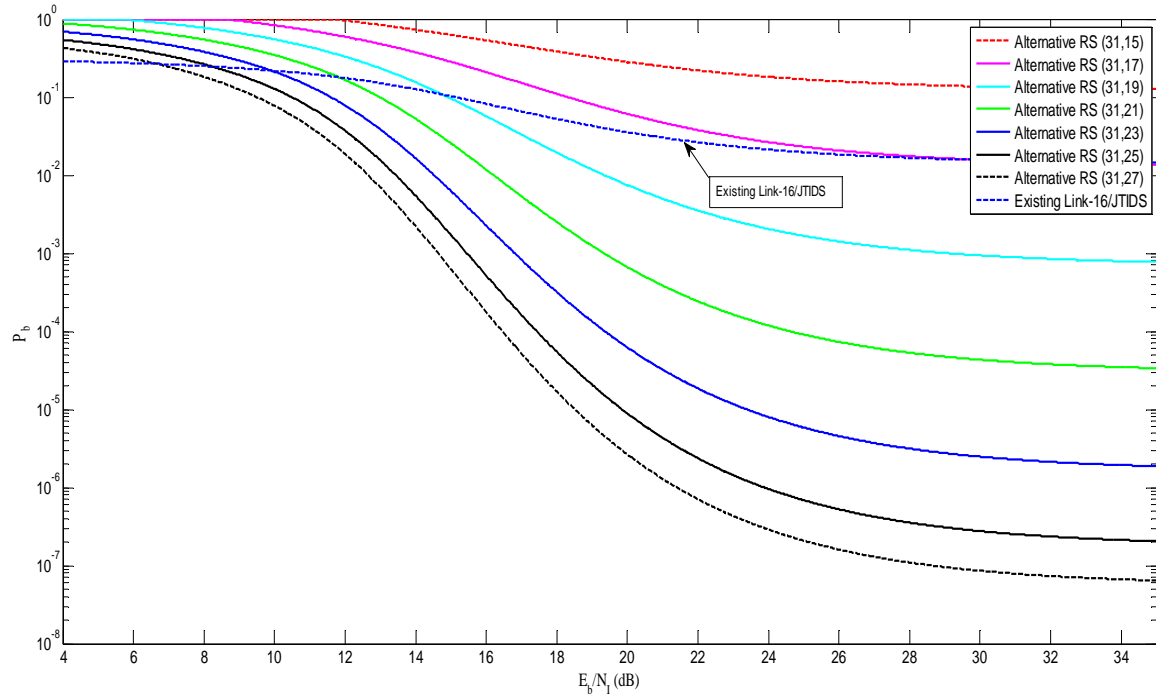


Figure 33. Performance of 32-ary CCSK Using the Alternative Error Correction Coding Scheme with Diversity and Noise-normalization in AWGN and PNI with  $\rho = 0.5$  when  $E_b / N_o = 8.0$  dB.

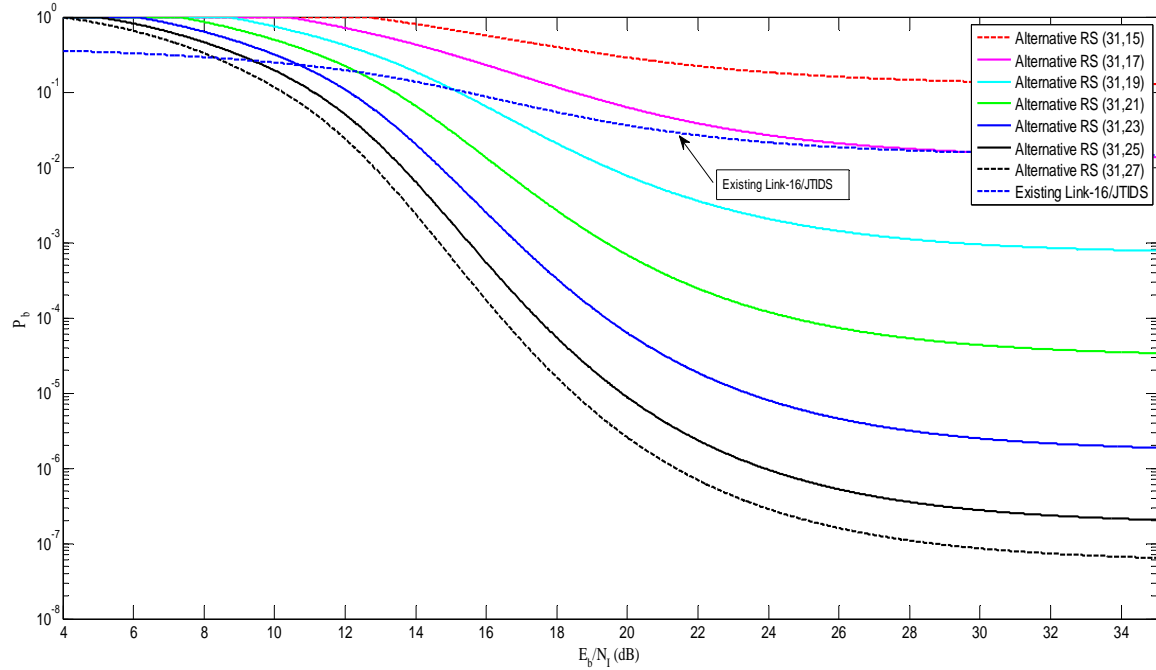


Figure 34. Performance of 32-ary CCSK Using the Alternative Error Correction Coding Scheme with Diversity and Noise-normalization in AWGN and PNI with  $\rho = 0.7$



when  $E_b / N_o = 8.0\text{dB}$ .

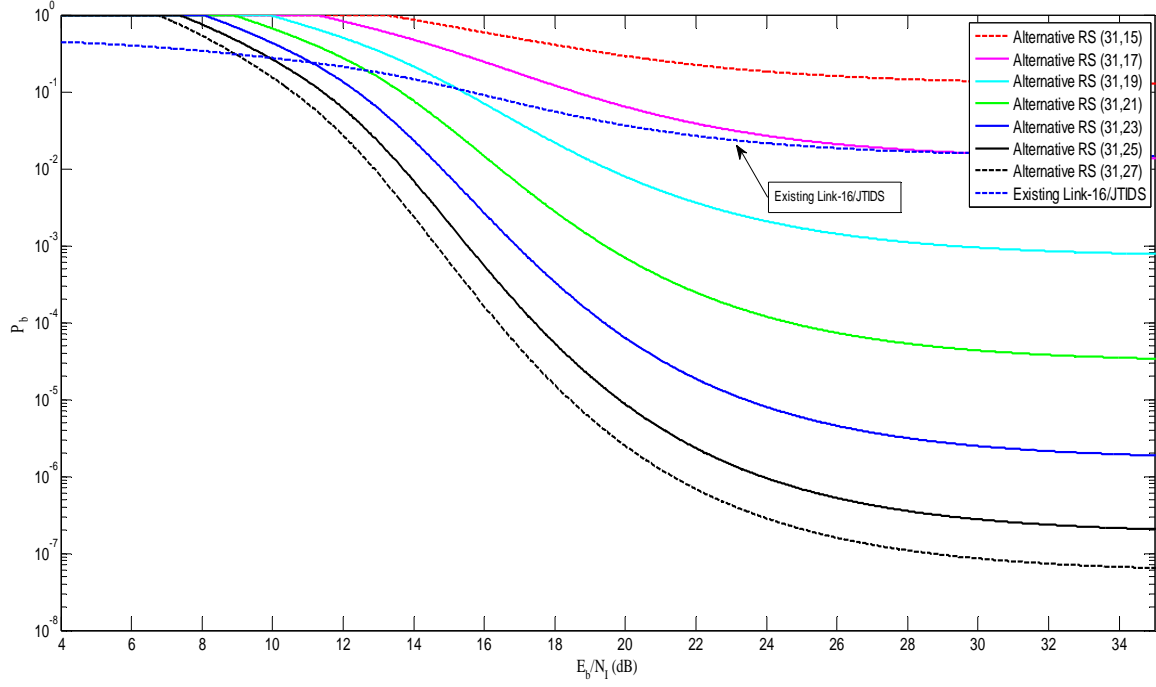


Figure 35. Performance of 32-ary CCSK Using the Alternative Error Correction Coding Scheme with Diversity and Noise-normalization in AWGN and PNI with  $\rho = 1.0$  when  $E_b / N_o = 8.0\text{dB}$ .

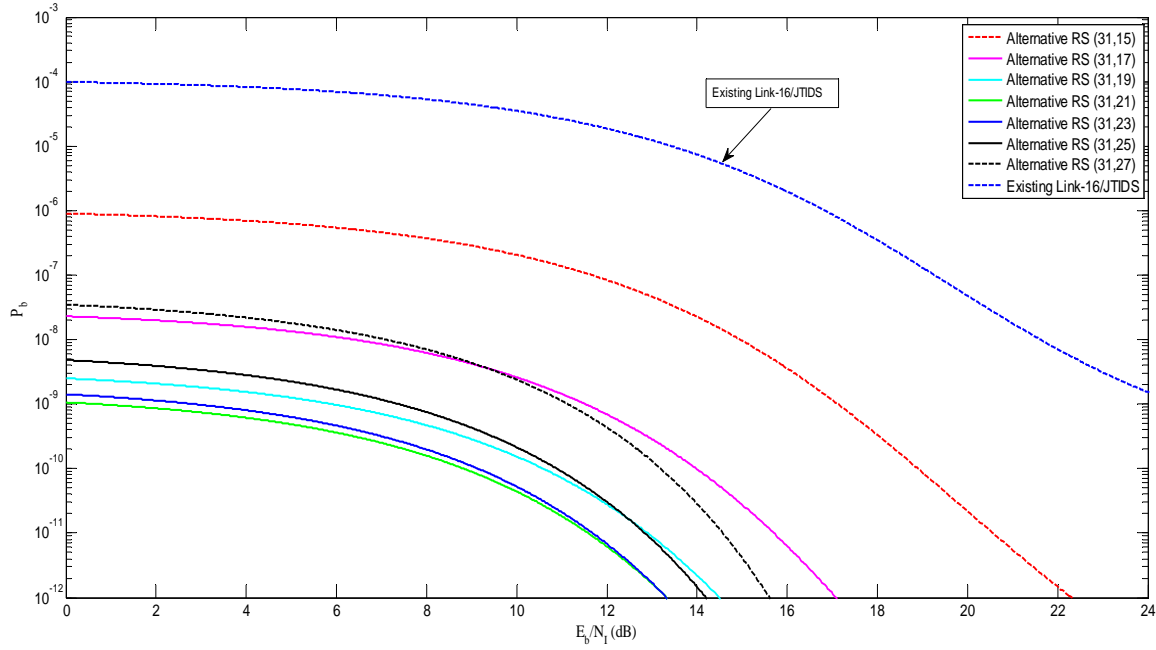


Figure 36. Performance of 32-ary CCSK Using the Alternative Error Correction Coding Scheme with Diversity and Noise-normalization in AWGN and PNI with  $\rho = 0.1$

when  $E_b / N_o = 10.0$  dB.

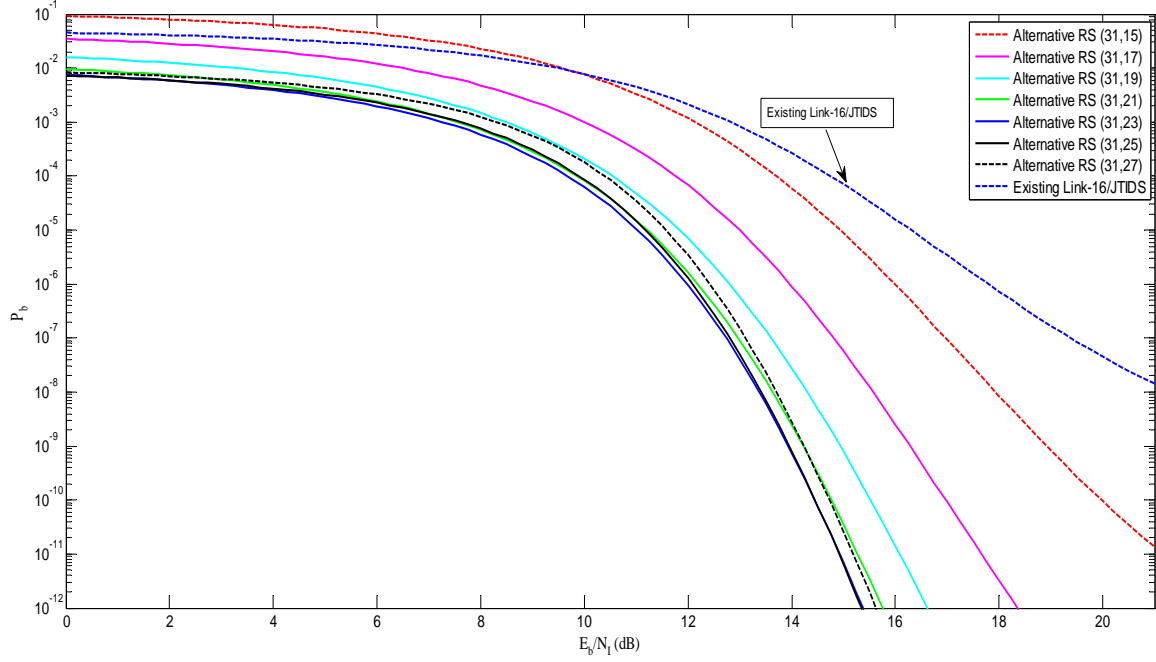


Figure 37. Performance of 32-ary CCSK Using the Alternative Error Correction Coding Scheme with Diversity and Noise-normalization in AWGN and PNI with  $\rho = 0.3$  when  $E_b / N_o = 10.0$  dB.

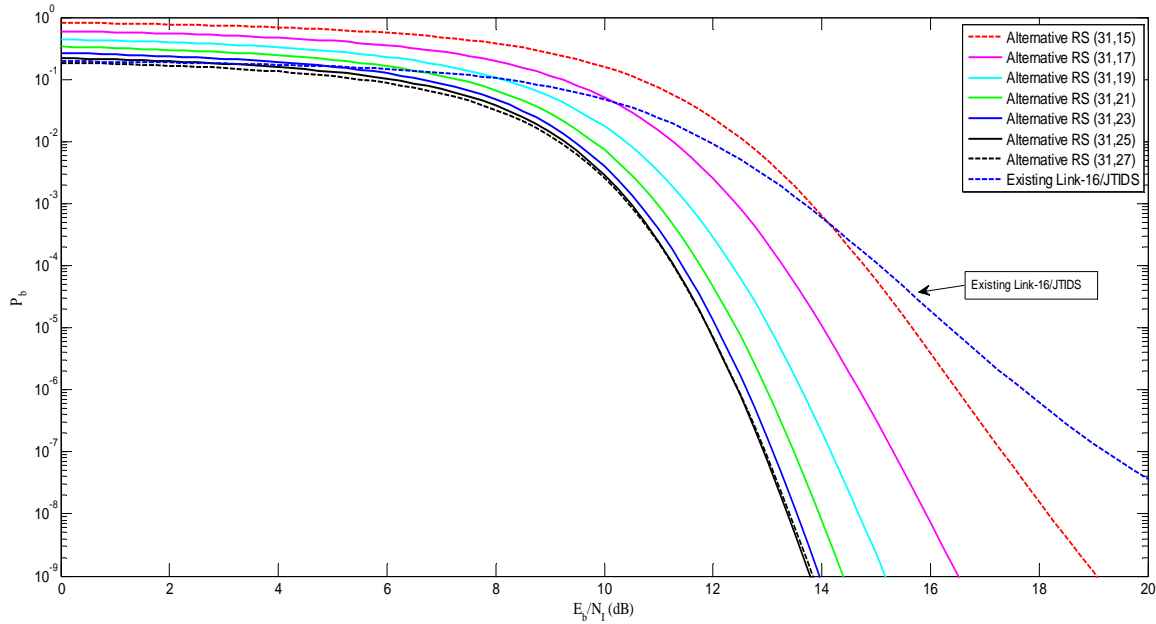


Figure 38. Performance of 32-ary CCSK Using the Alternative Error Correction Coding Scheme with Diversity and Noise-normalization in AWGN and PNI with  $\rho = 0.5$  when  $E_b / N_o = 10.0$  dB.

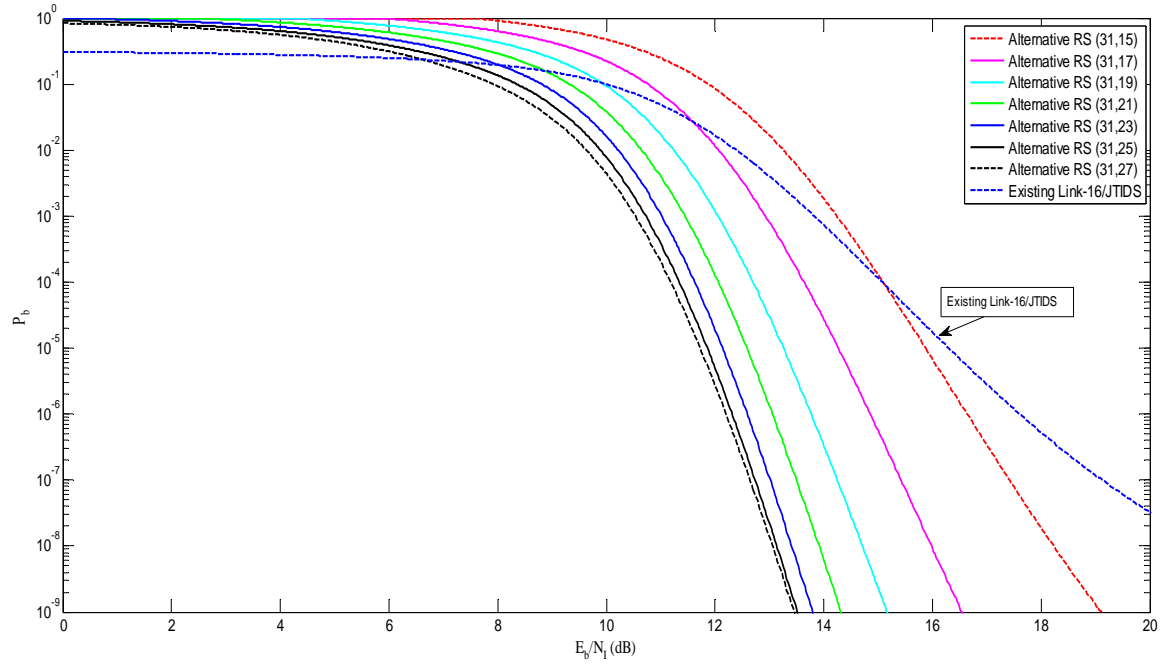


Figure 39. Performance of 32-ary CCSK Using the Alternative Error Correction Coding Scheme with Diversity and Noise-normalization in AWGN and PNI with  $\rho = 0.7$  when  $E_b / N_o = 10.0$  dB.

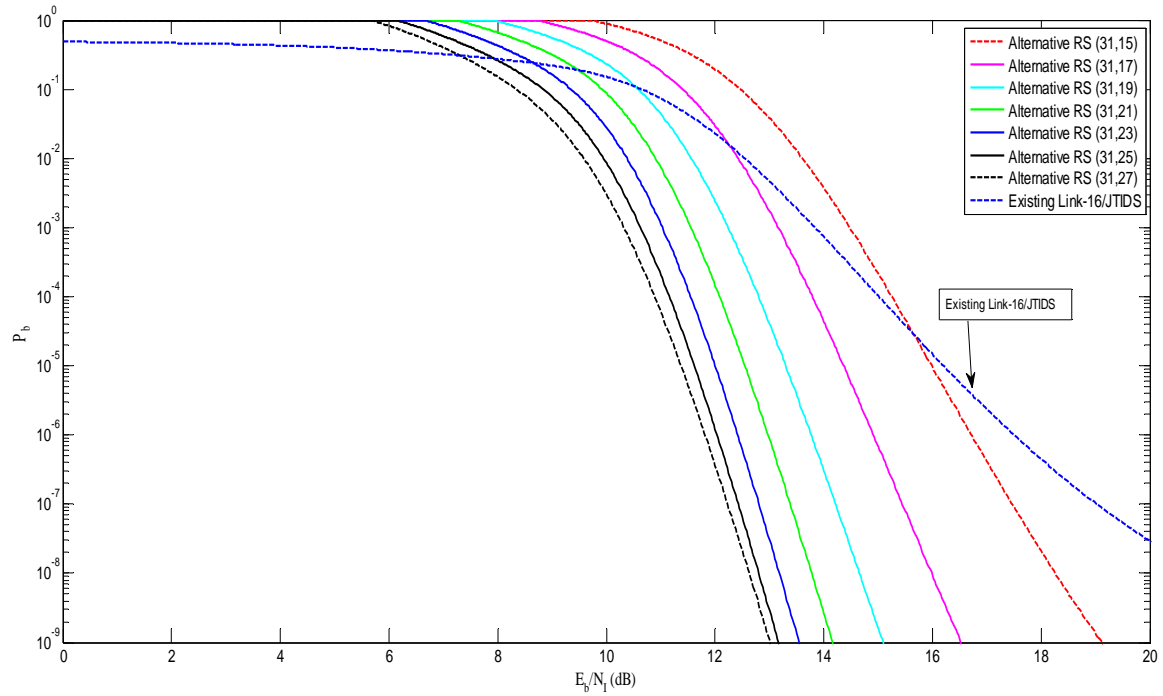


Figure 40. Performance of 32-ary CCSK Using the Alternative Error Correction Coding Scheme with Diversity and Noise-normalization in AWGN and PNI with  $\rho = 1.0$  when  $E_b / N_o = 10.0$  dB.

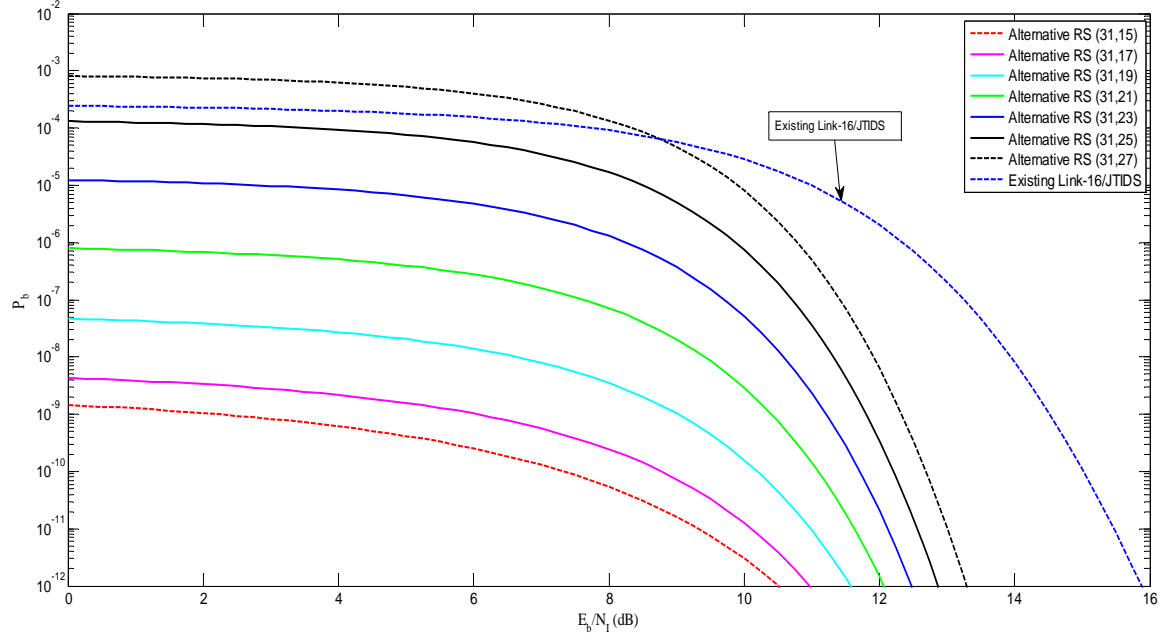


Figure 41. Performance of 32-ary CCSK Using the Alternative Error Correction Coding Scheme with Diversity and Noise-normalization in AWGN and PNI with  $\rho = 0.3$  when  $E_b / N_o = 13.0$  dB.

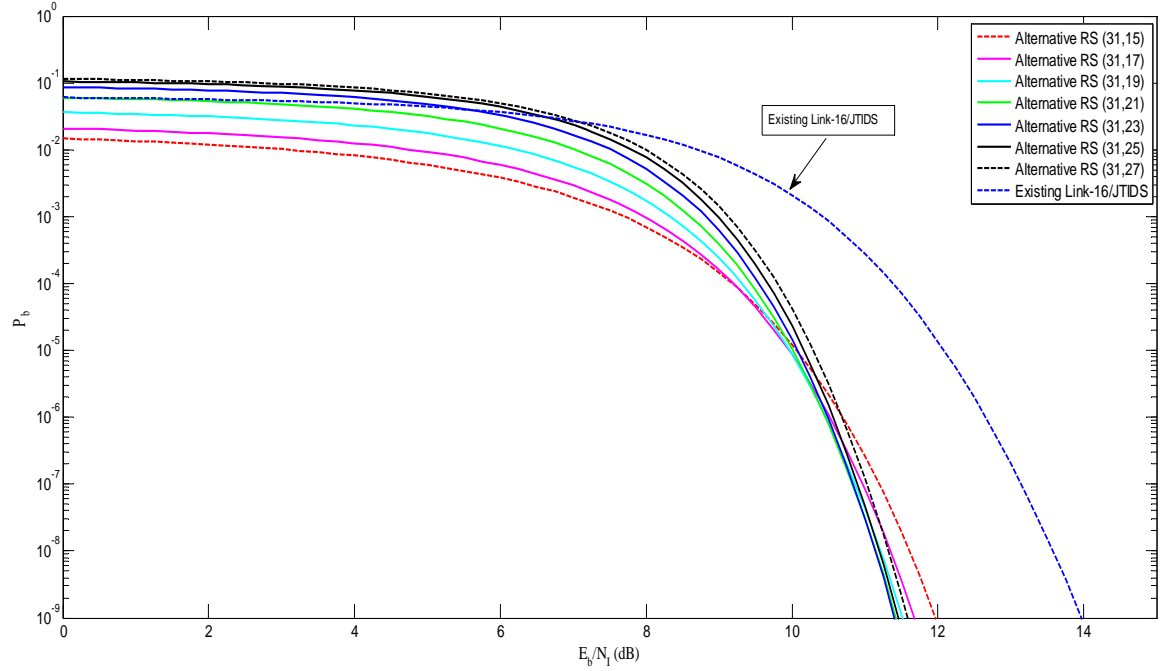


Figure 42. Performance of 32-ary CCSK Using the Alternative Error Correction Coding Scheme with Diversity and Noise-normalization in AWGN and PNI with  $\rho = 0.5$  when  $E_b / N_o = 13.0$  dB.

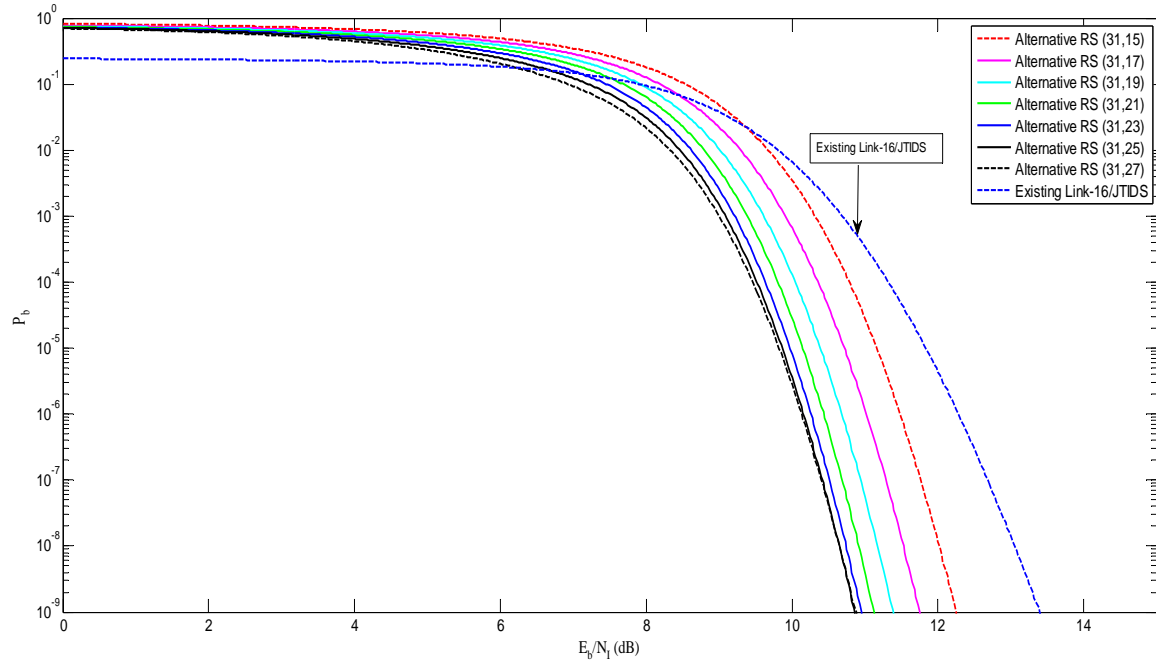


Figure 43. Performance of 32-ary CCSK Using the Alternative Error Correction Coding Scheme with Diversity and Noise-normalization in AWGN and PNI with  $\rho = 0.7$  when  $E_b / N_o = 13.0$  dB.

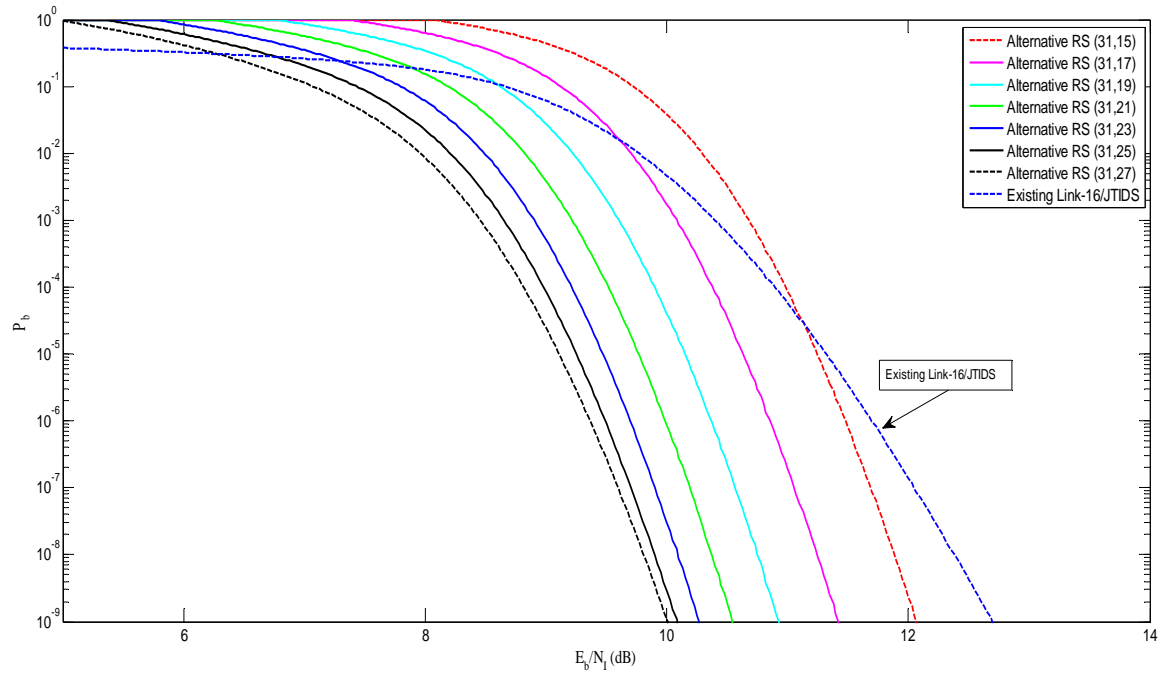


Figure 44. Performance of 32-ary CCSK Using the Alternative Error Correction Coding Scheme with Diversity and Noise-normalization in AWGN and PNI with  $\rho = 1.0$  when  $E_b / N_o = 13.0$  dB.

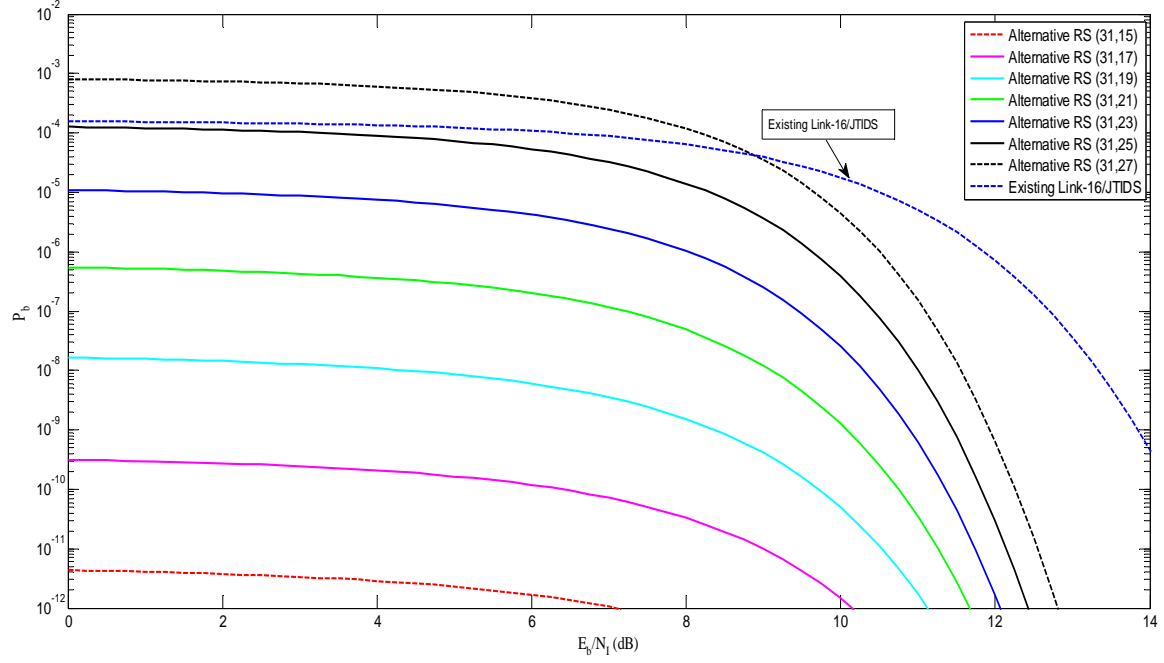


Figure 45. Performance of 32-ary CCSK Using the Alternative Error Correction Coding Scheme with Diversity and Noise-normalization in AWGN and PNI with  $\rho = 0.3$  when  $E_b / N_o = 15.0$  dB.

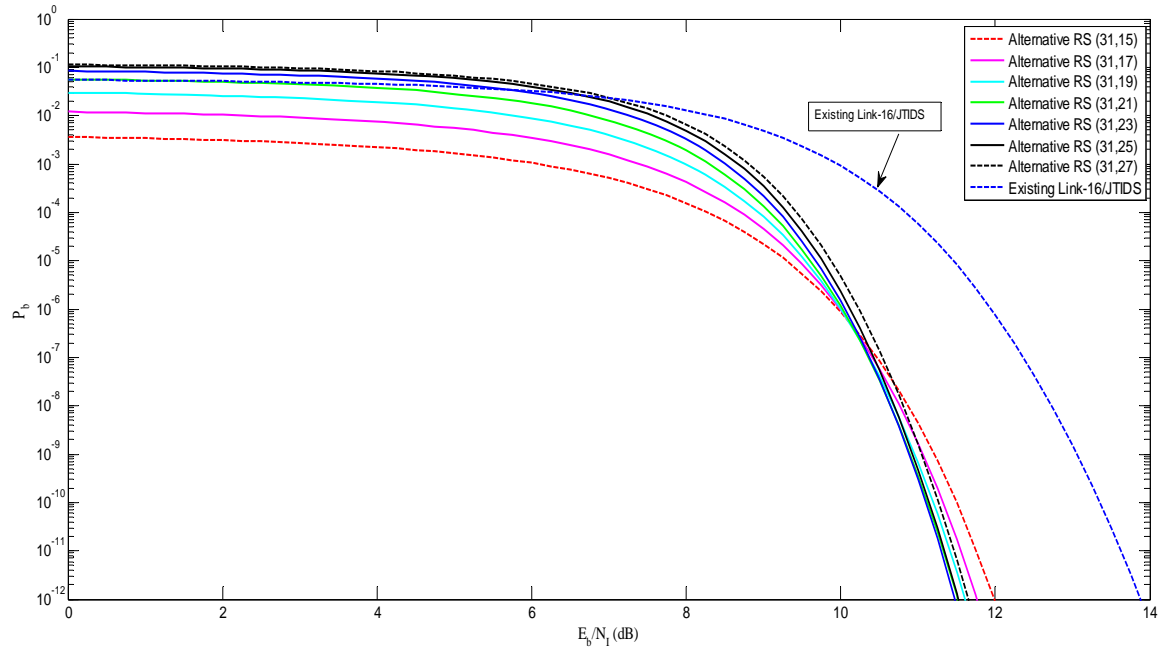


Figure 46. Performance of 32-ary CCSK Using the Alternative Error Correction Coding Scheme with Diversity and Noise-normalization in AWGN and PNI with  $\rho = 0.5$  when  $E_b / N_o = 15.0$  dB.

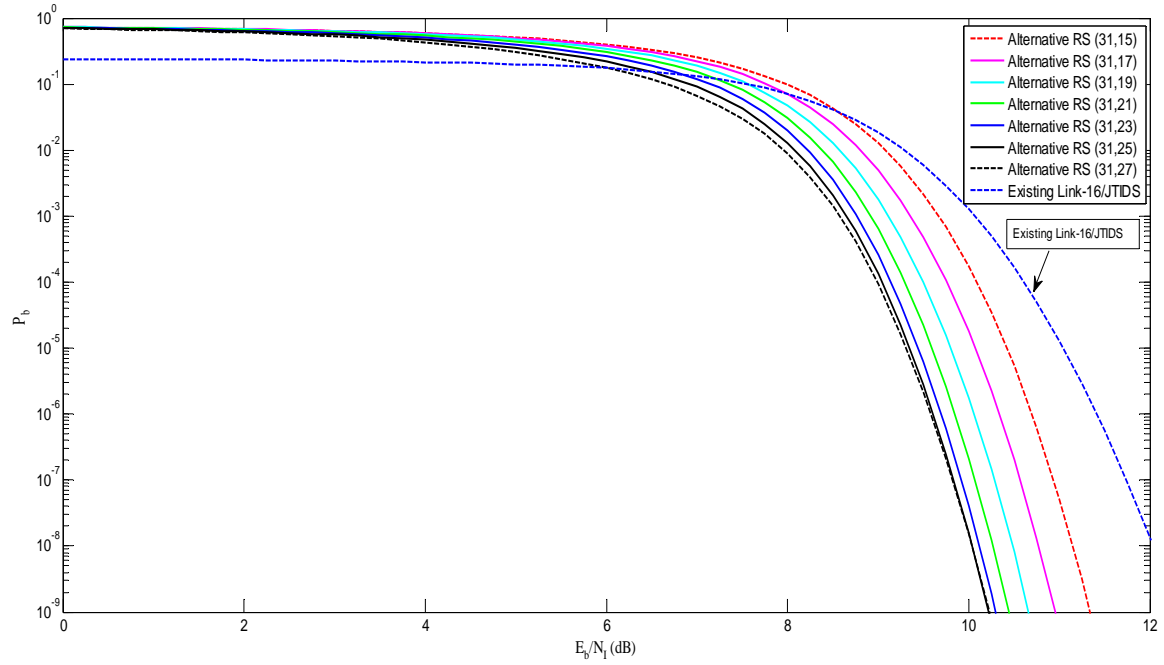


Figure 47. Performance of 32-ary CCSK Using the Alternative Error Correction Coding Scheme with Diversity and Noise-normalization in AWGN and PNI with  $\rho = 0.7$  when  $E_b / N_o = 15.0$  dB.

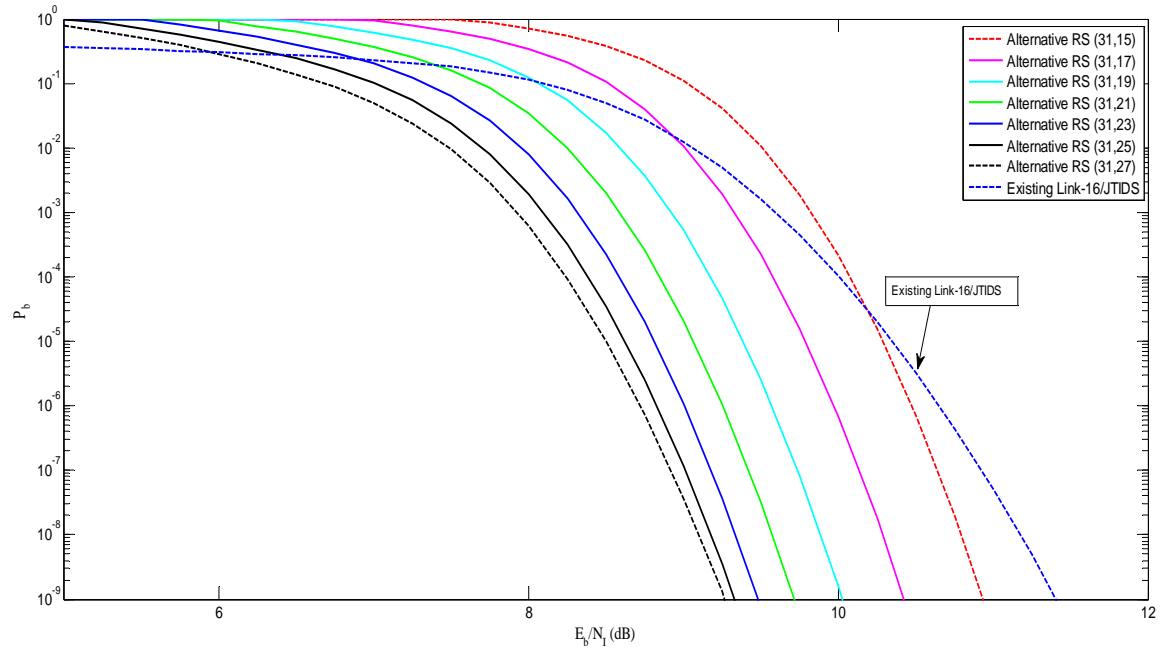


Figure 48. Performance of 32-ary CCSK Using the Alternative Error Correction Coding Scheme with Diversity and Noise-normalization in AWGN and PNI with  $\rho = 1.0$  when  $E_b / N_o = 15.0$  dB.

**C. COMPARISON OF THE PERFORMANCE OF THE ALTERNATIVE WAVEFORM WITH SLOPE DETECTION OR WITH QUADRATURE-CORRELATOR SQUARE-LAW DETECTION FOR NONCOHERENT DEMODULATION OF 32-ARY CCSK WITH DIVERSITY AND NOISE-NORMALIZATION IN AWGN AND PNI**

The use of slope detectors, compared to demodulation with matched filters or correlators, is best in terms of performance. In Figures 49 through 52, the alternative waveform performance with inner RS(31, 23), RS(31, 25) and RS(31, 27) codes are plotted for both slope detection and matched filter detection when  $E_b/N_0 = 12.0$  dB. The performance results for various values of  $\rho$  are summarized in Table 10.

The alternative waveform in all cases has outstanding performance when  $\rho = 0.1$ . As  $\rho$  increases, the degradation of the performance is very high when matched filters are employed instead of slope detectors, and this degradation can reach 10.0 dB. The noise-normalized receiver still cancels out the effects of pulse-noise interference.

$P_b$	$\rho$	RS(31,23) $E_b / N_t$ (dB) Matched filter	RS(31,23) $E_b / N_t$ (dB) Slope detector	RS(31,25) $E_b / N_t$ (dB) Matched filter	RS(31,25) $E_b / N_t$ (dB) Slope detector	RS(31,27) $E_b / N_t$ (dB) Matched filter	RS(31,27) $E_b / N_t$ (dB) Slope detector
$10^{-5}$	0.1	superior	superior	superior	superior	superior	superior
$10^{-5}$	0.3	17.1	5.8	16.6	8.8	16.6	10.1
$10^{-5}$	0.5	17.4	10.5	16.9	10.5	16.6	10.5
$10^{-5}$	0.7	17.3	10.3	16.8	10.3	16.5	10.3
$10^{-5}$	1	17.4	10.0	16.7	9.8	16.3	9.6

Table 10. Comparison of the Performance of the Alternative Waveform for Different Values of  $\rho$  for Noncoherent Demodulation with Matched Filter Detection and Slope Detection with  $E_b/N_0 = 12.0$  dB.

In AWGN, when slope detection is used, the performance of the alternative waveform with no diversity is improved about 3.0 dB relative to matched filter detection. How the sensitivity of these two different receivers is affected when AWGN and PNI are present is shown in Table 11. The results in Table 11 are based on the results shown in Figures 53 through 56.



$P_b$	$\rho$	RS(31,23) $E_b / N_I$ (dB) Matched filter	RS(31,23) $E_b / N_I$ (dB) Slope detector	RS(31,25) $E_b / N_I$ (dB) Matched filter	RS(31,25) $E_b / N_I$ (dB) Slope detector	RS(31,27) $E_b / N_I$ (dB) Matched filter	RS(31,27) $E_b / N_I$ (dB) Slope detector
$10^{-5}$	0.1	superior	superior	superior	superior	superior	superior
$10^{-5}$	0.3	8.8	5.8	11.8	8.8	13.1	10.1
$10^{-5}$	0.5	13.5	10.5	13.5	10.5	13.6	10.5
$10^{-5}$	0.7	13.4	10.3	13.3	10.3	13.3	10.3
$10^{-5}$	1	13.0	10.0	12.8	9.8	12.6	9.6

Table 11. Comparison of the Performance of the Alternative Waveform for Different Values of  $\rho$  for Noncoherent Demodulation with Matched Filter Detection with  $E_b/N_0 = 15.0$  dB and Slope Detection with  $E_b/N_0 = 12.0$  dB.

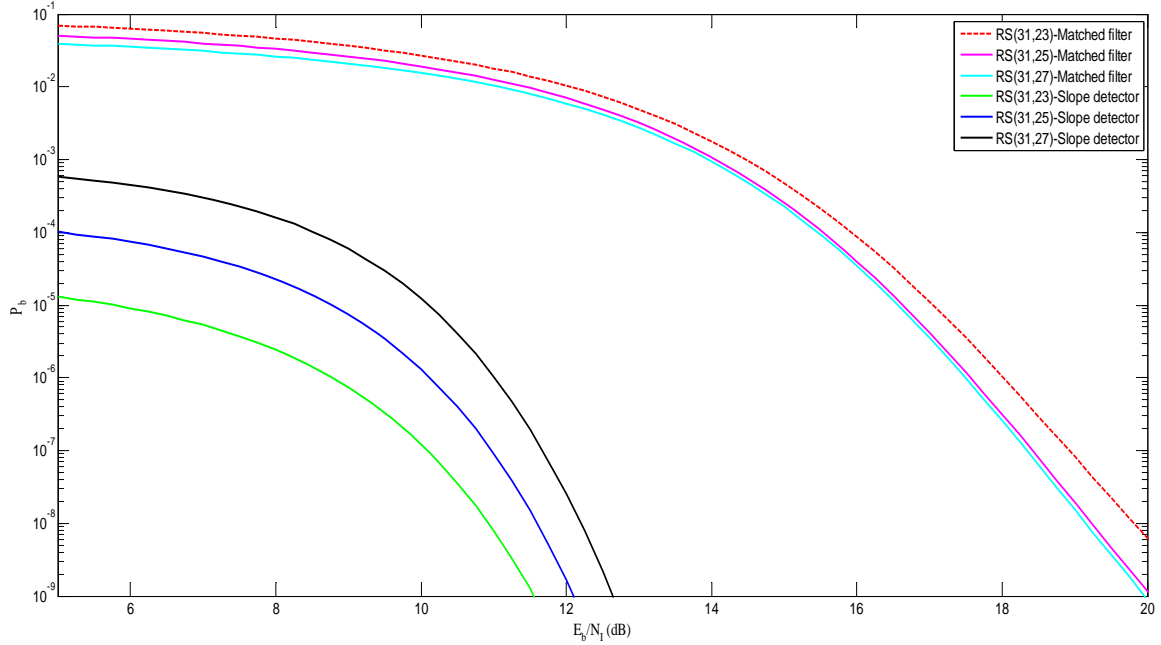


Figure 49. Performance of 32-ary CCSK Using the Alternative Error Correction Coding Scheme with Diversity and Noise-normalization in AWGN and PNI with  $\rho = 0.3$  for Both Matched Filter and Slope Detection when  $E_b / N_o = 12.0$  dB.

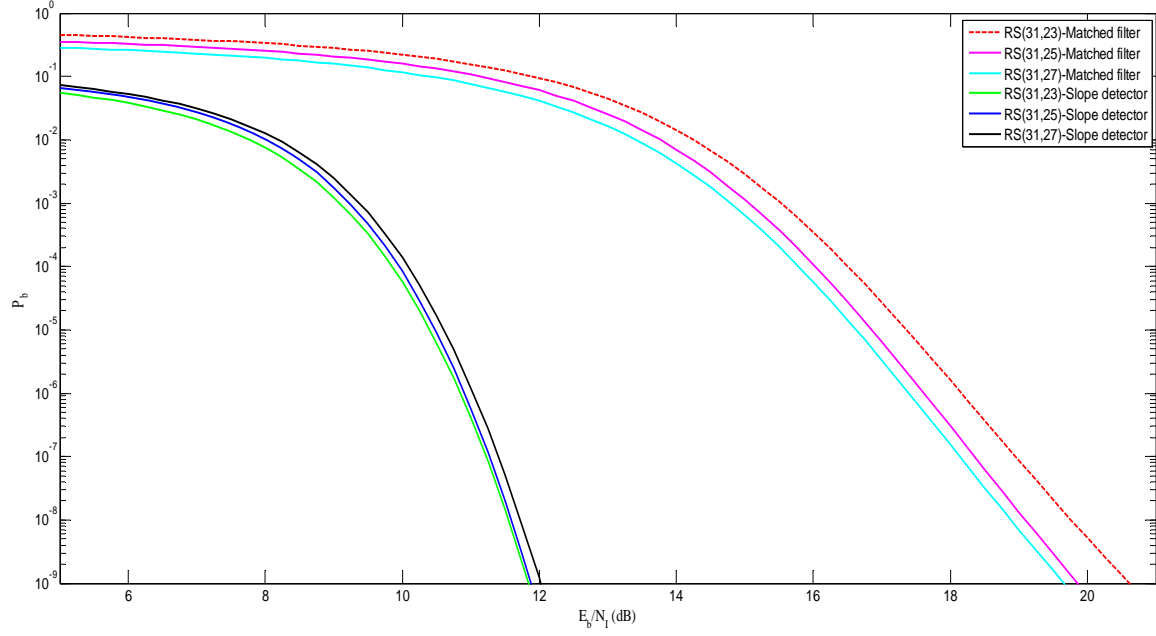


Figure 50. Performance of 32-ary CCSK Using the Alternative Error Correction Coding Scheme with Diversity and Noise-normalization in AWGN and PNI with  $\rho = 0.5$  for Both Matched Filter and Slope Detection when  $E_b / N_o = 12.0$  dB.

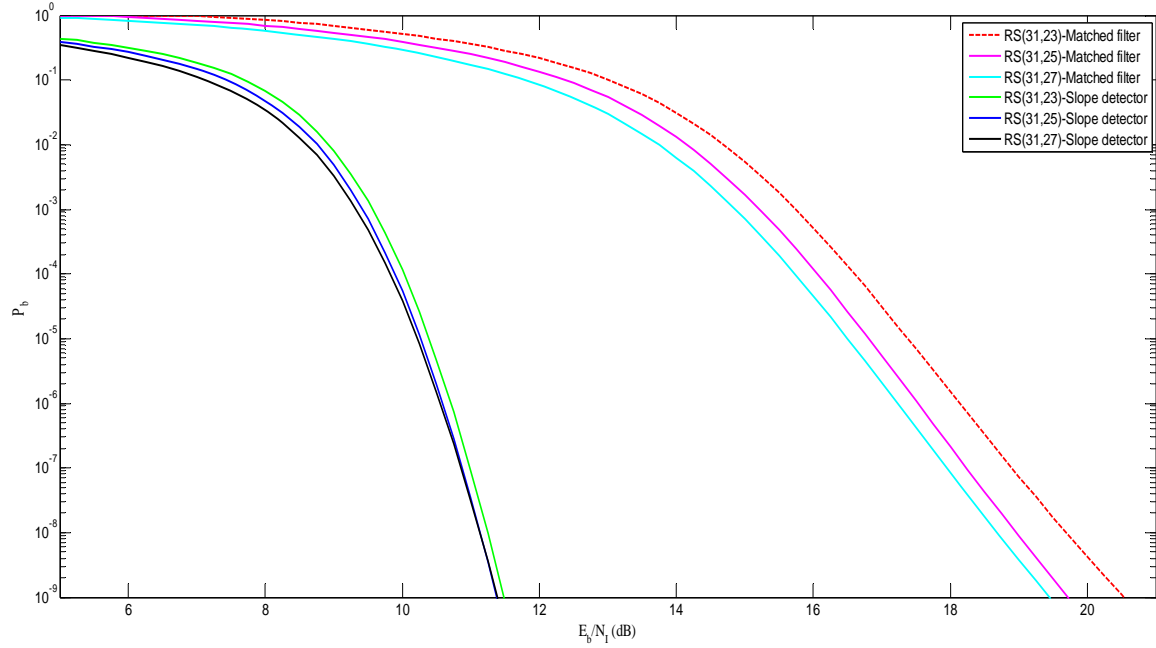


Figure 51. Performance of 32-ary CCSK Using the Alternative Error Correction Coding Scheme with Diversity and Noise-normalization in AWGN and PNI with  $\rho = 0.7$  for Both Matched Filter and Slope Detection when  $E_b / N_o = 12.0$  dB.

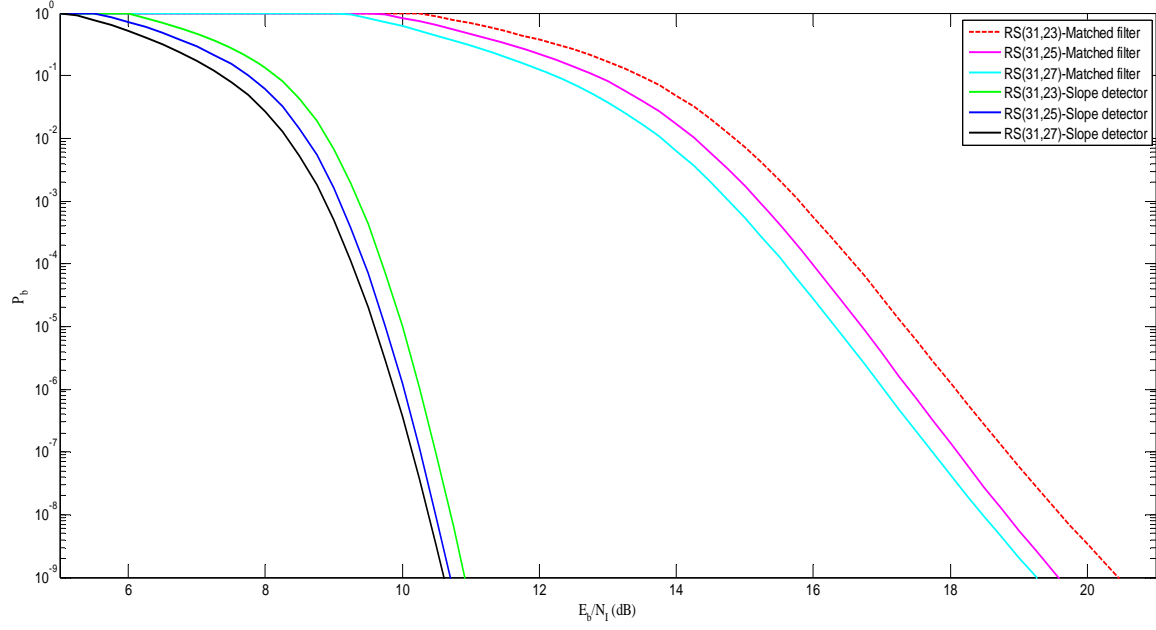


Figure 52. Performance of 32-ary CCSK Using the Alternative Error Correction Coding Scheme with Diversity and Noise-normalization in AWGN and PNI with  $\rho = 1.0$  for Both Matched Filter and Slope Detection when  $E_b / N_o = 12.0$  dB.

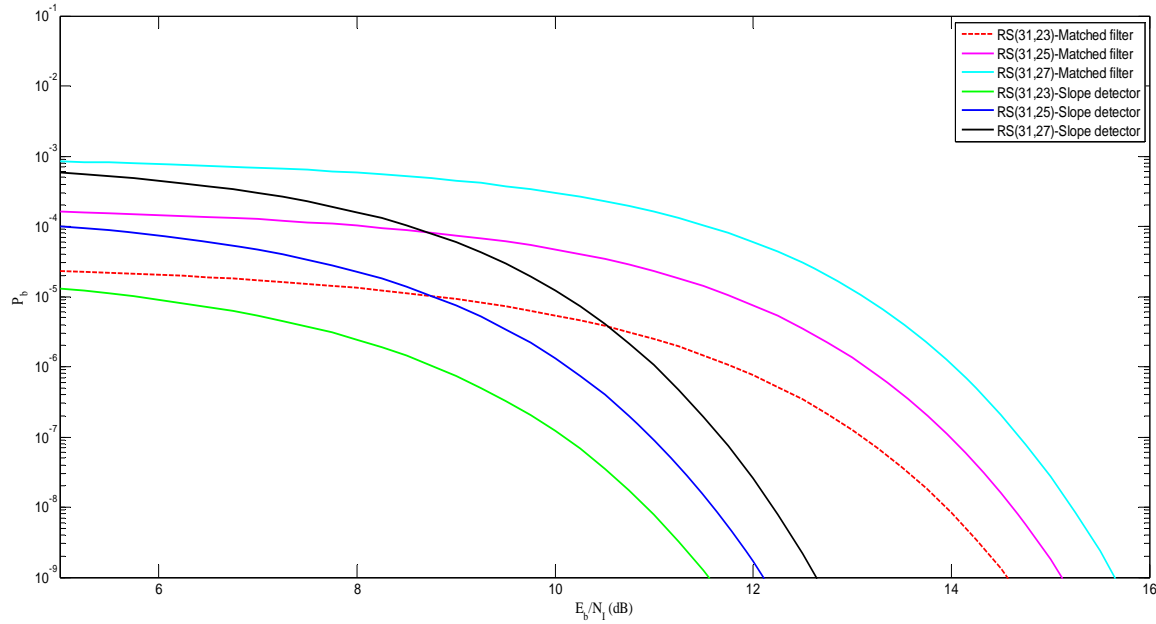


Figure 53. Performance of 32-ary CCSK Using the Alternative Error Correction Coding Scheme with Diversity and Noise-normalization in AWGN and PNI with  $\rho = 0.3$  for Matched Filter Detection with  $E_b / N_o = 15.0$  dB and Slope Detection with  $E_b / N_o = 12.0$  dB.

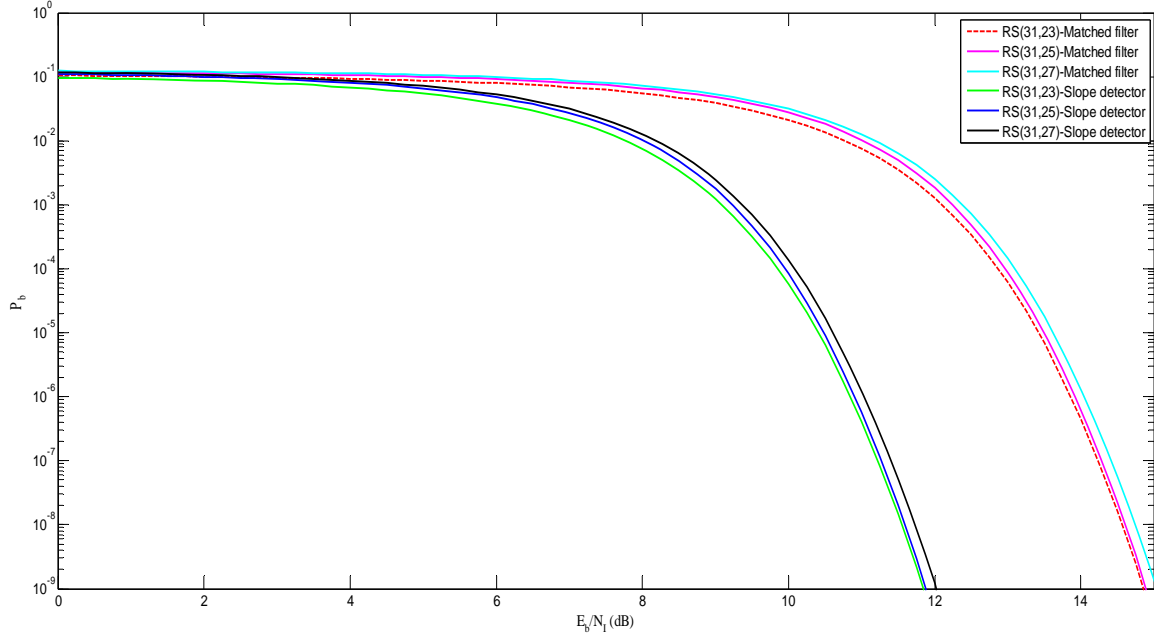


Figure 54. Performance of 32-ary CCSK Using the Alternative Error Correction Coding Scheme with Diversity and Noise-normalization in AWGN and PNI with  $\rho = 0.5$  for Matched Filter Detection with  $E_b / N_o = 15.0$  dB and Slope Detection with  $E_b / N_o = 12.0$  dB.

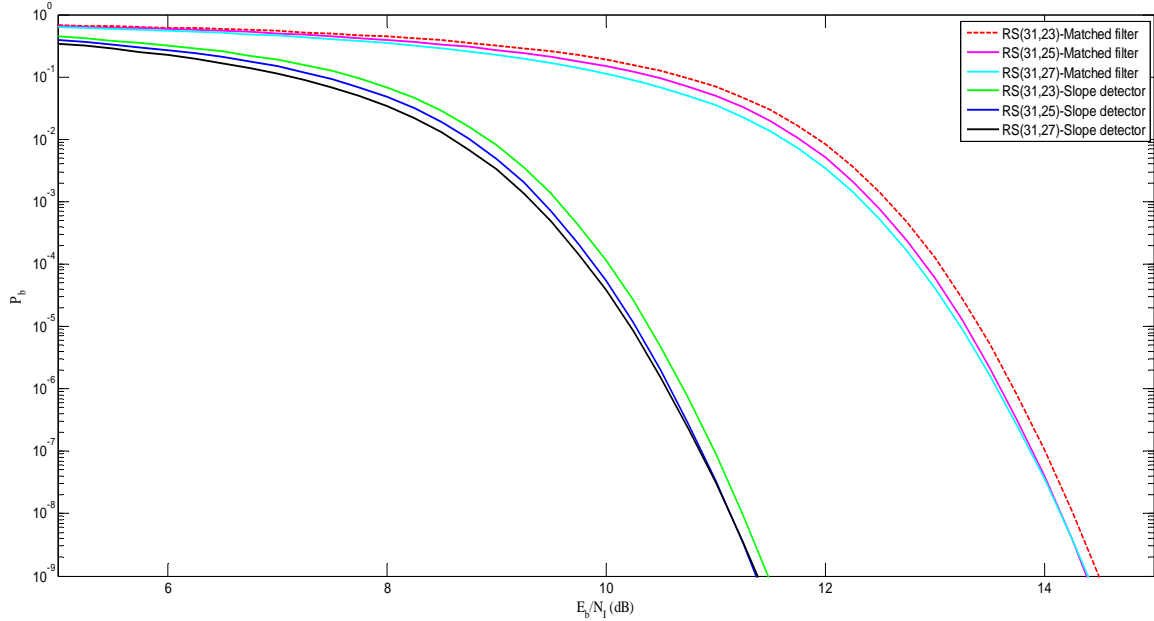


Figure 55. Performance of 32-ary CCSK Using the Alternative Error Correction Coding Scheme with Diversity and Noise-normalization in AWGN and PNI with  $\rho = 0.7$  for Matched Filter Detection with  $E_b / N_o = 15.0$  dB and Slope Detection with  $E_b / N_o = 12.0$  dB.

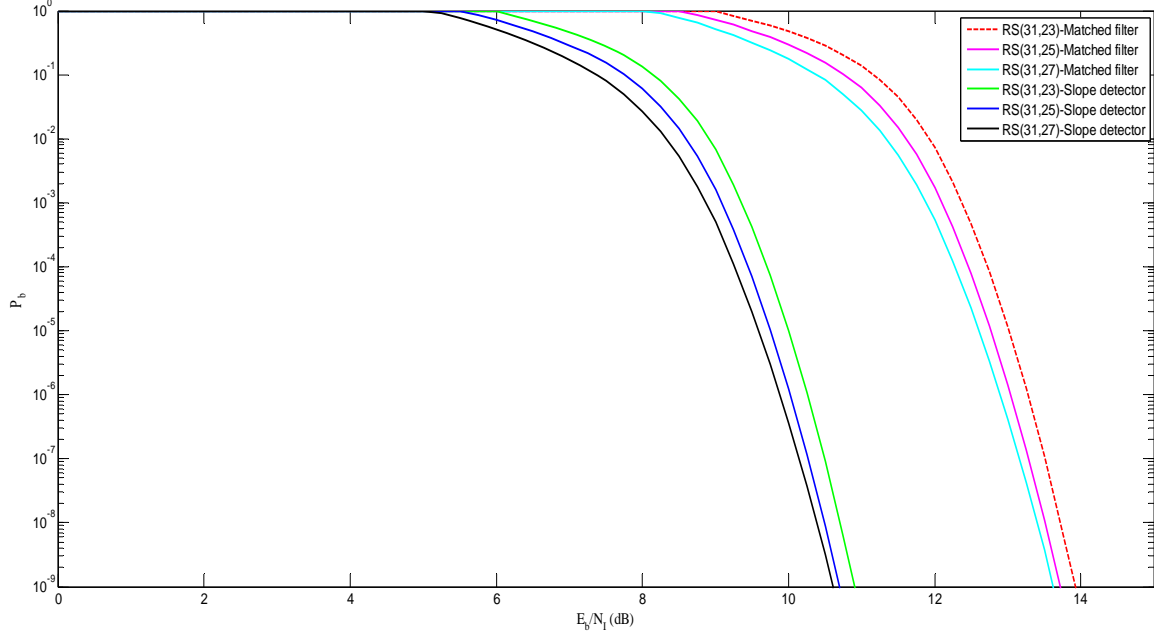


Figure 56. Performance of 32-ary CCSK Using the Alternative Error Correction Coding Scheme with Diversity and Noise-normalization in AWGN and PNI with  $\rho = 1.0$  for Matched Filter Detection with  $E_b / N_o = 15.0$  dB and Slope Detection with  $E_b / N_o = 12.0$  dB.

#### D. COMPARISON OF THE PERFORMANCE OF THE ALTERNATIVE WAVEFORM OBTAINED WITH HARD AND SOFT DECISION RS DECODING

In this section, the benefits of using soft decision RS decoding instead of hard decision RS decoding in both AWGN and pulse-noise interference are examined. In Figures 57 through 60, the alternative waveform with RS (31, 23), RS (31, 25) and RS (31, 27) inner codes are plotted for various  $\rho$ . The performance results are summarized in Table 12.

$P_b$	$\rho$	SD RS(31,23) $E_b / N_I$ (dB)	HD RS(31,23) $E_b / N_I$ (dB)	SD RS(31,25) $E_b / N_I$ (dB)	HD RS(31,25) $E_b / N_I$ (dB)	SD RS(31,27) $E_b / N_I$ (dB)	HD RS(31,27) $E_b / N_I$ (dB)
$10^{-5}$	0.1	superior	superior	superior	superior	superior	superior
$10^{-5}$	0.3	11.0	12.3	11.2	12.5	11.6	12.9
$10^{-5}$	0.5	12.1	12.8	11.9	12.6	11.9	12.7
$10^{-5}$	0.7	12.1	12.8	11.9	12.5	11.7	12.4
$10^{-5}$	1	12.0	12.6	11.6	12.2	11.4	12.0

Table 12. Comparison of the Performance of the Alternative Waveform for Different Values of  $\rho$  for Noncoherent Hard and Soft Decision RS Decoding in AWGN and PNI with Noise Normalization when  $E_b/N_0 = 8.0$  dB.

Based on the results shown in Table 12, the advantage of using soft decision RS decoding in the receiver when  $\rho > 0.5$  is negligible since the improvement does not exceed 1.0 dB. On the other hand, and up to a point, if the fraction of time when PNI is on is reduced, the employment of soft decision RS decoding results in higher gain. The least significant amount of improvement is observed for barrage noise interference ( $\rho = 1.0$ ).

In general, soft decision RS decoding outperforms hard decision, but the benefit of using it is marginal. Since hard decision decoding results in a simpler receiver, hard decision RS decoding is preferable.

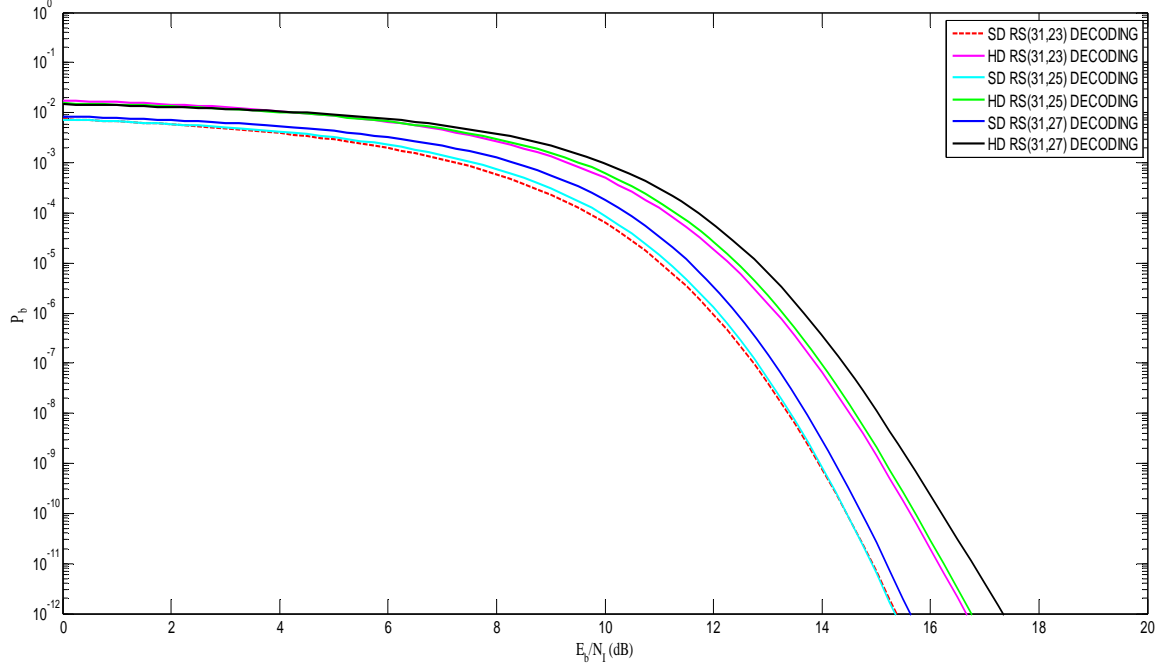


Figure 57. Performance of 32-ary CCSK Using the Alternative Error Correction Coding Scheme in AWGN and PNI with  $\rho = 0.3$ , Diversity, Noise-normalization, Hard and Soft Decision RS Decoding, and Noncoherent Demodulation.

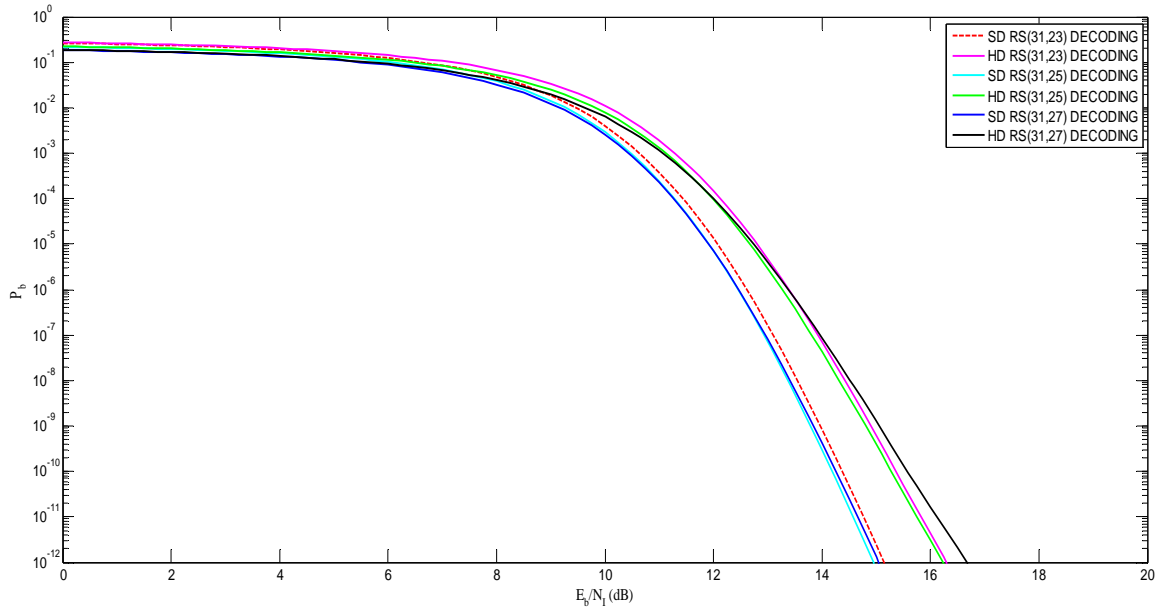


Figure 58. Performance of 32-ary CCSK Using the Alternative Error Correction Coding Scheme in AWGN and PNI with  $\rho = 0.5$ , Diversity, Noise-normalization, Hard and Soft Decision RS Decoding, and Noncoherent Demodulation.

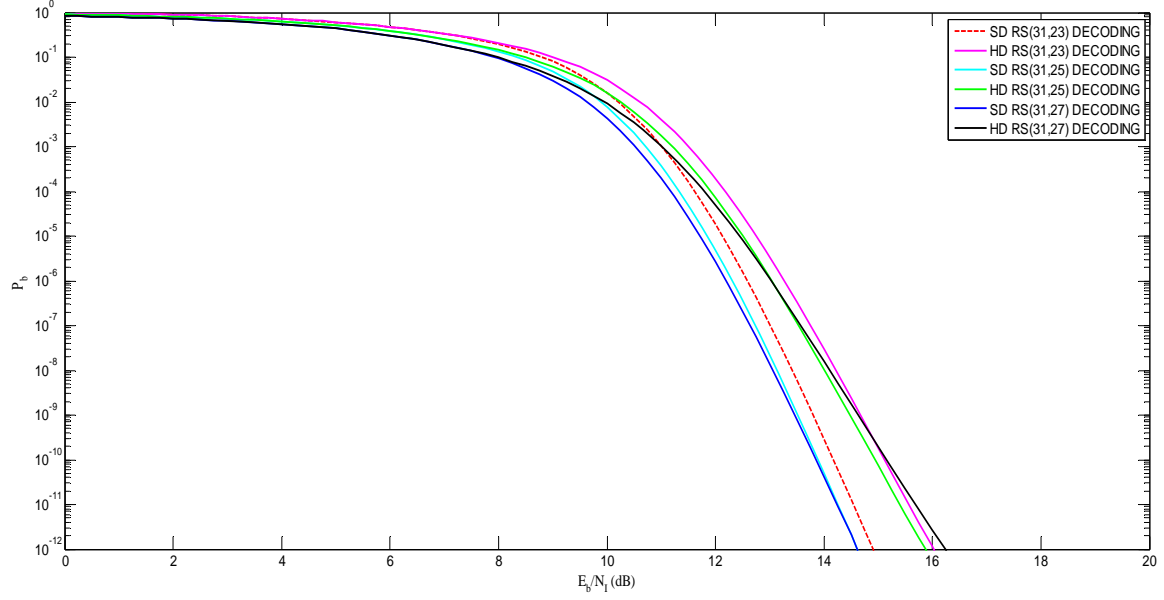


Figure 59. Performance of 32-ary CCSK Using the Alternative Error Correction Coding Scheme in AWGN and PNI with  $\rho = 0.7$ , Diversity, Noise-normalization, Hard and Soft Decision RS Decoding, and Noncoherent Demodulation.

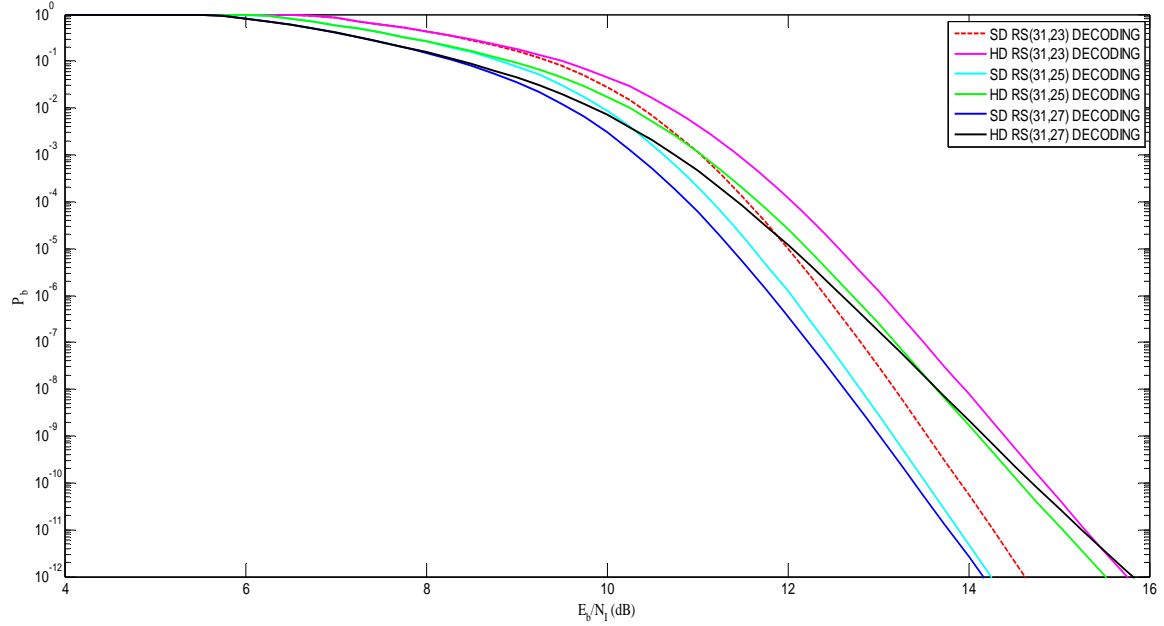


Figure 60. Performance of 32-ary CCSK Using the Alternative Error Correction Coding Scheme in AWGN and PNI with  $\rho = 1.0$ , Diversity, Noise-normalization, Hard and Soft Decision RS Decoding, and Noncoherent Demodulation.



## **E. CHAPTER SUMMARY**

In this chapter, the performance of the alternative waveform with a diversity of two, soft decision RS decoding, and noise-normalization in AWGN and PNI was investigated for noncoherent demodulation. The author concluded that the performance of the existing waveform was inferior when compared to the alternative waveform in all cases. The benefits of noise-normalization were shown to be very important since noise-normalization successfully cancelled the effects of pulse-noise interference. Finally, the use of soft decision (with increased receiver complexity) instead of hard decision RS decoding does not significantly improve the overall performance of the system.

THIS PAGE INTENTIONALLY LEFT BLANK

## VI. CONCLUSIONS AND FUTURE WORK

A JTIDS-type compatible waveform with an alternative error correction coding scheme, consistent with the existing JTIDS waveform, was examined in this thesis. The alternative scheme used a concatenated code with a  $(31, k)$  RS inner code and a rate  $4/5$  convolutional outer code. In the receiver, soft decision RS decoding was employed. The performance of the proposed waveform was analyzed for AWGN only, as well as for both AWGN and PNI. The effects of noise-normalization when PNI is present were investigated for both coherent and noncoherent demodulation.

Based on the results of the analyses in this thesis, the alternative waveform was found to improve performance relative to the original JTIDS. Specifically, when only AWGN was present, the alternative waveform with a diversity of two outperformed the original by 1.4 dB for both coherent and noncoherent demodulation.

When both AWGN and PNI were present, the alternative waveform again outperformed relative to the original JTIDS for all the cases considered. In this environment, noise-normalization was used in order to minimize the effects of pulse-noise interference. The performance results were very satisfactory since the degradation due to PNI essentially was cancelled. Thus, one of the worst types of jamming/interference was effectively countered.

The use of soft decision RS decoding was shown to have trivial benefits on the overall performance of the system relative to hard decision RS decoding. The improvement was negligible and, therefore, because of the increased complexity of soft decision receiver designs, this type of decoding is not recommended.

Future work should consider self-normalization instead of noise-normalization to reduce the effects of PNI since self-normalization is more practical to implement than noise-normalization for a frequency-hopped system with a real hop rate as fast as JTIDS (more than 77,000 hops/sec). Additionally, the effect of more aggressive SD decoding should be investigated. In this thesis, a conservative estimate of one additional error

corrected per block was assumed. It has been shown that, in some circumstances, an increase of three or four additional errors corrected per block is both possible and practical [14].

## LIST OF REFERENCES

- [1] I. Koromilas, "Performance analysis of the Link-16/JTIDS waveform with concatenated coding," M.S. thesis, Naval Postgraduate School, Monterey, CA, 2009.
- [2] T. Aivaliotis, "Performance analysis of a JTIDS/Link-16-type waveform using 32-ry orthogonal signaling with 32 chip baseband waveforms and concatenated code," M.S. thesis, Naval Postgraduate School, Monterey, CA, 2009.
- [3] C. Robertson, "Concatenated codes," lecture notes, Naval Postgraduate School, Monterey, CA, 2009.
- [4] Tri T. Ha, "Information theory and channel coding," lecture notes, Naval Postgraduate School, Monterey, CA, 2006.
- [5] C. Robertson, Notes, "Convolutional codes," lecture notes, Naval Postgraduate School, Monterey, CA, 2009.
- [6] J. G. Proakis and M. Salehi, *Digital Communications*, 4th ed. New York: McGraw Hill, 2008.
- [7] C. Robertson, "Linear block codes," lecture notes, Naval Postgraduate School, Monterey, CA, 2005.
- [8] B. Sklar, *Digital Communications: Fundamentals and Applications*, 2nd ed. New Jersey: Prentice Hall Inc., 2001.
- [9] Northrop Grumman Corporation, *Understanding Link-16: A Guidebook for New Users*, San Diego, CA, 2001.
- [10] Chi-Han Kao, "Performance analysis of a JTIDS/Link-16-type waveform transmitted over slow, flat nakagami fading channels in the presence of narrowband interference," Ph.D. dissertation, Naval Postgraduate School, Monterey, CA, 2008.
- [11] Tri T. Ha, "Demodulation (chapter 7)," lecture notes, Naval Postgraduate School, Monterey, CA, 2009.
- [12] C. Robertson, "Binary phase shift-keying," lecture notes, Naval Postgraduate School, Monterey, CA, 2009.
- [13] C. Robertson, "Frequency-hopped spread spectrum," lecture notes, Naval Postgraduate School, Monterey, CA, 2009.

- [14] K. Spyridis, “Hybrid hard and soft decision decoding of Reed-Solomon codes for M-ARY frequency-shift keying,” M.S. thesis, Naval Postgraduate School, Monterey, CA, 2010.

## INITIAL DISTRIBUTION LIST

1. Defense Technical Information Center  
Ft. Belvoir, Virginia
2. Dudley Knox Library  
Naval Postgraduate School  
Monterey, California
3. Chairman, Code IS  
Department of Information Sciences  
Naval Postgraduate School  
Monterey, California
4. Professor R. Clark Robertson  
Department of Electrical and Computer Engineering  
Naval Postgraduate School  
Monterey, California
5. Professor Terry Smith, Code IS/Smith  
Department of Information Sciences  
Naval Postgraduate School  
Monterey, California
6. Embassy of Greece  
Office of Naval Attaché  
Washington, District of Columbia
7. LTJG Katsaros Charalampos  
Hellenic Navy General Staff  
Athens, Greece